

Circulation Research

JOURNAL OF THE AMERICAN HEART ASSOCIATION



Extracellular Matrix Secretion by Cardiac Fibroblasts: Role of microRNA-29b and microRNA-30c

Melanie Abonnenc, Adam A Nabeebaccus, Ursula Mayr, Javier Barallobre-Barreiro, Xuebin Dong, Friederike Cuello, Sumon Sur, Ignat Drozdov, Sarah Langley, Ruifang Lu, Konstantina Stathopoulou, Athanasios Didangelos, Xiaoke Yin, Wolfram H Zimmermann, Ajay M Shah, Anna Zampetaki and Manuel Mayr

Circ Res. published online September 4, 2013;
Circulation Research is published by the American Heart Association, 7272 Greenville Avenue, Dallas, TX 75231
Copyright © 2013 American Heart Association, Inc. All rights reserved.
Print ISSN: 0009-7330. Online ISSN: 1524-4571

The online version of this article, along with updated information and services, is located on the World Wide Web at:

<http://circres.ahajournals.org/content/early/2013/09/03/CIRCRESAHA.113.302400>

Data Supplement (unedited) at:

<http://circres.ahajournals.org/content/suppl/2013/09/03/CIRCRESAHA.113.302400.DC1.html>

Permissions: Requests for permissions to reproduce figures, tables, or portions of articles originally published in *Circulation Research* can be obtained via RightsLink, a service of the Copyright Clearance Center, not the Editorial Office. Once the online version of the published article for which permission is being requested is located, click Request Permissions in the middle column of the Web page under Services. Further information about this process is available in the [Permissions and Rights Question and Answer](#) document.

Reprints: Information about reprints can be found online at:
<http://www.lww.com/reprints>

Subscriptions: Information about subscribing to *Circulation Research* is online at:
<http://circres.ahajournals.org//subscriptions/>

**Extracellular Matrix Secretion by Cardiac Fibroblasts:
Role of microRNA-29b and microRNA-30c**

Mélanie Abonnenc¹, Adam A. Nabeebaccus¹, Ursula Mayr¹, Javier Barallobre-Barreiro¹, Xuebin Dong¹, Friederike Cuello^{1,2}, Sumon Sur⁴, Ignat Drozdov^{1,3}, Sarah R. Langley¹, Ruifang Lu¹, Konstantina Stathopoulou^{1,2}, Athanasios Didangelos¹, Xiaoke Yin¹, Wolfram-Hubertus Zimmermann⁴, Ajay M. Shah¹, Anna Zampetaki¹, Manuel Mayr¹

¹King's BHF Centre, King's College London, UK; ²Department of Experimental Pharmacology and Toxicology, University Medical Centre Hamburg-Eppendorf, Germany; ³Centre for Bioinformatics-School of Physical Sciences and Engineering, and ; ⁴Institute of Pharmacology, University Medical Center, Georg-August-University and DZHK (German Center for Cardiovascular Research), partner site Goettingen, Germany.

Running title: MicroRNAs in Cardiac Fibroblasts



Circulation Research

Subject codes:

- [11] Other heart failure
- [108] Other myocardial biology
- [130] Animal models of human disease
- [141] Functional genomics
- [142] Gene expression

Address correspondence to:

Dr. Manuel Mayr
King's BHF Centre
King's College London,
125 Coldharbour Lane
London SE5 9NU
United Kingdom
Tel: +44 (0)20 7848 5132
Fax: +44 (0)20 7848 5296,
manuel.mayr@kcl.ac.uk

In August 2013, the average time from submission to first decision for all original research papers submitted to *Circulation Research* was 12.82 days.

ABSTRACT

Rationale: MicroRNAs (miRNAs), in particular miR-29b and miR-30c, have been implicated as important regulators of cardiac fibrosis.

Objective: To perform a proteomics comparison of miRNA effects on extracellular matrix (ECM) secretion by cardiac fibroblasts (CFs).

Methods and Results: Mouse CFs were transfected with pre-/anti-miR of miR-29b and miR-30c and their conditioned medium was analysed by mass spectrometry. MiR-29b targeted a cadre of proteins involved in fibrosis, including multiple collagens, matrix metalloproteinases, and leukemia inhibitory factor (LIF), insulin-like growth factor-1 (IGF-1) and pentraxin-3, three predicted targets of miR-29b. MiR-29b even attenuated the CF response to TGF β . In contrast, miR-30c had little effect on ECM production, but opposite effects with regards to LIF and IGF-1. Both miRNAs indirectly affected cardiac myocytes: Upon transfection with pre-miR-29b, the conditioned medium of CFs lost its ability to support adhesion of rat ventricular myocytes and led to a significant reduction of cardiac myocyte proteins (alpha-actinin, cardiac myosin-binding protein C and cardiac troponin I). Similarly, cardiomyocytes derived from mouse embryonic stem cells atrophied under pre-miR-29 conditioned medium whereas pre-miR-30c conditioned medium had a prohypertrophic effect. Levels of miR-29a, miR-29c and miR-30c but not miR-29b were significantly reduced in a mouse model of pathological but not physiological hypertrophy. Treatment with antagomirRs to miR-29b induced excess fibrosis after aortic constriction without overt deterioration in cardiac function.

Conclusions: Our proteomic analysis revealed novel molecular targets of miRNAs that are linked to a fibrogenic cardiac phenotype. Such comprehensive screening methods are essential to define the concerted actions of miRNAs in cardiovascular disease.

Keywords:

microRNA, proteomics, fibroblasts, fibrosis, animal model cardiovascular disease

Nonstandard Abbreviations and Acronyms:

| | |
|-------------|----------------------------------|
| CF | Cardiac fibroblast |
| ECM | Extracellular matrix |
| IGF-1 | Insulin-like growth factor 1 |
| LVH | Left ventricular hypertrophy |
| LIF | Leukemia inhibitory factor |
| miRNA | microRNA |
| MMP | Matrix metalloproteinase |
| NRVM | Neonatal rat ventricular myocyte |
| PTX-3 | Pentraxin 3 |
| TGF β | Transforming growth factor beta |

INTRODUCTION

MiRNAs have emerged as important regulators of cardiac fibrosis, a critical feature of structural myocardial remodeling in many cardiac diseases.¹⁻³ CFs communicate with cardiac myocytes via paracrine mechanisms, alterations in ECM, and direct cell-cell interactions.⁴ The miR-29 family suppresses the expression of several collagens and ECM proteins. MiR-29b is downregulated after myocardial infarction and in disease models for cardiac hypertrophy, possibly contributing to scar formation and fibrosis.⁵ Two other miRNAs, miR-30 and miR-133, display reduced expression during cardiac disease and show an inverse correlation to levels of connective tissue growth factor, collagen production, and fibrosis.⁶ Whereas miR-133 is expressed specifically in cardiac myocytes, miR-30 is present both in cardiac myocytes and CFs. MiR-21 has also been implicated in cardiac fibrosis, but its role is debated.^{7,8}

In this study, we applied a proteomics approach to investigate the targets of miR-29b and miR-30c in the secretome of CFs. Most studies rely on bioinformatic algorithms or mRNA analysis for the identification of direct targets. These algorithms are based on an incomplete understanding of miRNA-mRNA seed pairing and evolutionary conservation of miRNAs.⁹ They typically predict hundreds to thousands of target genes for one miRNA, but with limited overlap and even the most sensitive programs fail to identify known targets.¹⁰ Importantly, cell type context is not taken into consideration. The utilization of -omics methods is essential for a more comprehensive understanding of miRNA-mediated regulation of gene expression. MiRNAs function as posttranscriptional regulators of gene expression, either by inducing mRNA degradation or by blocking protein translation. A systems biology approach aiming at a global readout at the protein rather than the mRNA level may advance our insight into the coordinated regulation of direct as well as indirect targets driving cardiovascular phenotypes following miRNA manipulation³.

METHODS

An expanded Materials and Methods section is available in the online data supplement <http://circres.ahajournals.org>. Key techniques involved adaptations of previously published protocols, including those for miRNA measurements¹¹⁻¹³ and liquid chromatography tandem mass spectrometry (LC-MS/MS)¹⁴⁻¹⁵. For animal studies, procedures were performed in accordance with the Guidance on the Operation of the Animals (Scientific Procedures) Act, 1986 (United Kingdom).

RESULTS

ECM secretion by CFs.

Primary murine CFs were transfected with pre-/anti-miRs of miR-29b or miR-30c (Online Figure I) and their secretome was analysed by proteomics (Online Figure II). GO term enrichment confirmed that the majority of proteins identified belong to the extracellular region (Figure 1A), including low abundant proteins such as secreted proteases, protease inhibitors, growth factors and cytokines (Figure 1B). Online Table I lists 248 non-redundant extracellular proteins from two independent experiments. Proteins previously identified in other proteomic studies on fibroblasts, including one on CFs, are highlighted. Notably, our study provides the most detailed characterization of the CF secretome to date.

Effects of miR-29b and miR-30c.

Both, miR-29b and miR-30c are abundant miRNAs in CFs (Figure 1C). Based on three different algorithms (TargetScan, PicTar and Diana-microT), fewer common targets were predicted for miR-29b than miR-30c (Figure 1D). Yet, pre-miR-29b markedly attenuated protein secretion by CFs, whereas pre-miR-30c had comparably little effect (Figure 2A). In general, transfection with pre-miRs led to more pronounced protein changes than anti-miRs. In agreement with previous studies,¹⁶⁻¹⁹ pre-miR-29b reduced collagen (CO1A1, CO5A2) and MMP2 secretion (Figure 2B). Inhibition by anti-miR-29b also reduced the expression of other miR-29 family members (Online Figure I) but did not further stimulate collagen and MMP secretion in cultured CFs.

Proteomics for miRNA target identification.

To reveal predicted and novel targets of miR-29b and miR-30c, the normalized spectral counts of all extracellular proteins are presented in Online Table II and III. Besides conventional methods of statistical inference to detect differences in expression, we utilised a hierarchical Bayes estimation of generalized linear mixed effects model (Qspec). The false discovery rate (FDR) was calculated with a mixture model-based method of local FDR control based upon the Bayes factors (BF). Proteins with a BF>10, FDR<5% and a fold change >30% were considered to be significant. Regarding miR-30c, little is known about its extracellular targets. Recently, miR-30c has been shown to target plasminogen activator inhibitor-1 (PAI1)²⁰. Upon transfection with pre-miR-30c, plasminogen activator inhibitor-1 was decreased by 25%, but fell short of statistical significance in our analysis (BF=7, Online Table III). Instead, protein-lysine 6-oxidase (LYOX), responsible for the cross-linking of peptidyl lysine residues in precursors to fibrous collagen and elastin, displayed a significant reduction in CFs transfected with pre-miR-30c. It was only predicted as a direct target by one of the three bioinformatics algorithms (Online Figure III). Results after transfection with pre-miR-29b were much more pronounced (Online Table II, Figure 2C). Since target derepression can be stress dependent, the proteomics analysis of pre-miR-29b transfected CFs was repeated following stimulation with TGF β . Among the 186 extracellular proteins identified (Online Table IV), 92 (\approx 50%) reached an unadjusted p-value (ANOVA) <0.05, including 21 out of 25 (84%) predicted targets of miR-29b (Figure 3A). Again, Qspec was used to detect differential expression. Results are shown in Figure 3B.

Confirmation of direct and indirect targets.

The quantification of low abundance proteins by proteomics can be challenging in complex biological samples. Cytokines and growth factors, such as LIF and IGF-1, as well as a member of the pentraxin superfamily, PTX3 showed weak evidence for differential expression (unadjusted p-value <0.05) in the t-test. PTX3 and LIF had a BF>4 by Qspec. For independent validation, levels of IGF-1, LIF and PTX-3 were determined using commercial ELISAs. The ELISA data correlated well to the spectral counts obtained by proteomics in the miR-29b experiment (Figure 4A-C, Spearman correlation coefficients 0.75-0.90). IGF-1 (Figure 4A), LIF (Figure 4B), and PTX3 (Figure 4C) were suppressed by pre-miR-29b and increased after inhibition by anti-miR-29b. As expected for direct targets, there was complementarity between the miR-29b seed-matching sequence and the 3'-UTR region of the target mRNAs (LIF, IGF-1, PTX3, Figure 4D). To further confirm the functionality of the seed regions of miR-29b, we fused the 3' UTR of IGF-1, LIF and PTX3 to a luciferase reporter vector. Co-expression of synthetic miR-29b decreased IGF-1 and LIF (Online Figure IV) but not PTX3 3'UTR reporter activity (data not shown). Mimics of miR-29b had the same effect as pre-miR-29b on target gene repression (Online Figure V). In contrast, miR-30c had no seed-matching sequence in the 3' UTR of IGF-1, LIF, and PTX3. Yet, overexpression of miR-30c increased levels of IGF-1 (Figure 4A) and LIF (Figure 4B). Again, PTX3 remained unaffected (Figure 4C).

In vivo validation.

Next, adult C57Bl6 mice were treated with antagomiRs directed against miR-29b (3 consecutive i.p. injections at a dose of 80mg/kg/day, Figure 4E). At day 7, successful inhibition of cardiac miR-29b was confirmed by qPCR (Figure 4F). When we evaluated cardiac mRNA expression, IGF-1 levels were increased by \approx 50% compared to respective controls (Figure 4G). In plasma, levels of IGF-1 rose by \approx 25% (Figure 4H), confirming IGF-1 as a target of miR-29b *in vitro* and *in vivo*. Neither LIF nor PTX-3 showed significant changes in unstressed hearts or in plasma following antagomiR-29b treatment (data not shown).

Effects on cell adhesion.

To investigate whether miRNA-induced changes in the secretome of CF impact on cardiac myocyte adhesion, neonatal rat ventricular myocytes (NRVM) were cultured overnight on glass-coverslips, pre-coated with conditioned medium of CFs, previously transfected with pre-miR29b (Figure 5A) or anti-miR29b (Figure 5B). Cardiac myocytes were stained for cardiac myosin-binding protein C (cMyBP-C, green) and cardiac α -actinin (red). Nuclei were counterstained with DAPI (blue). Transfection with pre-miR29b markedly reduced the ability of the conditioned medium from CFs to support adhesion of NRVM (Figure 5A, Online Figure VI). The effect of pre-miR30c on NRVM adhesion was less pronounced. Only when untransfected CFs were seeded on plates pre-coated with conditioned medium of transfected CFs, pre- as well as anti-miR-29b resulted in significant changes in early adhesion (Online Figure VII).

Effects on cardiac myocytes.

Bidirectional crosstalk between CFs and cardiac myocytes is able to regulate the CF and cardiac myocyte phenotype.⁴ NRVM cultured on plastic dishes, precoated with conditioned medium of CFs previously transfected with pre-miR-29b, displayed reduced expression of alpha-actinin, cMyBP-C and cTnI, as demonstrated by western immunoblotting (Figure 5A). These cardiac markers were unaltered by anti-miR-29b or pre-miR-30c. In contrast, pre-coating with conditioned medium from CFs transfected with anti-miR-30c reduced alpha-actinin and cTnI expression in NRVM (Figure 5B). No difference was observed for cMyBP-C. To test whether the secretomes of transfected CFs have a direct activity on cardiomyocytes, specifically on cardiomyocyte size, we exposed a pure ($>95\%$) cardiomyocyte preparation derived from mouse embryonic stem cells (ESC) modified to express a neomycin resistance under the cardiomyocyte-restricted α MHC promoter, to conditioned medium from pre-miR-29 and pre-miR30c transfected CF. Under these conditions cardiomyocytes atrophied (pre-miR-29 conditioned medium) or conversely showed hypertrophic growth (pre-miR-30c conditioned medium; Figure 5C). Conditioned media from CFs transfected with anti-miRs did not alter cardiomyocyte size.

Cross-talk between miRNAs.

Our observation that miR-30c and miR-29b induced opposite effects in several experiments (Figures 4A-C, 5A-C), prompted us to investigate the possibility of a cross-talk between miR-30c and miR-29b in CFs: Indeed, overexpression of pre-miR-29b was sufficient to reduce the endogenous levels of miR-30c in CFs to a similar extent (\approx 50%) as TGF \square stimulation of CFs (Online Figure VIII). Even at a moderate level of miR-29b overexpression (~20 fold), the difference in miR-30c remained statistically significant, while many other miRNAs were not affected (data not shown).

MiR-29b in cardiac hypertrophy.

Attenuation of miR-29b expression has previously been linked to ECM remodelling post myocardial infarction.¹⁶ MiR-29c has also been reported as down-regulated in cardiac hypertrophy.²¹ Thus, we sought to explore whether endogenous miR-29b and miR-30c levels are affected in mouse models of pathological (transverse aortic constriction, TAC) and physiological (free running exercise) left ventricular hypertrophy (LVH). RNA was isolated from 23 left ventricular samples (Sham: n=6; TAC: n=6; Sedentary: n=6; Exercise: n=5). TaqMan qPCR revealed a significant decrease of miR-29a, miR-29c and miR-30c, but not of miR-29b in pathological LVH (Figure 6A). Physiological LVH was not associated with significant alterations in any of the miRNAs tested (Figure 6A). Yet, miR-29b was abundant in non-myocytes (Figure 6B) and putative miR-29 targets were differentially expressed after TAC (Figure 6C).

In vivo silencing of miR-29b.

To establish whether miR-29b can alter ECM protein expression in pathological hypertrophy, antagomiRs to miR-29b were injected in male C57/Bl6 mice on 3 consecutive days before TAC. Hearts were obtained 14 days post surgery. AntagomiR treatment exhibited a marked repression of miR-29b without significant attenuation of other miR-29 family members (Figure 7A). Inhibition of miR-29b did not affect cardiac volumes or cardiac function and overall regional wall hypertrophy remained concentric (Online Table V). Only in mice with the most pronounced inhibition of miR-29b, the posterior papillary muscle was occasionally more echobright and its base thickened (Online Figure IX). Histologically, excess perivascular fibrosis was observed (Figure 7B). Of note, miR-29b inhibition by antagomiRs emerged as significant determinant of myocardial expression for many direct and indirect targets identified by proteomics, including LIF and IGF-1 (Figure 7C). Detailed expression data after TAC are presented in Online Figure X.

DISCUSSION

The molecular mechanisms underlying cardiac fibrosis are of intense interest. MiR-29b and miR-30c are two key miRNAs that are enriched in CFs and involved in cardiac fibrosis. In the present study, we applied a proteomics approach to identify extracellular targets of miR-29b and miR-30c. MiR-29b had a much stronger effect on the extracellular proteome of CFs than miR-30c and even blocked the response of CFs to TGF \square , one of the master regulators of fibrosis. Besides its major effect on ECM proteins, miR-29b additionally altered the secretion of growth factors and cytokines, such as LIF and IGF-1. In contrast, miR-30c regulated fewer ECM proteins, but indirectly modulated the expression of LIF and IGF-1.

The secretome of mouse CFs.

Few large-scale proteomics studies focusing on the secretome of fibroblasts have been performed so far.²² Most studies investigated the secretome of feeder cells such as mouse embryonic fibroblasts, which support the growth of embryonic stem cells²³⁻²⁶ or dermal fibroblasts.^{27,28} Thus far, only one study used CFs and profiled 24 cytokines/chemokines in their conditioned medium.²⁹ No detailed proteomics analysis has been performed to date. The recognition that cardiac fibrosis is a prominent contributor to myocardial disease and that CFs interact with cardiac myocytes via paracrine mechanisms, alterations in matrix homeostasis, and direct cell-cell interactions has resulted in a growing interest in CFs over recent years.⁴ For example, ECM promotes efficient cardiac differentiation of human pluripotent stem cells.³⁰ To the best of our knowledge, our proteomic study presents the most extensive characterization of the CF secretome published so far. Among the 248 proteins identified are important proteins for ECM-receptor

interaction, focal adhesion, the TGF β signalling pathway, and cytokine-cytokine receptor interaction. Similar to our recent study on ECM remodeling in a porcine model of cardiac ischemia/reperfusion,³¹ this comprehensive map of the CF secretome will provide an important resource for future investigations into factors involved in CF-cardiac myocyte communication.

Proteomics for miRNA target identification.

Changes in cardiovascular phenotypes following miRNA manipulation are likely to be the result of multiple interactions. As miRNAs are fine-tuners of protein expression and the regulation of their target genes tends to be in the range of 20-50%, the secretome offers the distinct advantage that miRNA-induced changes accumulate and become more readily detectable by proteomics. The levels of miR-29b expression in our study are similar to previous publications in CFs¹⁶. An obvious concern is whether transfection with precursor miRNAs interferes with the cellular processing of non-coding RNAs. To exclude off-target effects, we compared two miRNAs, both of which play an important role in CFs and are likely to be processed in a similar manner upon transfection, in parallel to respective scrambled miRNA controls. Potential explanations for the more pronounced effect of pre-miRNAs over anti-miRs are as follows: 1) Transfection with miRNA precursors will saturate the available binding sites. This is informative about the maximal effect of a particular miRNA within the proteome, but does not imply that the expression of these proteins is under the control of the endogenous miRNA. 2) A tight regulation of expression is required, in particular for proteins that have important functions. Individual miRNAs modulate the expression of several targets, which often are effectors of the same biological process. Conversely, several miRNAs can target the same effector.¹ Diverse miRNAs can also act cooperatively or redundantly to regulate the effectors of the same biological process. Thus, derepression of a protein based on inhibition of a single miRNA is more difficult to achieve. 3) Most transgenic animals for miRNAs have no baseline phenotype, but develop a phenotype in response to a stress stimulus. Stress conditions are likely to alter the susceptibility of proteins for the control by endogenous miRNAs. The abundance of the mRNA is as important for miRNA target regulation as the concentration of the endogenous miRNA itself. Thus, proteins that change following the transfection of the precursor but do not change by antagonizing the endogenous miRNA in unstimulated cells or normal hearts could still be affected during a stress response. Currently, miRNA target identification is mainly performed in unstressed cells. Our proteomics analyses were performed at baseline and after TGF β stimulation. Moreover, confirmation of target repression was obtained by using miRNA mimics and by antagomiR treatment in a mouse model of pathological LVH.

Role of miR-29b in cardiac disease.

The miR-29 family is present with four copies in the genome and mainly expressed in fibroblasts. Unlike most miRNAs that are only present in the cytosol, miR-29 is also found in the nucleus. Following myocardial infarction, miR-29b is down-regulated in the region adjacent to the infarcted area, suggesting a pertinent role of this miRNA in cardiac remodelling.¹⁶ Besides its involvement in the development of cardiac fibrosis, the miR-29 family has been implicated in aortic aneurysm formation^{32, 33} and atherosclerosis¹⁸. Its modulatory effect on ECM protein secretion and potential importance in different cardiovascular diseases has made it a lead miRNA for therapeutic intervention. Thus far, the effect of miR-29b in CFs was mainly assessed at the mRNA level. Over-expression of miR-29b reduced expression of collagens whereas down-regulation of miR-29b with anti-miRs induced the expression of collagens *in vitro* and *in vivo*.¹⁶ Our proteomic data confirm that pre-miR-29b is a potent regulator of ECM synthesis. The effect of anti-miR-29b in cultured CF, however, was not as pronounced. While we failed to observe a significant change of miR-29b expression in two mouse models of LVH, this does not negate a potential role of miR-29b for initial ECM deposition during cardiac hypertrophy, as miRNA measurements were only performed at one time point (14 days post surgery or 28 days post exercise). In fact, treatment with antagomiRs to miR-29b increased ECM deposition after aortic constriction. Previous

studies with miR-29 inhibition were done in unstressed hearts and the expression of three collagen transcripts (Col1A1, Col1A2, and Col3A1) was only modestly increased¹⁶. After TAC, we did observe target derepression and increased perivascular fibrosis in response to miR-29b inhibition.

CF – cardiac myocyte interactions.

MiRNA levels in CFs may impact on cardiac myocytes with regards to their adhesive properties and growth characteristics. Recently, Castoldi *et al.* have demonstrated that miR-133a, a miRNA expressed in cardiac myocytes and involved in cardiac hypertrophy, also targets CO1A1, a target of miR-29b.¹⁷ Their data support the concept that myocardial fibrosis could be modulated not only by miRNAs expressed in CFs, but also by muscle-specific miRNAs, through a synergistic action on CO1A1 mRNA expression. However, little is known regarding the role of miR-29b in the communication between CFs and cardiac myocytes and its involvement in myocardial hypertrophy. Our data suggest that miR-29b is not only regulating ECM protein deposition but may also contribute to development of cardiac hypertrophy by targeting important growth factors and cytokines: among the potential targets of miR-29b were IGF-1, LIF and PTX3. PTX3 is a member of the pentraxin superfamily that plays an important role at the interface of inflammation and ECM remodeling.^{34,35} It has been suggested as a novel biomarker of left ventricular dysfunction and heart failure with normal ejection fraction.³⁵ Interestingly, various inflammatory molecular cascades, in particular toll-like receptor signaling, stimulate the expression of PTX3³⁶ and the promoter region of miR-29b shows at least 4 different binding sites for NK-kappaB.³⁷ LIF is a member of the IL-6 family that is synthesized by different cell types in the myocardium including cardiac myocytes and CFs.³⁸ Previous studies have demonstrated that LIF confers both hypertrophic and cytoprotective responses in adult cardiac myocytes via the gp130 and LIF receptor signaling complex.^{39,40} IGF-1 is a key regulator of growth, survival, and differentiation. In myocardial biology, IGF-1 and its signal transduction cascade are involved in development, cardiac myocyte size and survival, action potential, and excitation-contraction coupling.^{41,42} Interestingly, miR-29b and miR-30c exerted opposite effects on IGF-1 and LIF secretion by CFs and in most functional experiments. This is in agreement with previous reports that miRNAs in the same cell type could regulate the same targets counterbalancing each other.¹ To rule out indirect effects mediated via contaminating stroma cells, we exposed a highly purified cardiomyocyte population derived from ESCs to conditioned medium and observed that the pre-miR29b and pre-miR30c CF secretomes did indeed impart opposite effects on cardiomyocyte growth, i.e. atrophy and hypertrophy, respectively. These effects were likely mediated by soluble growth factors suggesting that the observed paracrine effects on cardiomyocytes may not only be due to adhesive ECM molecules.

Conclusion.

Our proteomics study provides the most comprehensive characterization of the mouse CF secretome to date. A particular strength is the proteome-wide analysis of miRNA function, which offers unique insight into the regulation of protein networks controlled by miR-29b and miR-30c. Direct and indirect targets were identified from a broader proteomics screen and validated *in vivo*. Many of these targets would not have been anticipated based on current bioinformatics prediction models. Addressing the complexity of miRNA-regulated gene expression is an essential step to facilitate a better understanding of their concerted actions in cardiac fibrosis.

SOURCES OF FUNDING

This work was funded by the British Heart Foundation. A.Z. is an Intermediate Fellow of the British Heart Foundation. M.M. is a Senior Fellow of the British Heart Foundation. S.S. is a member of the IRTG 1816 (project supervisors: M.M. and W.H.Z.).

DISCLOSURES

None.

REFERENCES

1. Small EM, Olson EN. Pervasive roles of microRNAs in cardiovascular biology. *Nature*. 2011;469:336-342.
2. Bauersachs J, Thum T. Biogenesis and regulation of cardiovascular microRNAs. *Circ Res*. 2011;109:334-347.
3. Zampetaki A, Mayr M. MicroRNAs in vascular and metabolic disease. *Circ Res*. 2012;110:508-522.
4. Kakkar R, Lee RT. Intramyocardial fibroblast myocyte communication. *Circ Res*. 2010;106:47-57.
5. Van Rooij E, Olson EN. Searching for miR-acles in cardiac fibrosis. *Circ Res*. 2009;104:138-140.
6. Duisters RF, Tijsen AJ, Schroen B, Leenders JJ, Lentink V, van der Made I, Herias V, van Leeuwen RE, Schellings MW, Barenbrug P, Maessen JG, Heymans S, Pinto YM, Creemers EE. miR-133 and miR-30 regulate connective tissue growth factor: implications for a role of microRNAs in myocardial matrix remodeling. *Circ Res*. 2009;104:170-178.
7. Thum T, Gross C, Fiedler J, Fischer T, Kissler S, Bussen M, Galuppo P, Just S, Rottbauer W, Frantz S, Castoldi M, Soutschek J, Koteliansky V, Rosenwald A, Basson MA, Licht JD, Pena JT, Rouhanifard SH, Muckenthaler MU, Tuschl T, Martin GR, Bauersachs J, Engelhardt S. MicroRNA-21 contributes to myocardial disease by stimulating MAP kinase signalling in fibroblasts. *Nature*. 2008;456:980-984.
8. Patrick DM, Kauppinen S, van Rooij E, Olson EN. Response to Thum et al. *J Clin Invest*. 2011;121:462-463.
9. Thomas M, Lieberman J, Lal A. Desperately seeking microRNA targets. *Nat Struct Mol Biol*. 2010;17:1169-1174.
10. Alexiou P, Maragkakis M, Papadopoulos GL, Reczko M, Hatzigeorgiou AG. Lost in translation: an assessment and perspective for computational microRNA target identification. *Bioinformatics*. 2009;25:3049-3055.
11. Zampetaki A, Kiechl S, Drozdov I, Willeit P, Mayr U, Prokopi M, Mayr A, Weger S, Oberholzer F, Bonora E, Shah A, Willeit J, Mayr M. Plasma microRNA profiling reveals loss of endothelial miR-126 and other microRNAs in type 2 diabetes. *Circ Res*. 2010;107:810-817.
12. Zampetaki A, Willeit P, Tilling L, Drozdov I, Prokopi M, Renard JM, Mayr A, Weger S, Schett G, Shah A, Boulanger CM, Willeit J, Chowienczyk PJ, Kiechl S, Mayr M. Prospective study on circulating MicroRNAs and risk of myocardial infarction. *J Am Coll Cardiol*. 2012;60:290-299.
13. Willeit P, Zampetaki A, Dudek K, Kaudewitz D, King A, Kirkby NS, Crosby-Nwaobi R, Prokopi M, Drozdov I, Langley SR, Sivaprasad S, Markus HS, Mitchell JA, Warner TD, Kiechl S, Mayr M. Circulating microRNAs as novel biomarkers for platelet activation. *Circ Res*. 2013;112:595-600.
14. Didangelos A, Yin X, Mandal K, Saje A, Smith A, Xu Q, Jahangiri M, Mayr M. Extracellular matrix composition and remodeling in human abdominal aortic aneurysms: a proteomics approach. *Mol Cell Proteomics*. 2011;10:M111 008128.
15. Yin X, Bern M, Xing Q, Ho J, Viner R, Mayr M. Glycoproteomic analysis of the secretome of human endothelial cells. *Mol Cell Proteomics*. 2013;12:956-978.

16. van Rooij E, Sutherland LB, Thatcher JE, DiMaio JM, Naseem RH, Marshall WS, Hill JA, Olson EN. Dysregulation of microRNAs after myocardial infarction reveals a role of miR-29 in cardiac fibrosis. *Proc Natl Acad Sci U S A*. 2008;105:13027-13032.
17. Castoldi G, di Gioia CR, Bombardi C, Catalucci D, Corradi B, Gualazzi MG, Leopizzi M, Mancini M, Zerbini G, Condorelli G, Stella A. MiR-133a regulates collagen 1A1: potential role of miR-133a in myocardial fibrosis in angiotensin II dependent hypertension. *J Cell Physiol*. 2012;227:850-856.
18. Chen KC, Wang YS, Hu CY, Chang WC, Liao YC, Dai CY, Juo SH. OxLDL up-regulates microRNA-29b, leading to epigenetic modifications of MMP-2/MMP-9 genes: a novel mechanism for cardiovascular diseases. *FASEB J*. 2011;25:1718-1728.
19. Luna C, Li G, Qiu J, Epstein DL, Gonzalez P. Role of miR-29b on the regulation of the extracellular matrix in human trabecular meshwork cells under chronic oxidative stress. *Mol Vis*. 2009;15:2488-2497.
20. Marchand A, Proust C, Morange P-E, Lompré A-M, Trégouët D-A. miR-421 and miR-30c Inhibit SERPINE 1 Gene Expression in Human Endothelial Cells. *PLOS One*. 2012;7(8): e44532.
21. van Rooij E, Sutherland LB, Liu N, Williams AH, McAnally J, Gerard RD, Richardson JA, Olson EN. A signature pattern of stress-responsive microRNAs that can evoke cardiac hypertrophy and heart failure. *Proc Natl Acad Sci U S A*. 2006;103:18255-18260.
22. Skalnikova H, Motlik J, Gadher SJ, Kovarova H. Mapping of the secretome of primary isolates of mammalian cells, stem cells and derived cell lines. *Proteomics*. 2011;11:691-708.
23. Bendall SC, Hughes C, Campbell JL, Stewart MH, Pittock P, Liu S, Bonneil E, Thibault P, Bhatia M, Lajoie GA. An enhanced mass spectrometry approach reveals human embryonic stem cell growth factors in culture. *Mol Cell Proteomics*. 2009;8:421-432.
24. Chin AC, Fong WJ, Goh LT, Philp R, Oh SK, Choo AB. Identification of proteins from feeder conditioned medium that support human embryonic stem cells. *J Biotechnol*. 2007;130:320-328.
25. Buhr N, Carapito C, Schaeffer C, Hovasse A, Van Dorsselaer A, Viville S. Proteome analysis of the culture environment supporting undifferentiated mouse embryonic stem and germ cell growth. *Electrophoresis*. 2007;28:1615-1623.
26. Lim JW, Bodnar A. Proteome analysis of conditioned medium from mouse embryonic fibroblast feeder layers which support the growth of human embryonic stem cells. *Proteomics*. 2002;2:1187-1203.
27. Prowse AB, McQuade LR, Bryant KJ, Van Dyk DD, Tuch BE, Gray PP. A proteome analysis of conditioned media from human neonatal fibroblasts used in the maintenance of human embryonic stem cells. *Proteomics*. 2005;5:978-989.
28. Xie L, Tsaprailis G, Chen QM. Proteomic identification of insulin-like growth factor-binding protein-6 induced by sublethal H₂O₂ stress from human diploid fibroblasts. *Mol Cell Proteomics*. 2005;4:1273-1283.
29. LaFramboise WA, Scalise D, Stoodley P, Graner SR, Guthrie RD, Magovern JA, Becich MJ. Cardiac fibroblasts influence cardiomyocyte phenotype in vitro. *Am J Physiol Cell Physiol*. 2007;292:C1799-1808.
30. Zhang J, Klos M, Wilson GF, Herman AM, Lian X, Raval KK, Barron MR, Hou L, Soerens AG, Yu J, Palecek SP, Lyons GE, Thomson JA, Herron TJ, Jalife J, Kamp TJ. Extracellular matrix promotes highly efficient cardiac differentiation of human pluripotent stem cells: the matrix sandwich method. *Circ Res*. 2012;111:1125-1136.
31. Barallobre-Barreiro J, Didangelos A, Schoendube FA, Drozdov I, Yin X, Fernandez-Caggiano M, Willeit P, Puntmann VO, Aldama-Lopez G, Shah AM, Domenech N, Mayr M. Proteomics analysis of cardiac extracellular matrix remodeling in a porcine model of ischemia/reperfusion injury. *Circulation*. 2012;125:789-802.
32. Boon RA ST, Heydt S, Fischer A, Hergenreider E, Horrevoets AJ, Vinciguerra M, Rosenthal N, Sciacca S, Pilato M, van Heijningen P, Essers J, Brandes RP, Zeiher AM, Dimmeler S.

MicroRNA-29 in aortic dilation: implications for aneurysm formation. *Circ Res*. 2011;109:1115-1119.

33. Maegdefessel L, Azuma J, Toh R, Merk DR, Deng A, Chin JT, Raaz U, Schoelmerich AM, Raiesdana A, Leeper NJ, McConnell MV, Dalman RL, Spin JM, Tsao PS. Inhibition of microRNA-29b reduces murine abdominal aortic aneurysm development. *J Clin Invest*. 2012;122:497-506.
34. Mantovani A, Garlanda C, Doni A, Bottazzi B. Pentraxins in innate immunity: from C-reactive protein to the long pentraxin PTX3. *J Clin Immunol*. 2008;28:1-13.
35. Kaess BM, Vasan RS. Heart failure: pentraxin 3 - a marker of diastolic dysfunction and HF? *Nat Rev Cardiol*. 2011;8:246-248.
36. Bottazzi B, Garlanda C, Cotena A, Moalli F, Jaillon S, Deban L, Mantovani A. The long pentraxin PTX3 as a prototypic humoral pattern recognition receptor: interplay with cellular innate immunity. *Immunol Rev*. 2009;227:9-18.
37. Mott JL, Kurita S, Cazanave SC, Bronk SF, Werneburg NW, Fernandez-Zapico ME. Transcriptional suppression of mir-29b-1/mir-29a promoter by c-Myc, hedgehog, and NF-kappaB. *J Cell Biochem*. 2010;110:1155-1164.
38. Wollert KC, Drexler H. The role of interleukin-6 in the failing heart. *Heart Fail Rev*. 2001;6:95-103.
39. Kodama H, Fukuda K, Pan J, Makino S, Baba A, Hori S, Ogawa S. Leukemia inhibitory factor, a potent cardiac hypertrophic cytokine, activates the JAK/STAT pathway in rat cardiomyocytes. *Circ Res*. 1997;81:656-663.
40. Wang F, Seta Y, Baumgarten G, Engel DJ, Sivasubramanian N, Mann DL. Functional significance of hemodynamic overload-induced expression of leukemia-inhibitory factor in the adult mammalian heart. *Circulation*. 2001;103:1296-1302.
41. Santini MP, Tsao L, Monassier L, Theodoropoulos C, Carter J, Lara-Pezzi E, Slonimsky E, Salimova E, Delafontaine P, Song YH, Bergmann M, Freund C, Suzuki K, Rosenthal N. Enhancing repair of the mammalian heart. *Circ Res*. 2007;100:1732-1740.
42. Elia L, Contu R, Quintavalle M, Varrone F, Chimenti C, Russo MA, Cimino V, De Marinis L, Frustaci A, Catalucci D, Condorelli G. Reciprocal regulation of microRNA-1 and insulin-like growth factor-1 signal transduction cascade in cardiac and skeletal muscle in physiological and pathological conditions. *Circulation*. 2009;120:2377-2385.

ONLINE FIRST

FIGURE LEGENDS

Figure 1: The secretome of mouse CFs. **A**, Simplified GO term enrichment graph of the proteins identified in the conditioned medium of CFs (Online Table I). The functional annotation tool “David 6.7” has been used to perform the GO term annotation. The default background dataset of *Mus Musculus* was selected for the GO term enrichment calculation. **B**, Classification of the relevant extracellular proteins identified in secretome of CFs. **C**, Expression levels of miR-29 and miR-30c compared to other selected miRNAs in mouse CFs. The higher Ct values inversely correlate with miRNA expression levels. U6 was used as normalisation control. **D**, Pie charts illustrating common targets for miR-29 and miR-30c in three target prediction algorithms (TargetScan, PicTar, Diana).

Figure 2: Comparison of miR-29b and miR-30c. **A**, Frequency distribution of protein changes after the transfection of CFs either with pre-miR-29b, anti-miR-29b, pre-miR-30c or anti-miR-30c. A log₂ fold change of -1 or 1 was used as cut-off. Protein fractions with a log₂ fold change lower than -1 or higher than 1 are highlighted in grey. Log₂ (fold change) is calculated using the normalized spectral counts and averaged for the 3 biological replicates. The data were fitted with a Gaussian function showing a normal distribution of the values in our dataset. All proteins are listed in Online Table II and III. **B**, 30 µl of conditioned medium from CFs transfected with pre-miR-29b and anti-miR-29b was separated by SDS-PAGE before validation of known targets by immunoblotting (CO1A2, CO5A2) and gel zymography (MMP-2). The corresponding silver-stained gels are presented below. **C**, The log(fold change) for each of the differentially secreted proteins on overexpression of pre-miR-29b is illustrated. The identified targets predicted by at least one prediction algorithm (TargetScan, PicTar, Diana) are highlighted.

Figure 3: TGFβ1 stimulation. **A**, Attenuation of the CF response to TGFβ1 following transfection with pre-miR-29b. Proteins identified in the conditioned medium of CFs after stimulation with TGFβ1 (10ng/ml) are listed in Online Table IV. The heat map displays only predicted miR-29b targets reaching a p-value (ANOVA) <0.05. **B**, Effect of pre-miR-29b in the presence of TGFβ1. The log(fold change) for each of the differentially secreted proteins on overexpression of pre-miR-29b is illustrated. The identified targets predicted by at least one prediction algorithm (TargetScan, PicTar, Diana) are highlighted.

Figure 4: Confirmation of miR-29b targets. Correlation between the protein concentration of IGF-1 (**A**), LIF (**B**), PTX3 (**C**) in the conditioned medium of CFs transfected by ELISA and by proteomics. The Spearman coefficients of correlations to the ELISA measurements and the normalised spectral counts (SCs) in the miR-29b experiment are given (left panel). Concentration of IGF-1, LIF, PTX3 after overexpression (middle panel) or inhibition (right panel) of miR-29b and miR-30c as measured by ELISA. **D**, Alignment of LIF, IGF-1 and PTX3 3'-UTR mRNA region with the sequence of miR-29b. The vertical bars and bold characters indicate 3' -UTR sequences of the miR-29b binding site of each target gene. **E**, Schematic representation of the antagoniR experiment. Relative expression of miR-29b (**F**) and IGF-1 (**G**) in the heart of antagoniR-treated mice. **H**, IGF-1 concentration in plasma of antagoniR-treated mice. * denotes P<0.05; ** P<0.01; *** P<0.001; “ns” non-significant; “CTL” control.

Figure 5: Functional assay on cardiac myocytes. **A, B** NRVM were plated onto glass-coverslips, pre-coated with conditioned medium of CFs previously transfected with control pre (Con), pre-miR-29b or pre-miR-30c or control anti (Con), anti-miR-29b or anti-miR-30c. Nuclei were labeled with DAPI (blue), cMyBP-C and α-actinin were labeled with specific antibodies (green and red, respectively). For quantitation see Online Figure VI. Representative immunoblots for cardiac α-actinin, cMyBP-C or cTnI. Bar charts reflect quantitative data of 6 independent experiments. **C**, Effect of conditioned medium of CF on cell area of ESC-derived cardiomyocytes. ** denotes P<0.05; ** P<0.01; *** P<0.001; “Con” control.

Figure 6: MiR-29b and cardiac hypertrophy. **A**, MiRNA-expression in models of pathological (TAC) and physiological hypertrophy (Exercise), with their respective controls (n=5-6 per group). **B**, In situ hybridisation for miR-29b demonstrating predominantly nuclear staining in non-myocytes of pressure-overloaded hearts. Size bar indicates 50 µm. **C**, Heatmap of qPCR results of potential miR-29 targets. The proteins above the black line are transcripts that showed a difference in pathological hypertrophy by t-test (p-value < 0.05). The transcripts above the red line are those that remained significant after a Bonferroni correction. There were no significant differences in mRNA expression in physiological hypertrophy.

Figure 7: MiR-29b and target derepression in cardiac hypertrophy. **A**, Knock-down of miR-29 family members following antagomiR-29b treatment in two independent TAC experiments (n=9 per group, mean±SEM, *** P<0.001). **B**, ECM accumulation in Masson's Trichrome Staining. Size bar indicates 50 µm. **C**, Correlation between the efficiency of miR-29b knockdown and derepression of 27 putative miR-29b targets as quantified by qPCR (upper panel). Distribution of correlations between putative miR-29b targets and the efficiency of miR-29 a,b and c knockdown (lower panel).



Circulation Research

ONLINE FIRST

Novelty and Significance

What Is Known?

- MicroRNAs are involved in the pathogenesis of cardiac fibrosis.
- MicroRNA-29b suppresses extracellular matrix production.

What New Information Does This Article Contribute?

- We report proteomics analysis of the proteins secreted (secretome) from cardiac fibroblasts.
- We identify extracellular proteins that are targeted by microRNA-29b and microRNA-30c.

Comprehensive read-outs are required for assessing microRNA (miRNA) targets. We used a proteomics approach to analyze miRNA targets in the secretome of cardiac fibroblasts. We also assessed the effects of two key miRNAs (miR-29b and miR-30c) in cardiac fibroblasts side-by-side. Using this method we uncovered not only previously known direct targets, which are related to fibrosis, but also several new direct and indirect targets of miR-29b and miR-30c. Our data suggest that proteomics methods are more effective for identifying miRNA targets at the protein level than the use of mRNA profiling or bioinformatics prediction algorithms. Changes in individual miRNA targets should be interpreted in the wider context of other protein alterations, including the indirect effects of miRNAs. Studying the role of miRNAs in regulating protein secretion is a promising strategy to explore the importance of miRNAs in cardiovascular biology.

Research

ONLINE FIRST

Figure 1

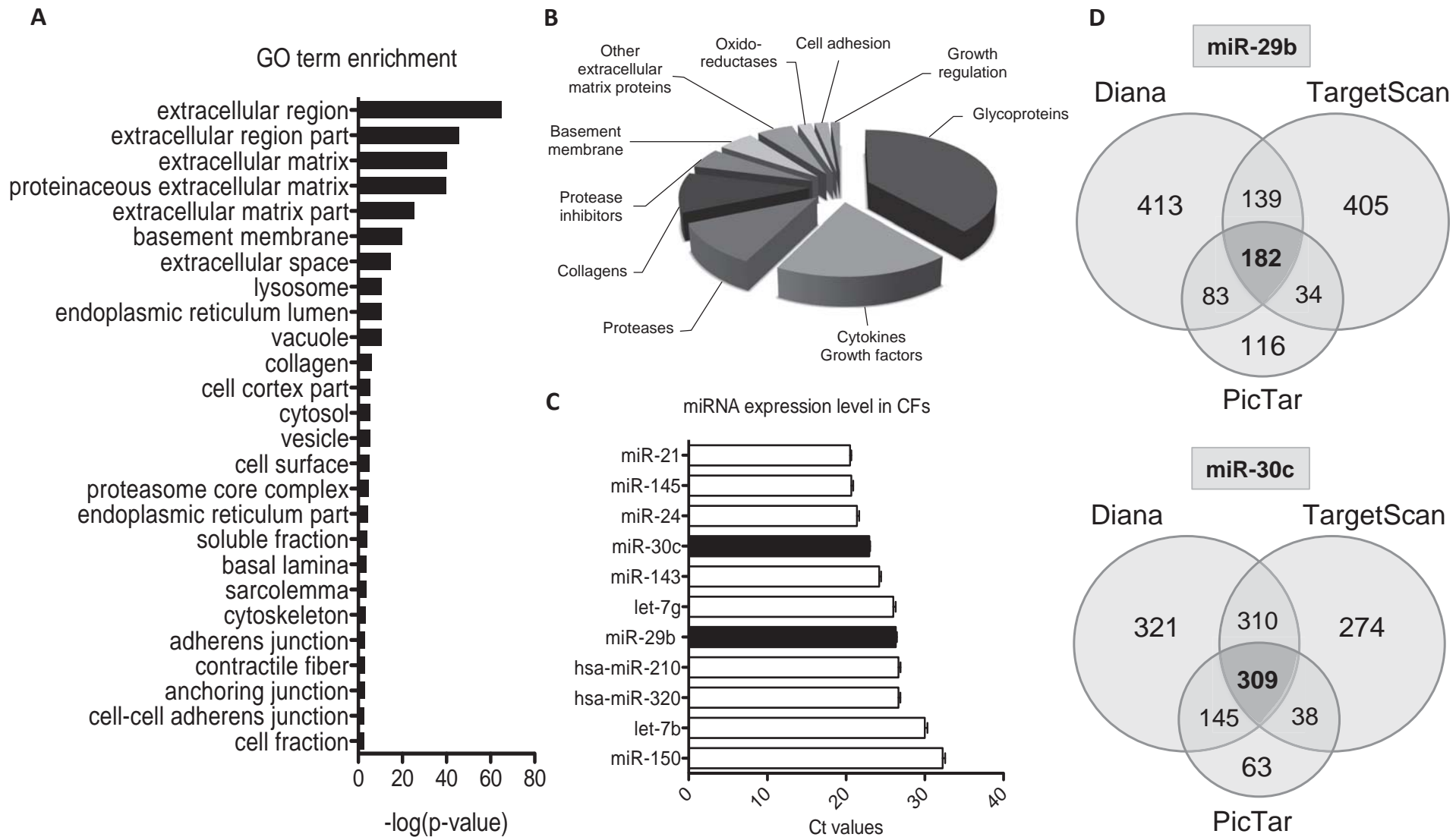


Figure 2

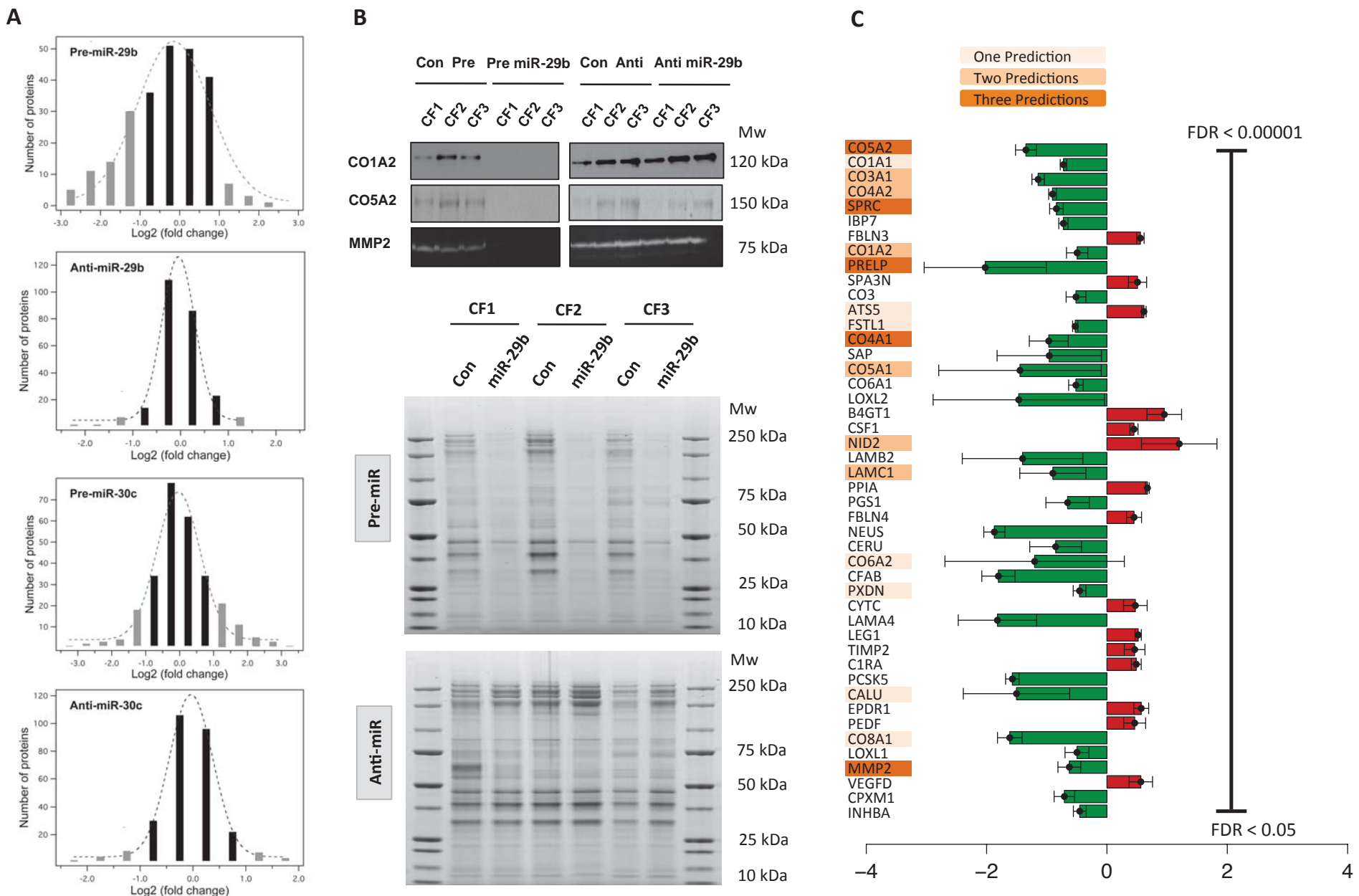


Figure 3

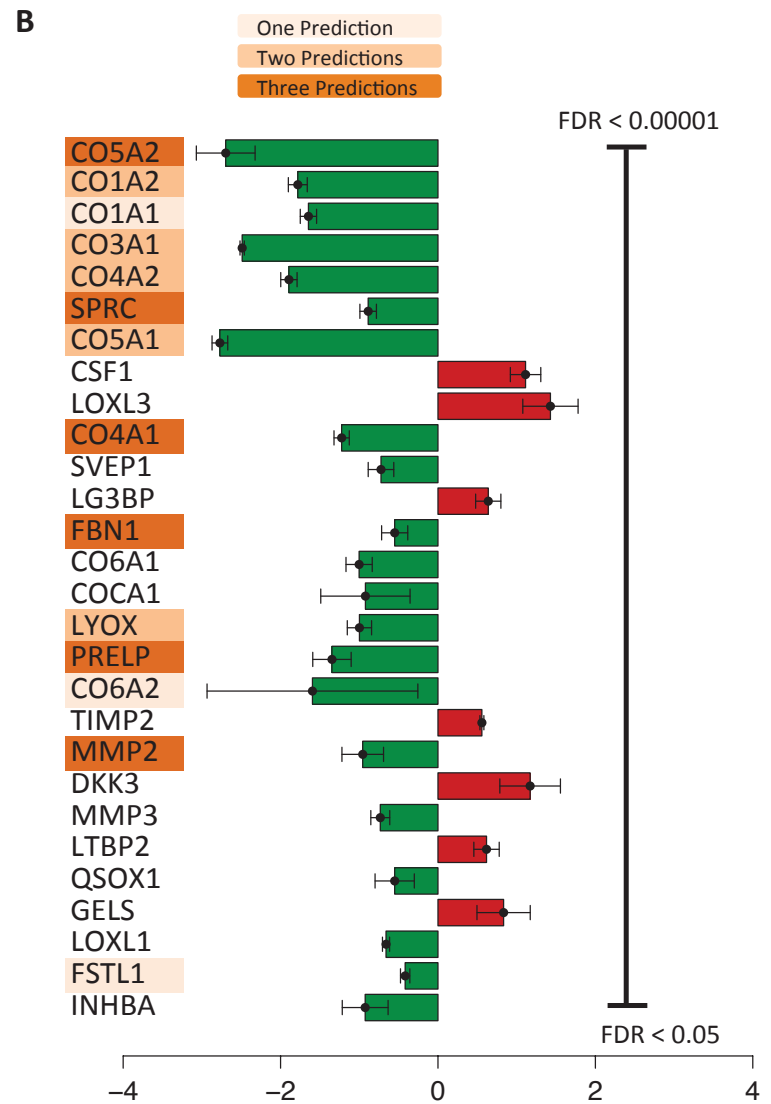
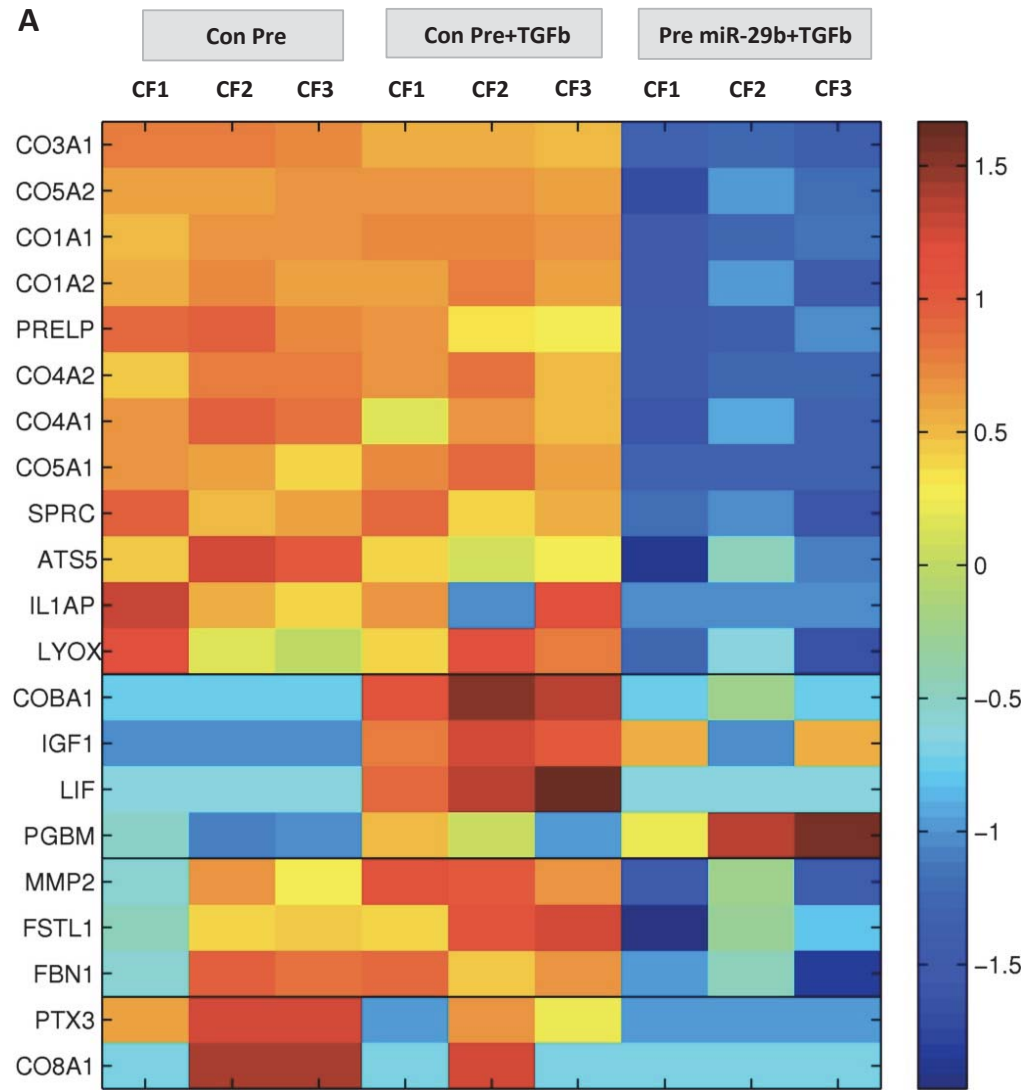


Figure 4

Downloaded from <http://circres.ahajournals.org/> at King's College London on September 18, 2013

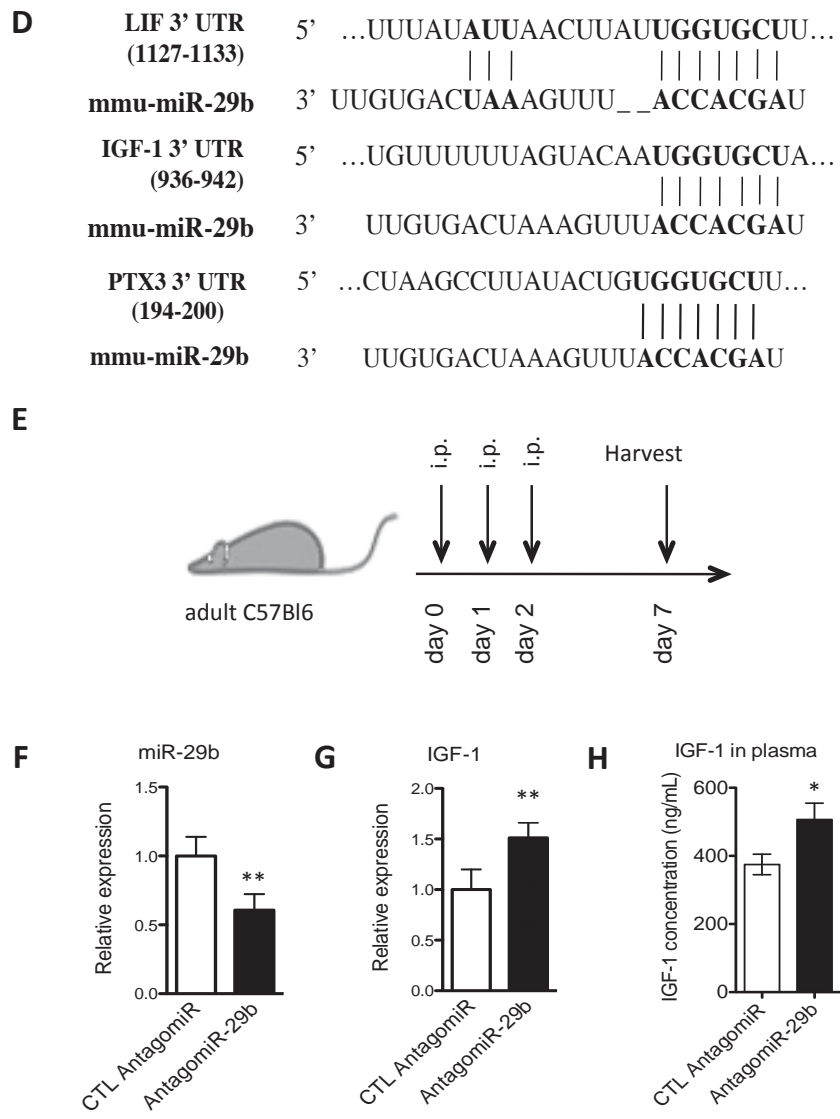
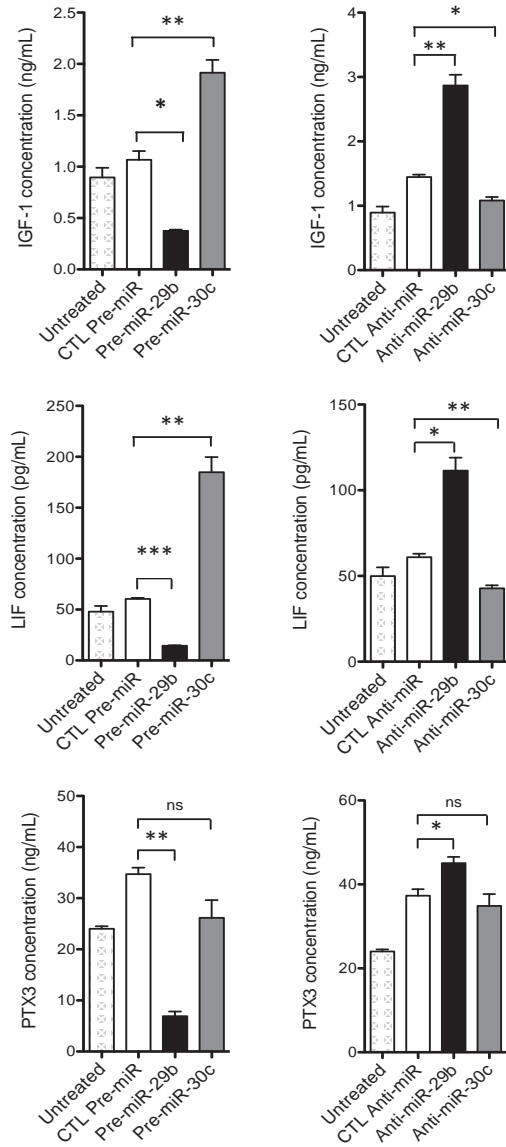
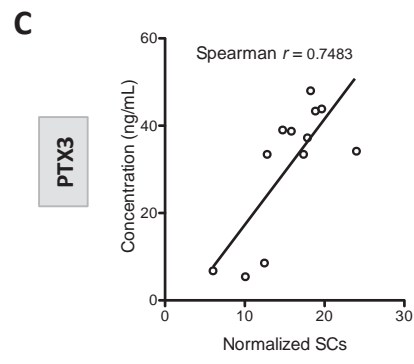
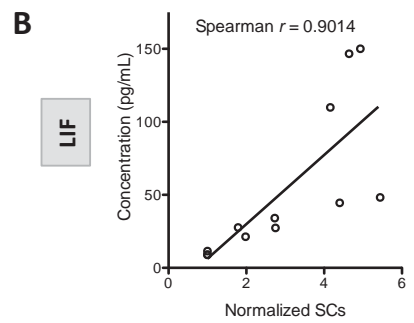
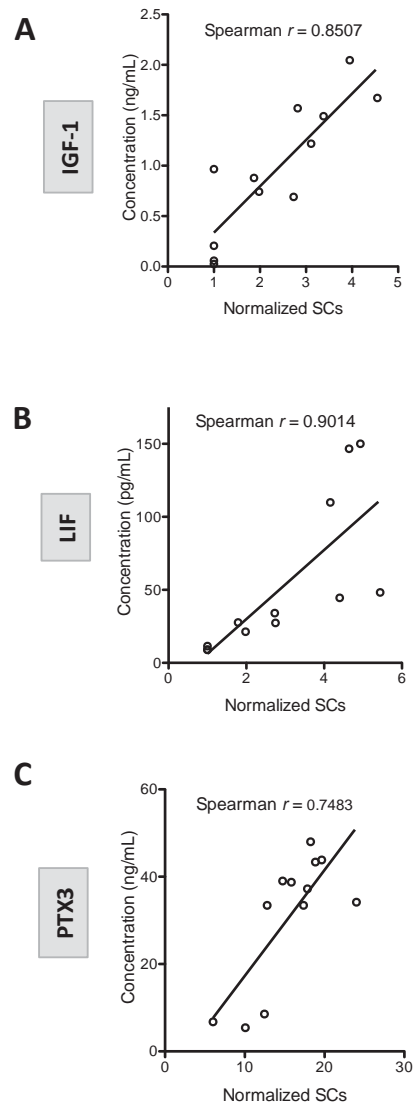


Figure 5

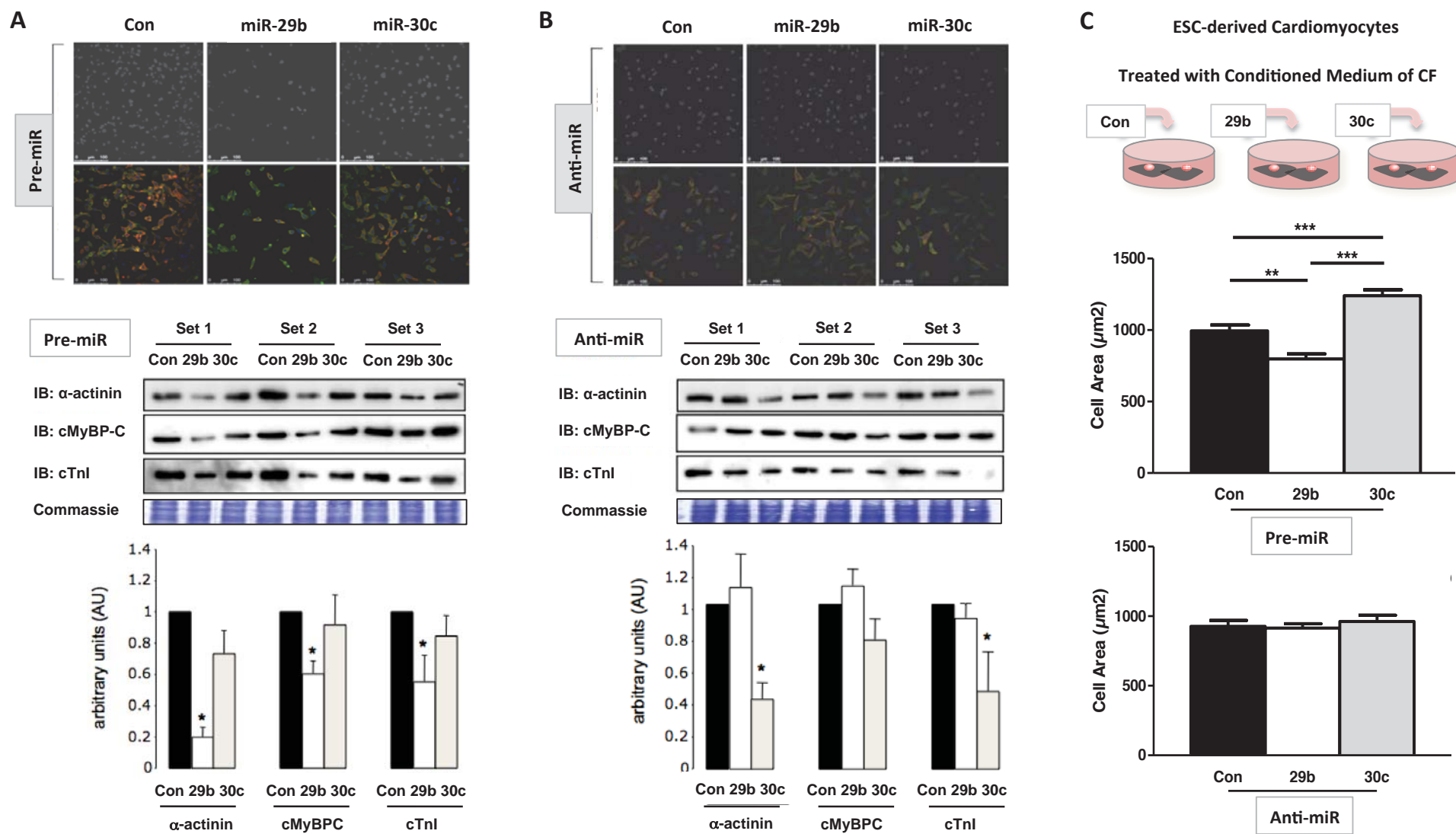


Figure 6

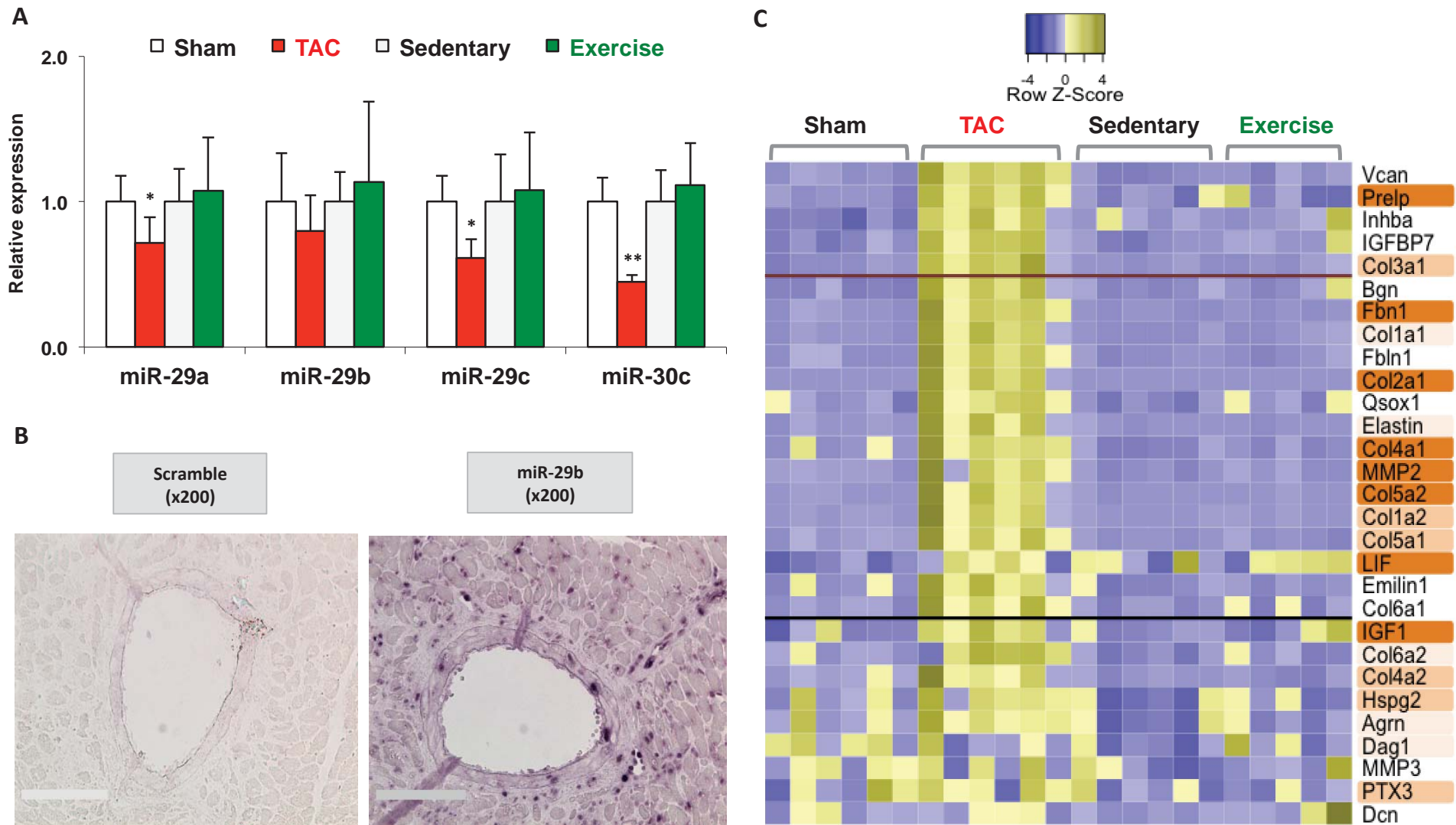
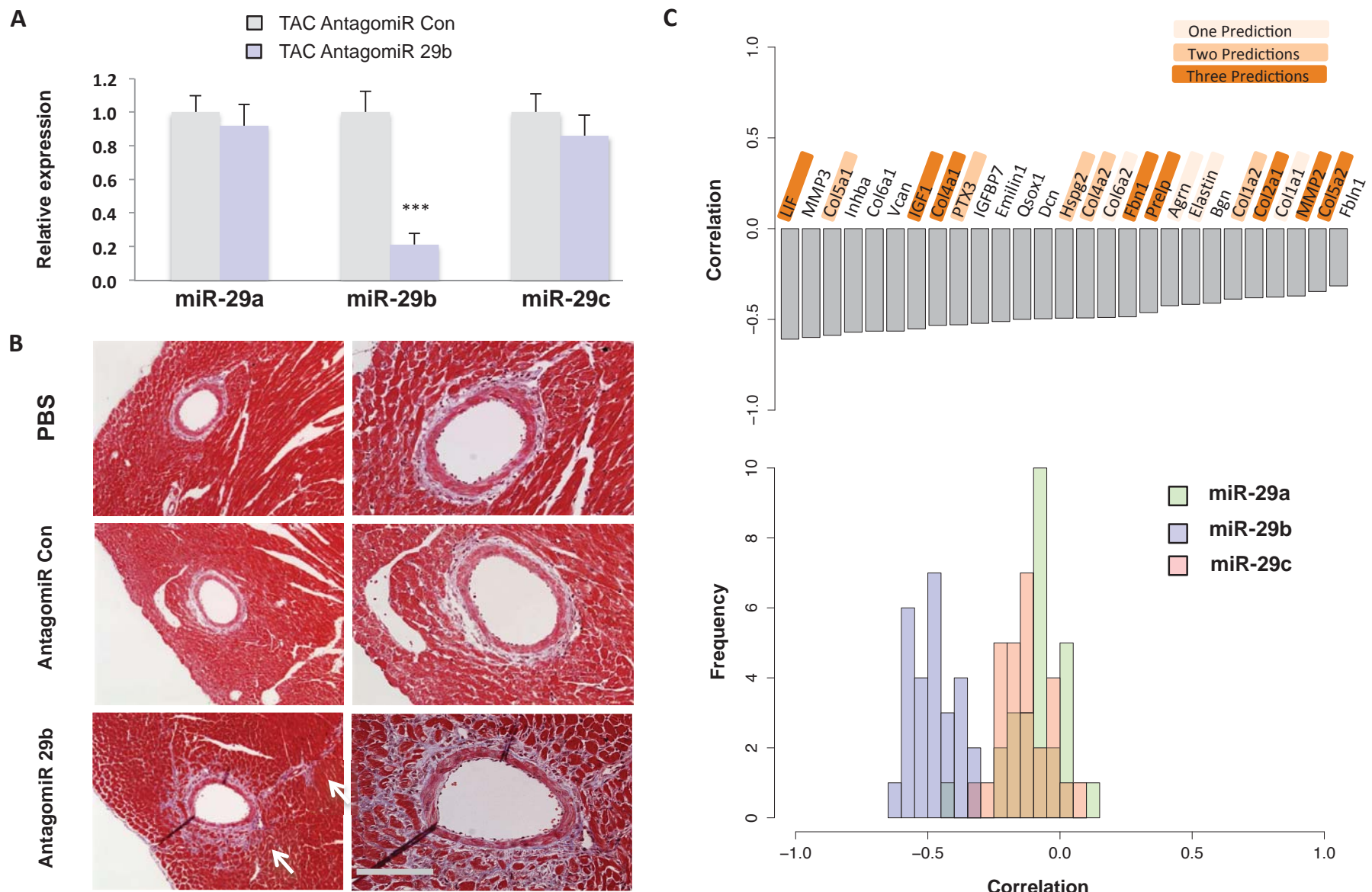


Figure 7



SUPPLEMENTAL MATERIAL

Extracellular Matrix Secretion by Cardiac Fibroblasts: Role of microRNA-29b and microRNA-30

Mélanie Abonnenc*, Adam Nabeebaccus*, Ursula Mayr*, Javier Barallobre-Barreiro*,
Xuebin Dong*, Friederike Cuello*,[§], Sumon Sur[†], Ignat Drozdov*,[#], Sarah R.
Langley*, Ruifang Lu*, Konstantina Stathopoulou*,[§], Athanasios Didangelos*,
Xiaoke Yin*, Wolfram-Hubertus Zimmermann[†], Ajay Shah*,
Anna Zampetaki*, Manuel Mayr*

* King's BHF Centre, King's College London, UK

[§] Department of Experimental Pharmacology and Toxicology, University Medical
Centre Hamburg-Eppendorf, Germany

[#] Centre for Bioinformatics-School of Physical Sciences and Engineering

[†] Institute of Pharmacology, University Medical Center, Georg-August-University and
DZHK (German Center for Cardiovascular Research), partner site Goettingen,
Germany

Running Title: Proteomics for microRNAs in cardiac fibroblasts

Corresponding author:

Prof. Manuel Mayr, King's BHF Centre, King's College London,
125 Coldharbour Lane, London SE5 9NU, UK.

Fax number: +44 (0)20 7848 5296

Tel number: +44 (0)20 7848 5132

E-mail: manuel.mayr@kcl.ac.uk

ONLINE MATERIALS AND METHODS

Isolation of mouse cardiac fibroblasts (CFs). Primary mouse CFs were isolated from the hearts of male C57BL6 mice (5-6 week-old, n=3) by standard collagenase-based digestion and maintained as separate cell lines. Two independent experiments (cardiac fibroblast isolation) were performed. Briefly, the hearts were diced into small pieces, carefully washed in ice-cold phosphate buffered saline (PBS, Sigma-Aldrich) to remove plasma contaminants. The pieces were pre-digested in collagenase II solution for 10 min. The collagenase II solution was replaced and the tissue pieces were incubated for 45 min – 1h at 37°C. The digested tissue pieces were washed in complete medium before plating. Primary mouse CFs were cultured on gelatin 0.1% and grown in DMEM medium supplemented with L-Glutamine, 10% heat-inactivated FBS and antibiotics (100 U/ml penicillin and 100 µg/ml streptomycin) at 37°C in a humidified atmosphere of 95% air / 5% CO₂. Cells were detached with 0.05% trypsin for passaging. After two passages the cell population is mainly composed of cardiac fibroblasts. Immunostaining of vimentin has been carried out at passage 2 indicating that the cell population are predominantly CFs (**Online Figure I**). Cells at passage 2-4 were used in all experiments.

Pre-miR and anti-miR transfection. Cells were plated at 60-70% confluence on the day before transfection. Mouse Pre-miR™ miRNA precursors were synthesized by Applied Biosystems/Ambion and Mercury™ LNA-antimiRs by Exiqon. The following sequences were used: LNA-29b: ACTGATTCAAATGGRGCT; LNA-30c: TGAGAGTGTAGGATGTTAC, LNA-CTL: GTGTAACACGTCTATACGCCCA, Pre-miR-29b: UAGCACCAUUUGAAAUCAGUGUU; Pre-miR-30c: UGUAAACAUCC-UACACUCUCAGC; Pre-miR-CTL2: sequence not specified. LNA inhibitors and precursor miRNA were transfected at a final concentration of 100 nM using lipofectamine™ RMAiMAX (Invitrogen) according to the manufacturer's recommendations.

TGFβ1 stimulation of CFs. The day following the transfection of CFs with the miRNA constructs, the cells were carefully washed in serum-free medium and then, stimulated with TGFβ1 (from Peprotech) at a final concentration of 10 ng/mL in serum-free medium for 72h. After stimulation, the conditioned medium and RNA were harvested for analysis.

Conditioned medium for proteomics analysis. CFs were carefully washed in serum-free medium to maximize the removal of proteins from the serum and then incubated in fresh serum-free medium for 72 hours (“conditioned medium”). The conditioned medium was collected and centrifuged at 3000 g for 10 min to remove cell debris. The supernatant was transferred into a new tube and stored at -80°C. 2 mL of conditioned medium was first desalting using Zeba Spin desalting columns (Thermo Scientific), vacuum dried and resuspended in 60 µL of ddH₂O. 30 µL was used for the proteomic analysis and 30 µL to run a SDS-PAGE gel for immunoblotting.

MicroRNA target prediction. The prediction of mir-29b and miR-30c targets was performed with the following algorithms: Targetscan 5.2 (<http://www.targetscan.org/>), PicTar (<http://pictar.mdc-berlin.de/>) and DIANA MicroT v.4.0 (<http://diana.cs.cslab.ece.ntua.gr/>).

RNA isolation from cells. Total RNA was prepared using the miRNeasy kit (Qiagen) according to the manufacturer's recommendations. In brief, cells were lysed with 700 μ l of QIAzol reagent. Following a brief incubation at ambient temperature, 140 μ l of chloroform were added and the solution was mixed vigorously. The samples were then centrifuged at 12,000 rpm for 15 min at 4°C. The upper aqueous phase was carefully transferred to a new tube and 1.5 volumes of ethanol were added. The samples were then applied directly to columns and washed according to the company's protocol. Total RNA was eluted in 25 μ l of nuclease free H₂O.

MegaPlex reverse transcription and pre-amplification. To assess levels of specific miRNA in cells 20 ng of RNA from the 25 μ l eluate were diluted in a volume of 3 μ l and used as input in each reverse transcription (RT) reaction. A RT reaction and pre-amplification step were set up according to the company's recommendations. Briefly, miRNAs were reverse transcribed using the Megaplex Primer Pools (Rodent Pool A v.2.0) from Applied Biosystems. RT reaction was performed according to the company's recommendations (0.8 μ l of Pooled Primers were combined with 0.2 μ l of 100mmol/L dNTPs with dTTP, 0.8 μ l of 10x Reverse-Transcription Buffer, 0.9 μ l of MgCl₂ (25mmol/L), 1.5 μ l of Multiscribe Reverse-Transcriptase and 0.1 μ l of RNAsin (20U/ μ l) to a final volume of 7.5 μ l. The RT-PCR reaction was set as follows: 16°C for 2 min, 42°C for 1 min and 50°C for 1 sec for 40 cycles and then incubation at 85°C for 5 min using a Veriti thermocycler (Applied Biosystems). The RT reaction products were further amplified using the Megaplex PreAmp Primers (Rodent Pool A v2.0). A 1.25 μ l aliquot of the RT product was combined with 6.25 μ l of Pre-amplification Mastermix (2x) and 1.25 μ l of Megaplex PreAmp Primers (10x) to a final volume of 12.5 μ l. The pre-amplification reaction was performed by heating the samples at 95°C for 10 min, followed by 12 cycles of 95°C for 15 sec and 60°C for 4 min. Finally, samples were heated at 95°C for 10 min to ensure enzyme inactivation. Pre-amplification reaction products were diluted to a final volume of 50 μ l. RT-PCR and pre-amplification products were stored at -20°C.

Taqman qPCR assay. Taqman miRNA assays were used to assess the expression of individual miRNA. 0.5 μ l of pre-amplification product were combined with 0.25 μ l of Taqman miRNA Assay (20X) (Applied Biosystems) and 2.5 μ l of the Taqman Universal PCR Master Mix No AmpErase UNG (2X) to a final volume of 5 μ l. QPCR was performed on an Applied Biosystems 7900HT thermocycler at 95°C for 10 min, followed by 40 cycles of 95°C for 15 sec and 60°C for 1 min. All samples were run in duplicates and standardize to U6/sno-135/sno-202 using SDS2.2 software (Applied Biosystems).

Immunoblot analysis of CF proteins: Samples were mixed with 4X denaturing sample buffer, heated at 95°C for 10 min and separated on a Bis-Tris discontinuous 4-12% polyacrylamided gradient gels (NuPage, Invitrogen). Proteins were then transferred on nitrocellulose membranes. Membranes were blocked with 5% fat-free milk powder in PBS-Tween and probed for 16h at 4°C with primary antibodies to: CO1A2 (rabbit, Abcam ab96723), CO5A2 (mouse, Santa Cruz, sc-59903). All antibodies were used at 1:500 dilution in 5% BSA. The membranes were treated with the appropriate secondary, horseradish peroxidase (HRP) conjugated antibodies (Dako) at 1:2000 dilution. Finally, the blots were imaged using enhanced chemilluminescence (ECL, GE Healthcare) and films were developed on a Xograph

processor. The densitometry for the lanes from developed films was measured using the ImageJ software (v.1.44o, <http://imagej.nih.gov/ij> NIH, USA).

Gelatin zymography. Samples were mixed with non-reducing Tris-Glycine SDS sample buffer (2X) and applied without boiling to a Novex® 10% zymogram (gelatin, Life Technologies) gel. After electrophoresis, the gel was developed at 37°C overnight according to the manufacturer's recommendations. The gel was stained with Coomassie staining.

Enzyme-linked immunosorbent assay (ELISA). IGF-1, LIF and PTX-3 in the conditioned medium of CFs were quantified by ELISAs from R&D Systems.

Luciferase reporter assays. The 3' untranslated regions of mouse IGF-1, LIF and PTX3 harboring putative binding sites of the miR-29 family were cloned into the dual-luciferase reporter vector psiCheck2 (Promega). The following primer sets were used for this study:

Igf1 forward 'AGAGAGTTAACACACCTCTCCCACGTAGCTCA'
Igf1 reverse 'TATTCTCGAGGACTGAGGTCACAGGGTGGT'

LIF forward 'AGAGAGTTAAACTAGGAGTCAGGGAAGGAGCA'
LIF reverse 'TATTCTCGAGGCCAGCTCTGATTGACC'

PTX3 forward 'CGAGAGTTAAACTGAAGGGAAGGCTTGAGAGA'
PTX3 reverse 'TATTCTCGAGCGTCCCTGTTCAGAGTCC'

The reporter vectors (100 ng of psiCheck2 construct) were transfected together with 30-100 nM of miR-29b mimic or the mimic negative control (CON) in triplicate into SMCs plated in 6-well plates using Lipofectamine 2000 (Lifetech) as described above. After 48 h, the Renilla and firefly luciferase activities were assessed after harvesting cells in 200 µL Glo Lysis Buffer (Promega). 30 µL of each lysate were analyzed using Dual-Glo Luciferase reagents (Promega). Renilla 3'UTR-coupled luciferase activity was normalized to constitutive firefly luciferase activity for each well.

Gel-LC-MS/MS. Samples were denatured with 4X sample loading buffer at 96°C for 5 min and then separated in Bis-Tris discontinuous 4-12% polyacrylamide gradient gels (NuPage, Invitrogen). Protein standards were run along side the samples (pre-stained All Blue, Precision Plus, BioRad Laboratories). After electrophoresis, the gels were stained using Coomassie staining. Each gel lane was cut into 16 bands. Subsequently, all gel bands were subjected to in-gel tryptic digestion using an Investigator ProGest (Digilab) robotic digestion system. Tryptic peptides were separated on a nanoflow LC system (Dionex UltiMate 3000, UK) and eluted with a 70-min gradient (4-25% B in 35 min, 25-40% B in 5 min, 100% B in 10 min and 2% B in 20min where A is 2% ACN, 0.1% formic acid in HPLC H₂O and B is 90% ACN, 0.1% formic acid in HPLC H₂O). The column (Dionex PepMap C18, 25 cm length, 75µm i.d, 3 µm particle size) was coupled to a nanospray source (Picoview). Spectra were collected from a high-mass accuracy analyzer (LTQ Orbitrap XL, ThermoFisher Scientific) using full ion scan mode over the mass-to-charge (*m/z*) range 450-1600. MS/MS was performed on the top six ions in each MS scan using the data-

dependent acquisition mode with dynamic exclusion enabled. MS/MS mass spectra were extracted by extract_msn.exe version 5.0. Charge state deconvolution and deisotoping were not performed. All MS/MS samples were analyzed using Mascot (Matrix Science, London, UK; version 2.3). Mascot was set up to search the SwissProt_57.15 database (selected for *Mus musculus*, 16230 entries) assuming the digestion enzyme trypsin. Two missed cleavages were allowed. Mascot was searched with a fragment ion mass tolerance of 0.80 Da and a parent ion tolerance of 10.0 ppm. Iodoacetamide derivative of cysteine was specified in Mascot as a fixed modification. Oxidation of methionine was specified in Mascot as a variable modification. Scaffold (version Scaffold_3_00_08, Proteome Software Inc., Portland, OR) was used to validate MS/MS based peptide and protein identifications. Peptide identifications were accepted if they could be established at greater than 95.0% probability as specified by the Peptide Prophet algorithm.¹ Protein identifications were accepted if they could be established at greater than 99.0% probability and contained at least 2 independent peptides. Protein probabilities were assigned by the Protein Prophet algorithm.² Proteins that contained similar peptides and could not be differentiated based on MS/MS analysis alone were grouped to satisfy the principles of parsimony.

Isolation and culture of neonatal rat ventricular myocytes (NRVM). Primary cultures of NRVM were prepared from neonatal (day 0-2) Sprague-Dawley rats, as described previously³. In brief, hearts were excised, the atria trimmed off and the ventricles cut into small pieces. Cardiac myocytes were dispersed by a series of incubations at 37°C in Ca²⁺-free HEPES-buffered solution containing (in mmol/L) NaCl 120, HEPES 20, NaH₂PO₄ 0.8, glucose 5, KCl 5, MgSO₄ 0.4, pancreatin (0.6 mg/mL) and 0.5 mg/mL type II collagenase (Worthington Biochemicals). The dispersed cells were pre-plated for 1 hour to reduce fibroblast contamination. Unattached NRVM were then seeded in 24-well plates or on glass coverslips, which were pre-coated overnight at 37°C with conditioned medium of CFs, previously transfected with control pre, 29b or 30c pre-miR or control anti, 29b or 30c anti-miR at a final density of 200 000 cells/well or coverslip in DMEM/M199 4:1 (v/v) supplemented with 10 % horse serum, 5 % fetal calf serum and 100 IU/mL penicillin/streptomycin. After 24 hours in culture, unattached NRVM were washed off and cells were transferred to maintenance medium (DMEM/M199 4:1 (v/v), 100 IU/mL penicillin/streptomycin) for 24 hours, before harvesting cells from 24-well plates in Laemmli sample buffer for western immunoblot analysis or fixing cells from glass coverslips for immunocytochemistry and confocal microscopy.

Immunoblot analysis of NRVM proteins. Immunoblot analysis was carried out as described previously³. In brief, NRVM protein samples were resolved by 10 % SDS-PAGE, transferred to polyvinylidene difluoride membranes and subjected to immunoblotting. Primary antibody was detected by sheep anti-mouse secondary antibody linked to HRP (GE Healthcare). Specific protein bands were detected by enhanced chemiluminescence.

Immunolabelling of cardiac myocytes. NRVM were washed twice with PBS and fixed by incubation in 4% paraformaldehyde (PFA) in PBS for 10 min and washed twice with PBS. Cells were permeabilised by incubation in 0.2% Triton X-100 in PBS for 5 min and unspecific binding sites blocked by incubation in 5 % non-specific goat serum in 1 % BSA/TBS pH 7.5 containing (in mmol/L) Trizma base 20, NaCl 155,

EGTA 2, MgCl₂ 2 for 20 min. Primary and secondary antibodies were diluted using 1 % BSA/TBS. Incubation with primary antibodies was carried out overnight at 4°C, incubation with secondary antibodies was carried out at room-temperature for 4 hours. After final washing with PBS, the cardiac myocytes were mounted with coverslips in 0.1M Tris-HCl (pH 9.5)-glycerol (3:7) including 50 mg/mL *n*-propyl gallate as an anti-fading reagent (Messerli et al. 1993).

Antibodies and fluorescent reagents. The monoclonal mouse anti cardiac α -actinin antibody was obtained from Sigma and was used at a dilution of 1:1000 for western immunoblotting and 1:100 for immunocytochemistry. The polyclonal rabbit antibody to cardiac myosin-binding protein C was a kind gift from Prof. Mathias Gautel, King's College London and was used at a dilution of 1:50 for immunocytochemistry and 1:30000 for western immunoblotting. The polyclonal rabbit antibody to cardiac troponin I was obtained from Cell Signaling Technology and was used at a dilution of 1:1000. For double immunofluorescence labeling, a combination of Cy3 anti-mouse (1:500) and Cy5 anti-rabbit (1:100) conjugated secondary antibodies was used. The secondary antibodies were purchased from Jackson ImmunoResearch. 4',6-Diamidino-2-phenylindole dihydrochloride (DAPI 1 mg/ml 1:100) was purchased from Sigma.

Confocal microscopy. The specimens were analyzed using confocal microscopy on an inverted microscope (Leica SP5 system, Mannheim, Germany) equipped with blue diode, argon and helium neon lasers, using a 63x/1.4NA oil immersion lens.

Modification and culture of murine embryonic stem cells. The murine cardiomyocyte-selectable embryonic stem cell (ESC) line (α MHC-neoR "A6-line"; R1 background ⁴) was generated by electroporation of a plasmid encoding for a neomycin resistance gene (neoR), under the control of the cardiomyocyte restricted α -myosin heavy chain (α MHC) promotor, as described previously⁵. α MHC ESCs were cultured on irradiated murine embryonic fibroblasts (MEFs; 25,500 cells/cm²) in ESC culture medium consisting of: DMEM (high glucose, no pyruvate, 25 mmol/l HEPES), 15% fetal bovine serum (FBS), 1000 U/ml LIF, 2 mmol/l glutamine, 1x non-essential amino acids, 1 mmol/l Na-pyruvate, 30 μ mol/l adenosine, 30 μ mol/l cytidine, 30 μ mol/l uridine, 30 μ mol/l guanosine, 30 μ mol/l thymidine, 50 U/ml penicillin, 50 μ g/ml streptomycin, and 100 μ mol/l 2-mercaptoethanol. ES-colonies were detached every 48 hrs in 0.25% trypsin-EDTA and split at a 1:5 ratio.

Differentiation of α MHC-NeoR ESCs. ESCs were washed in phosphate buffered saline (PBS) and separated into single cells in 0.25% trypsin-EDTA. Cells were resuspended in differentiation medium consisting of: Iscove medium supplemented with 20% FBS, 2mmol/l glutamine, 1x non-essential amino acids, 50 U/ml penicillin, 50 μ g/ml streptomycin, 100 μ mol/l 2-mercaptoethanol and 0.5 mM L-ascorbic acid 2-phosphate. Spinner flasks equipped with a bulb-shaped glass stirrer (Techne) were inoculated with 50 ml of medium containing 10x10⁶ cells and stirred at 60 rpm, at 37°C in a 5% CO₂ incubator. Flasks were filled up to 100ml after 24 hrs, followed by half medium exchange every 48 hrs. Cardiomyocyte (CM) selection at day 11 was initiated by the addition of 400 μ g/ml Geneticin (G418) to eliminate non-cardiomyocytes. At day 16, CMs were harvested and dissociated into single cells with collagenase 1 for 1 hr and with 0.25% trypsin-EDTA for 3-6mins. Cells were subsequently resuspended in differentiation medium.

Treatment of ESC-derived CM with conditioned medium from transfected CF.

Purified ESC-derived CMs were cultured (8000 cells/well) for 6 days on a flat-bottom 96-well plate, coated with gelatine (0.1%). Cells were initially cultured for 24 hrs in differentiation medium, followed by 5 days with the following 50% conditioned media (Pre-miR (Control; 29b; 30c); Anti-miR (Control; 29b; 30c)) supplemented with 50% differentiation medium, with medium. Culture medium was exchanged changed after 48 hrs. Cells were thereafter fixed in 4% buffered formaldehyde at room temperature for 15 mins, and then subsequently washed in PBS (x2) prior to immunostaining. Fixed cells were blocked and permeabilized for 90 mins at room temperature in PBS (pH.7.4) containing 5% FBS, 1% bovine serum albumin (BSA) and 0.5% Triton X-100. Subsequent incubation with a mouse monoclonal α -actinin primary antibody (IgG1; clone: EA-53; 1:1,000 from 1 mg/ml stock; Sigma) was for 60 mins at room temperature, followed by a goat anti-mouse Alexa 488 secondary antibody (1:400 from 1 mg/ml stock; Invitrogen) and 4',6-diamidino-2-phenylindole (DAPI; 1 μ g/ml; Invitrogen) for 60 mins in the dark at room temperature. Cells were subsequently washed in buffer (x2) after each incubation step and thereafter stored in PBS. Imaging was performed with a Zeiss Axiovert 200 inverted fluorescence microscope equipped with a shutter (Visitron System; MAC 6000) and a AxioCam MRm camera (Zeiss). Image J software (National Institutes of Health) was used to determine cell area from images. Cell area was determined by measuring the α -actinin fluorescence staining of the cells. Cell clumps with >5 DAPI stained nuclei were excluded from the analysis. Data are presented as mean +/- SEM. Statistical analysis was performed using 1-way ANOVA followed by Bonferroni's multiple comparison test. A value of P<0.05 was considered statistically significant.

Animal models. Procedures were performed in accordance with the Guidance on the Operation of the Animals (Scientific Procedures) Act, 1986 (United Kingdom). Pathological cardiac hypertrophy was induced by the minimally invasive transverse aortic constriction (TAC), as previously described⁶. C57BL/6 mice 8-10 weeks of age were used. Sham constriction involved identical surgery apart from band placement. Physiological cardiac hypertrophy was achieved by a voluntary wheel running program⁷. Briefly, 8-10 weeks old C57BL/6 mice were initially introduced together into the running cage to learn from each other to run on the wheel. After a 7 day training period, mice were randomly housed individually and left to run up to 4 weeks. The running wheel is connected by a light triggered counting system, running time and distance is monitored and recorded with LabChart7. The average running distance was over 4km/day. Age-matched mice were also randomly assigned to the sedentary control group. They were housed in identical cages except for a non-rotating wheel for the same amount of time. 2 weeks TAC and 4 weeks exercise running resulted in 65% and 14% increase compared to controls in terms of heart weight/tibia length ratio, respectively.

In vivo silencing of miR-29b. AntagomiR constructs from Fidelity Biosystems were resuspended in sterile PBS at 37°C and stored at -20°C. The sequences of the antagomiR constructs were: Control Antagomir: 5'-A*A*GGCAAGCUGACCCUGAA*G*U*U* Chol*T-3', AntagomiR-29b: A*A*CACUGAUUUCAAAUGGUG*C*U*A*-Chol*T-3'. C57BL6 mice were treated by intraperitoneal injection with a dose of 80 mg/kg/day of antagomiR constructs at day 0, day 1 and day 2. Non-operated mice were sacrificed at day 7 and the plasma and

cardiac tissues were collected. For the *in vivo* model of pathological hypertrophy, pressure overload was induced at day 3 by aortic constriction in wild-type mice anesthetized with an isoflurane/O₂ mixture (2/98%). Sham surgery (n = 4) comprised an identical procedure with the exception of constriction. Cardiac tissues were obtained at 2 weeks post-surgery. Only left ventricles were used for further analysis. RNA was extracted using the RNeasy kit (Qiagen) with cDNA produced using the High Capacity Reverse transcriptase kit (Applied Biosystems). Transcript expression was quantified using TaqMan mRNA probes (Applied Biosystems).

Transthoracic echocardiography. The method for *in vivo* echocardiography was taken from Bauer *et al.*⁸ Studies were performed with a Vevo 2100 Imaging System (VisualSonics, Toronto, Canada) using a 22-55 MHz ultra-high frequency linear-array transducer. Mice were maintained under light anaesthesia with 1% isoflurane and 2L/min oxygen flow. Mice were fixed to a heated platform with simultaneous recording of heart rate and respiratory rate. Heart rate was maintained at >500 bpm (as described in Bauer *et al*⁸). Images were obtained in both parasternal long axis and short axis views. A B-mode image in parasternal long axis view was captured (to view both the apex and left ventricular outflow tract). In addition an M-mode of the widest part of the parasternal long axis B-mode image was taken (the midpoint between apex and base of the heart). The short axis images were obtained by a 90-degree rotation of the transducer from its long axis orientation. A B-mode image was acquired at the mid-papillary muscle level. An M-mode was also taken at this level. Conventional echocardiographic measurements were obtained from M-mode images acquired in the parasternal long axis and short axis views as described above. Measurements included left ventricular end-systolic and end-diastolic diameters and volumes, ejection fraction, fractional shortening, stroke volume and cardiac output. Short axis B-mode images taken at the papillary muscle level were used to measure interventricular septal (IVS) and left ventricular posterior wall (LVPW) thicknesses in both systole and diastole (IVS;s, IVS;d and LVPW;s, LVPW;d respectively). Measurements were taken from 3 separate cardiac cycles and then averaged (as described in Bauer *et al*⁸). Data are presented as group mean +/- SE. Group parameters (control versus antagomiR treated after TAC) were analysed with an unpaired Student's t-test. Long axis B-mode images could not be included in the analyses in view of the abnormal papillary muscle thickening leading to inaccurate values for echocardiographic parameters.

In situ hybridization. MiRNA *in situ* hybridisation was performed as described previously⁹. Fixed paraffin-embedded 4 µm mouse heart sections were used. After deparaffinization and proteinase K (Sigma) treatment, the sections were fixed with 4% paraformaldehyde for 10 min. Then, the slides were incubated with hybridisation buffer at 60 degree for 1h, and hybridised with 40nM DIG-labelled miR-29b or scramble probe (Exiqon) overnight. The next day, slides were incubated with anti-DIG_AP Fab fragments (Roche) in blocking buffer at the cold room overnight, and washed with PBS plus 0.1%Tween 20 and 0.1M Tris-HCL (pH9.5). MiR-29b was visualized with BM purple solution (Roche) for 1-2 days at room temperature until the staining was developed.

Statistics. Statistical analysis was performed with Graphpad Prism 5 using the Student's *t* test. A *p* value of <0.05 was considered significant. Correlations were analyzed using the Spearman method. Data are presented as mean and error bars

depict the standard deviation. Igor Pro v.6 (WaveMetrics) was used for graphics. For the generation of heatmaps, protein spectral counts were log-transformed to increase the signal of proteins with low spectral counts with respect to the “highly abundant” proteins¹⁰. Subsequently, proteins were excluded if normalized spectra counts did not exceed 5 in at least 5 samples. Overall, 51 (>30%) were retained for analysis. Co-expressions between all pairs of normalized protein spectra counts across primary cell culture and treated CFs were expressed through Pearson correlation coefficients (PCCs). Partial Correlation and an Information Theory (PCIT) algorithm was used to detect meaningful protein–protein associations from a co-expression matrix^{11, 12}. We used the Qspec software proposed by Choi *et al.*¹³ as a second measure to detect differential expression across the TGF-beta stimulated proteomics data. Qspec utilises a hierarchical Bayes estimation of generalized linear mixed effects model (GLMM) to share information across the protein levels. This eliminates some of the assumptions needed for standard statistical tests and can increase the power of the analysis when there are a limited number of replicates available. The false discovery rate (FDR) is calculated with mixture model-based method of local FDR control based upon the Bayes factors. We considered proteins with a Bayes Factor <10 and an FDR < 5%, including those with fold changes above 30%, to be significant.

ONLINE REFERENCES

1. Keller A, Nesvizhskii AI, Kolker E, Aebersold R. Empirical statistical model to estimate the accuracy of peptide identifications made by ms/ms and database search. *Anal Chem.* 2002;74:5383-5392
2. Nesvizhskii AI, Keller A, Kolker E, Aebersold R. A statistical model for identifying proteins by tandem mass spectrometry. *Anal Chem.* 2003;75:4646-4658
3. Cuello F, Bardswell SC, Haworth RS, Yin X, Lutz S, Wieland T, Mayr M, Kentish JC, Avkiran M. Protein kinase d selectively targets cardiac troponin i and regulates myofilament ca²⁺ sensitivity in ventricular myocytes. *Circ Res.* 2007;100:864-873
4. Nagy A, Rossant J, Nagy R, Abramow-Newerly W, Roder JC. Derivation of completely cell culture-derived mice from early-passage embryonic stem cells. *Proc Natl Acad Sci U S A.* 1993;90:8424-8428
5. Klug MG, Soonpaa MH, Koh GY, Field LJ. Genetically selected cardiomyocytes from differentiating embryonic stem cells form stable intracardiac grafts. *J Clin Invest.* 1996;98:216-224
6. Hu P, Zhang D, Swenson L, Chakrabarti G, Abel ED, Litwin SE. Minimally invasive aortic banding in mice: Effects of altered cardiomyocyte insulin signaling during pressure overload. *Am J Physiol Heart Circ Physiol.* 2003;285:H1261-1269
7. De Bono JP, Adlam D, Paterson DJ, Channon KM. Novel quantitative phenotypes of exercise training in mouse models. *American journal of physiology. Regulatory, integrative and comparative physiology.* 2006;290:R926-934
8. Bauer M, Cheng S, Jain M, Ngoy S, Theodoropoulos C, Trujillo A, Lin FC, Liao R. Echocardiographic speckle-tracking based strain imaging for rapid cardiovascular phenotyping in mice. *Circ Res.* 2011;108:908-916
9. Caruso P, Dempsie Y, Stevens HC, McDonald RA, Long L, Lu R, White K, Mair KM, McClure JD, Southwood M, Upton P, Xin M, van Rooij E, Olson EN, Morrell NW, MacLean MR, Baker AH. A role for mir-145 in pulmonary arterial hypertension: Evidence from mouse models and patient samples. *Circ Res.* 2012;111:290-300
10. Carvalho PC, Hewel J, Barbosa VC, Yates JR, 3rd. Identifying differences in protein expression levels by spectral counting and feature selection. *Genet Mol Res.* 2008;7:342-356
11. Reverter A, Chan EK. Combining partial correlation and an information theory approach to the reversed engineering of gene co-expression networks. *Bioinformatics.* 2008;24:2491-2497
12. Watson-Haigh NS, Kadarmideen HN, Reverter A. Pcit: An r package for weighted gene co-expression networks based on partial correlation and information theory approaches. *Bioinformatics.* 2010;26:411-413
13. Choi H, Fermin D, Nesvizhskii AI. Significance analysis of spectral count data in label-free shotgun proteomics. *Mol Cell Proteomics.* 2008;7:2373-2385

Online Table I: List of extracellular proteins identified in the secretome of mouse CFs. The secretome was prepared as described followed by a gel LC-MS/MS analysis using a LTQ-Orbitrap XL. Only the control samples are considered to characterize the proteins present in the secretome of CFs. 6 controls are used in each experiment (Exp.1 and Exp.2). The maximal value of the controls is shown in the Table.

Online Table II: List of extracellular protein changes in the secretome of CFs following overexpression or inhibition of miR-29b. The normalized spectral counts are averaged for the 3 biological replicated to calculate the ratio in protein expression. A paired t-test was used to evaluate the significance of the observed protein expression changes.

Online Table III: List of extracellular protein changes in the secretome of CFs following overexpression or inhibition of miR-30c. The normalized spectral counts are averaged for the 3 biological replicated to calculate the ratio in protein expression. A paired t-test was used to evaluate the significance of the observed protein expression changes.

Online Table IV: List of extracellular protein changes in the secretome of CFs following overexpression of miR-29b in the presence of TGF-beta. The normalized spectral counts are averaged for the 3 biological replicated to calculate the ratio in protein expression. An ANOVA test was used to evaluate the significance of the observed protein expression changes.

Online Table V: Echocardiography data of antagomiR-29b treated hearts after TAC. The analysis (n=9 per group) is based on two independent experiments.

Online-Table I: Extracellular proteins in the secretome of CFs

| # | Protein name | Accession Number | Molecular Weight (kDa) | Exp. 1 | | | | Exp.2 | | | | Cited in Ref |
|---|--------------|------------------|------------------------|----------------------|-------------------|------------|---------------------------------|----------------------|-------------------|------------|---------------------------------|--------------|
| | | | | Distinct peptides, n | Unique spectra, n | % coverage | Number of total ass. Spectra, n | Distinct peptides, n | Unique spectra, n | % coverage | Number of total ass. Spectra, n | |
| Cytokines & growth factors | | | | | | | | | | | | |
| 394 Brain-derived neurotrophic factor | BDNF_MOUSE | 28 | 2 | 2 | 12% | 4 | - | - | - | - | - | - |
| 101 Bone morphogenetic protein 1 | BMP1_MOUSE | 112 | 18 | 20 | 20% | 72 | 8 | 8 | 9% | - | 24 | |
| 533 Bone morphogenetic protein 6 | BMP6_MOUSE | 56 | 2 | 2 | 5% | 3 | - | - | - | - | - | |
| 218 BMP-binding endothelial regulator protein | BMPER_MOUSE | 76 | 3 | 3 | 6% | 11 | - | - | - | - | - | |
| 570 C-C motif chemokine 2 | CCL2_MOUSE | 16 | 2 | 2 | 6% | 2 | - | - | - | - | - | [a][g] |
| 133 Cytokine receptor-like factor 1 | CRLF1_MOUSE | 47 | 4 | 4 | 11% | 17 | 5 | 5 | 14% | - | 11 | |
| 24 Macrophage colony-stimulating factor 1 | CSF1_MOUSE | 61 | 6 | 10 | 15% | 57 | 6 | 9 | 15% | - | 49 | |
| 67 Connective tissue growth factor | CTGF_MOUSE | 38 | 12 | 12 | 32% | 46 | 9 | 9 | 24% | - | 24 | |
| 46 EGF-containing fibulin-like extracellular matrix protein 1 | FBLN3_MOUSE | 55 | 21 | 28 | 54% | 140 | 12 | 14 | 33% | - | 44 | |
| 58 EGF-containing fibulin-like extracellular matrix protein 2 | FBLN4_MOUSE | 49 | 13 | 17 | 33% | 46 | 8 | 11 | 25% | - | 41 | |
| 510 Growth-regulated alpha protein | GROA_MOUSE | 10 | 3 | 3 | 46% | 4 | - | - | - | - | - | |
| 55 Insulin-like growth factor-binding protein 2 | IGBP2_MOUSE | 33 | 9 | 11 | 45% | 51 | 5 | 7 | 26% | - | 26 | [a][b] |
| 399 Insulin-like growth factor-binding protein 3 | IGBP3_MOUSE | 32 | - | - | - | - | 2 | 2 | 7% | - | 3 | [a][e] |
| 71 Insulin-like growth factor-binding protein 4 | IGBP4_MOUSE | 28 | 4 | 6 | 23% | 37 | 3 | 6 | 17% | - | 18 | [a][d][f] |
| 409 Insulin-like growth factor-binding protein 6 | IGBP6_MOUSE | 25 | 2 | 2 | 15% | 4 | - | - | - | - | - | [a][e] |
| 15 Insulin-like growth factor-binding protein 7 | IGBP7_MOUSE | 29 | 14 | 22 | 56% | 105 | 14 | 21 | 58% | - | 92 | [a][b][d] |
| 467 Insulin-like growth factor 1 | IGF1_MOUSE | 17 | 2 | 2 | 16% | 3 | - | - | - | - | - | |
| 214 Interleukin-1 receptor accessory protein | IL1AP_MOUSE | 66 | 3 | 3 | 4% | 6 | 3 | 3 | 6% | - | 6 | |
| 64 Inhibin beta A chain | INHBA_MOUSE | 47 | 10 | 12 | 28% | 38 | 10 | 12 | 25% | - | 29 | [a] |
| 330 Inhibin beta B chain | INHBB_MOUSE | 45 | 3 | 3 | 12% | 5 | 4 | 4 | 14% | - | 6 | |
| 257 Leukemia inhibitory factor | LIF_MOUSE | 22 | 2 | 2 | 11% | 4 | 3 | 3 | 16% | - | 7 | [a][b][g] |
| 278 Latent-transforming growth factor beta-binding protein 1 | LTBP1_MOUSE | 187 | 3 | 3 | 2% | 4 | 2 | 2 | 2% | - | 4 | [a][g] |
| 34 Latent-transforming growth factor beta-binding protein 2 | LTBP2_MOUSE | 196 | 9 | 12 | 7% | 30 | 11 | 14 | 7% | - | 40 | |
| 120 Latent-transforming growth factor beta-binding protein 4 | LTBP4_MOUSE | 179 | 10 | 10 | 8% | 18 | - | - | - | - | - | |
| 210 Macrophage migration inhibitory factor | MIF_MOUSE | 13 | 2 | 2 | 17% | 4 | 2 | 2 | 17% | - | 4 | [a] |
| 495 Beta-nerve growth factor | NGF_MOUSE | 27 | 2 | 2 | 8% | 5 | - | - | - | - | - | |
| 23 Pigment epithelium-derived factor | PEDF_MOUSE | 46 | 13 | 15 | 33% | 47 | 14 | 17 | 29% | - | 56 | [b] |
| 333 Platelet-derived growth factor D | PDGF_D_MOUSE | 43 | 3 | 4 | 11% | 12 | 3 | 3 | 11% | - | 6 | |
| 589 Retinoic acid receptor responder protein 2 | RARR2_MOUSE | 18 | 2 | 2 | 17% | 2 | - | - | - | - | - | |
| 261 Transforming growth factor beta-2 | TGFB2_MOUSE | 48 | 3 | 3 | 9% | 9 | 4 | 4 | 12% | - | 8 | |
| 246 Vascular endothelial growth factor A | VEGFA_MOUSE | 25 | 2 | 3 | 14% | 8 | 2 | 4 | 14% | - | 6 | [g] |
| 196 Vascular endothelial growth factor C | VEGFC_MOUSE | 46 | 3 | 4 | 9% | 5 | 2 | 3 | 6% | - | 6 | |
| 116 Vascular endothelial growth factor D | VEGFD_MOUSE | 41 | 4 | 4 | 13% | 26 | 4 | 4 | 13% | - | 14 | |
| Collagens | | | | | | | | | | | | |
| 1 Collagen alpha-1(I) chain | COL1A1_MOUSE | 138 | 55 | 76 | 54% | 592 | 56 | 79 | 53% | - | 441 | [d][e][f] |
| 3 Collagen alpha-2(I) chain | COL1A2_MOUSE | 130 | 46 | 67 | 48% | 637 | 37 | 50 | 38% | - | 350 | [d][e][f] |
| 2 Collagen alpha-1(III) chain | COL3A1_MOUSE | 139 | 48 | 66 | 47% | 447 | 47 | 67 | 46% | - | 350 | [e][f] |
| 75 Collagen alpha-1(IV) chain | COL4A1_MOUSE | 161 | 25 | 29 | 24% | 79 | 3 | 3 | 3% | - | 17 | |
| 20 Collagen alpha-2(IV) chain | COL4A2_MOUSE | 167 | 40 | 50 | 37% | 268 | 18 | 21 | 15% | - | 87 | |
| 41 Collagen alpha-1(V) chain | COL5A1_MOUSE | 184 | 7 | 8 | 6% | 34 | 8 | 10 | 7% | - | 31 | |
| 5 Collagen alpha-2(V) chain | COL5A2_MOUSE | 145 | 44 | 60 | 45% | 371 | 36 | 49 | 38% | - | 226 | [d] |
| 12 Collagen alpha-1(VI) chain | COL6A1_MOUSE | 108 | 22 | 27 | 29% | 143 | 24 | 31 | 27% | - | 145 | [d][e][f] |
| 33 Collagen alpha-2(VII) chain | COL6A2_MOUSE | 110 | 10 | 10 | 13% | 40 | 17 | 20 | 20% | - | 73 | [e] |
| 251 Collagen alpha-1(VIII) chain | COL8A1_MOUSE | 74 | 6 | 6 | 10% | 26 | 4 | 4 | 6% | - | 7 | |
| 105 Collagen alpha-1(XI) chain | COL8A1_MOUSE | 181 | 5 | 5 | 4% | 9 | 4 | 4 | 4% | - | 16 | |
| 268 Collagen alpha-1(XII) chain | COL9A1_MOUSE | 340 | 24 | 25 | 10% | 46 | 5 | 5 | 2% | - | 6 | [e] |
| 227 Collagen alpha-1(XIV) chain | COL9A1_MOUSE | 193 | 2 | 2 | 2% | 3 | 7 | 7 | 5% | - | 12 | |
| 93 Collagen alpha-1(XV) chain | COL9A1_MOUSE | 140 | 3 | 3 | 3% | 5 | 8 | 8 | 7% | - | 18 | |
| 492 Collagen alpha-1(XVIII) chain | COL1A1_MOUSE | 182 | 2 | 2 | 2% | 5 | - | - | - | - | - | |
| Proteases | | | | | | | | | | | | |
| 259 protein 10 | ADA10_MOUSE | 84 | 8 | 8 | 11% | 16 | 4 | 4 | 5% | - | 6 | |
| Disintegrin and metalloproteinase domain-containing | ADA12_MOUSE | 99 | - | - | - | - | 2 | 2 | 3% | - | 3 | |
| 384 protein 12 | ADA15_MOUSE | 93 | 3 | 3 | 4% | 7 | 2 | 2 | 3% | - | 4 | |
| Disintegrin and metalloproteinase domain-containing | ADA17_MOUSE | 93 | 3 | 3 | 5% | 4 | 2 | 2 | 3% | - | 3 | |
| 290 protein 15 | ADAM9_MOUSE | 92 | 2 | 3 | 4% | 5 | 2 | 3 | 4% | - | 6 | |
| Disintegrin and metalloproteinase domain-containing | ATL4_MOUSE | 113 | 3 | 3 | 6% | 5 | - | - | - | - | - | |
| 385 protein 17 | AT52_MOUSE | 135 | 4 | 6 | 6% | 18 | 4 | 5 | 6% | - | 9 | |
| Disintegrin and metalloproteinase with thrombospondin | AT55_MOUSE | 102 | 9 | 13 | 10% | 33 | 8 | 10 | 8% | - | 24 | |
| 56 motifs 2 | AT57_MOUSE | 182 | 2 | 2 | 2% | 2 | - | - | - | - | - | |
| A disintegrin and metalloproteinase with thrombospondin | CBPE_MOUSE | 53 | 7 | 8 | 16% | 20 | 8 | 10 | 22% | - | 33 | |
| 150 Probable carboxypeptidase X1 | CPXMI_MOUSE | 81 | 7 | 8 | 15% | 14 | 7 | 7 | 12% | - | 12 | |
| 218 Serine protease HTRA1 | HTRA1_MOUSE | 51 | 5 | 6 | 15% | 13 | 3 | 3 | 7% | - | 10 | |
| 143 Macrophage metalloelastase | MMP12_MOUSE | 55 | 9 | 9 | 16% | 21 | - | - | - | - | - | |
| 149 Matrix metalloproteinase-19 | MMP19_MOUSE | 59 | 2 | 3 | 7% | 4 | 5 | 7 | 15% | - | 15 | |
| 208 72 type IV collagenase | MMP2_MOUSE | 74 | 13 | 15 | 21% | 29 | 7 | 8 | 11% | - | 13 | [d][e][f] |
| 90 Stromelysin-1 | MMP3_MOUSE | 54 | 16 | 16 | 29% | 63 | 7 | 7 | 15% | - | 17 | [f] |
| 550 Neutrophil collagenase | MMP8_MOUSE | 53 | 2 | 2 | 5% | 3 | - | - | - | - | - | |
| 300 Pappalysin-1 | PAPP1_MOUSE | 181 | 7 | 7 | 5% | 10 | 3 | 3 | 3% | - | 5 | |
| 274 Proprotein convertase subtilisin/kexin type 5 | PCSK5_MOUSE | 209 | 7 | 7 | 6% | 17 | 2 | 3 | 2% | - | 11 | |
| 555 Proprotein convertase subtilisin/kexin type 9 | PCSK9_MOUSE | 75 | 2 | 2 | 4% | 3 | - | - | - | - | - | |
| 244 Serine protease 23 | PRS23_MOUSE | 43 | 3 | 3 | 10% | 6 | 3 | 3 | 10% | - | 6 | |
| Protease inhibitors | | | | | | | | | | | | |
| 354 CD109 antigen | CD109_MOUSE | 162 | 8 | 8 | 7% | 14 | 3 | 3 | 3% | - | 4 | |
| 42 Cystatin-C | CYTC_MOUSE | 16 | 10 | 14 | 55% | 63 | 6 | 7 | 34% | - | 32 | |
| 95 Glia-derived nexin | GDN_MOUSE | 44 | 7 | 8 | 21% | 17 | 7 | 9 | 22% | - | 21 | |
| 166 Neuroserpin | NEUS_MOUSE | 46 | 5 | 5 | 13% | 11 | 5 | 5 | 15% | - | 11 | |
| 9 Plasminogen activator inhibitor 1 | PAI1_MOUSE | 45 | 23 | 30 | 55% | 177 | 23 | 29 | 55% | - | 139 | [b][e] |
| 13 Serine protease inhibitor A3N | SPA3N_MOUSE | 47 | 13 | 18 | 32% | 97 | 17 | 20 | 42% | - | 102 | |
| 459 Tissue factor pathway inhibitor | TFPI1_MOUSE | 35 | 2 | 2 | 7% | 7 | - | - | - | - | - | |
| 62 Metalloproteinase inhibitor 1 | TIMP1_MOUSE | 23 | 9 | 10 | 38% | 48 | 6 | 7 | 40% | - | 24 | [d][e] |
| 70 Metalloproteinase inhibitor 2 | TIMP2_MOUSE | 24 | 9 | 12 | 24% | 45 | 7 | 9 | 24% | - | 21 | [e][f] |
| 325 Metalloproteinase inhibitor 3 | TIMP3_MOUSE | 24 | 3 | 3 | 16% | 5 | 3 | 3 | 17% | - | 7 | |
| Basement membrane | | | | | | | | | | | | |
| 291 Annexin A2 | ANXA2_MOUSE | 39 | 4 | 4 | 14% | 7 | 3 | 4 | 12% | - | 7 | |
| 355 Laminin subunit alpha-1 | LAMA1_MOUSE | 338 | - | - | - | - | 3 | 3 | 1% | - | 4 | |
| 130 Laminin subunit alpha-2 | LAMA2_MOUSE | 343 | 12 | 12 | 5% | 18 | 21 | 22 | 8% | - | 38 | |
| 102 Laminin subunit alpha-4 | LAMA4_MOUSE | 202 | 12 | 12 | 8% | 29 | 8 | 8 | 6% | - | 22 | [e] |
| 65 Laminin subunit beta-1 | LAMB1_MOUSE | 197 | 6 | 6 | 4% | 9 | 19 | 20 | 12% | - | 40 | [e] |
| 104 Laminin subunit beta-2 | LAMB2_MOUSE | 196 | 13 | 14 | 9% | 25 | 11 | 11 | 8% | - | 27 | |
| 18 Laminin subunit gamma-1 | LAMC1_MOUSE | 177 | 13 | 14 | 12% | 31 | 25 | 36 | 21% | - | 103 | |
| Basement membrane-specific heparan sulfate | PGBM_MOUSE | 398 | 14 | 15 | 4% | 33 | 26 | 27 | 9% | - | 53 | [e][f] |
| 31 proteoglycan core protein | SPRC_MOUSE | 34 | 15 | 20 | 44% | 138 | 18 | 25 | 43% | - | 212 | [e] |
| 4 SPARC | TETN_MOUSE | 22 | - | - | - | - | 3 | 3 | 15% | - | 9 | |
| 248 Tetranectin | | | | | | | | | | | | |
| Glycoproteins | | | | | | | | | | | | |
| 296 Adipocyte enhancer-binding protein 1 | AEBP1_MOUSE | 128 | - | - | - | - | 4 | 4 | 4% | - | 9 | |
| 281 Agrin | AGRIN_MOUSE | 208 | 3 | 3 | 2% | 6 | 5 | 5 | 3% | - | 6 | |

| | | | | | | | | | | |
|---|---------------|-----|----|----|-----|-----|----|----|-----|-----|
| 359 Acid sphingomyelinase-like phosphodiesterase 3a | ASM3A_MOUSE | 50 | 2 | 2 | 6% | 4 | 2 | 2 | 6% | 4 |
| 194 Beta-1,4-galactosyltransferase 1 | B4GALT1_MOUSE | 44 | 5 | 5 | 12% | 10 | 5 | 6 | 12% | 11 |
| 183 Biotinidase | BTD_MOUSE | 58 | 5 | 5 | 13% | 7 | 4 | 4 | 10% | 9 |
| 106 Calumenin | CALU_MOUSE | 37 | 5 | 6 | 18% | 17 | 5 | 6 | 17% | 22 |
| 94 Clusterin | CLUS_MOUSE | 52 | 10 | 13 | 27% | 34 | 6 | 7 | 20% | 13 |
| 463 Cartilage oligomeric matrix protein | COMP_MOUSE | 82 | 2 | 2 | 3% | 3 | - | - | - | - |
| 344 Collagen triple helix repeat-containing protein 1 | CTHR1_MOUSE | 26 | 4 | 4 | 20% | 9 | 2 | 2 | 8% | 5 |
| 73 Dystroglycan | DAG1_MOUSE | 97 | 7 | 8 | 9% | 24 | 8 | 9 | 11% | 19 |
| 118 Dickkopf-related protein 3 | DKK3_MOUSE | 38 | 6 | 7 | 21% | 17 | - | - | - | - |
| 392 Dentin matrix protein 4 | DMP4_MOUSE | 66 | - | - | - | - | 2 | 2 | 5% | 3 |
| 11 Extracellular matrix protein 1 | ECM1_MOUSE | 63 | 22 | 33 | 47% | 182 | 19 | 25 | 42% | 111 |
| 22 EMILIN-1 | EMIL1_MOUSE | 108 | 17 | 23 | 18% | 67 | 20 | 27 | 20% | 75 |
| 427 EMILIN-2 | EMIL2_MOUSE | 117 | - | - | - | - | 2 | 2 | 2% | 2 |
| 144 Mammalian ependymin-related protein 1 | EPDR1_MOUSE | 25 | 4 | 4 | 23% | 13 | 4 | 4 | 23% | 8 |
| 505 Protein FAM20A | F20A_MOUSE | 62 | 3 | 3 | 7% | 4 | - | - | - | - |
| 573 Protein FAM20B | F20B_MOUSE | 47 | 2 | 2 | 5% | 2 | - | - | - | - |
| 284 Protein FAM3C | FAM3C_MOUSE | 25 | 4 | 4 | 23% | 8 | 3 | 3 | 17% | 6 |
| 16 Fibrillin-1 | FBN1_MOUSE | 312 | 53 | 61 | 24% | 127 | 42 | 46 | 19% | 113 |
| 296 Fetuin-B | FETUB_MOUSE | 43 | 2 | 3 | 8% | 7 | - | - | - | - |
| 6 Fibronectin | FINC_MOUSE | 272 | 58 | 80 | 31% | 529 | 36 | 50 | 20% | 220 |
| 44 Fibromodulin | FMOD_MOUSE | 43 | 4 | 6 | 14% | 22 | 6 | 8 | 18% | 31 |
| 574 Follistatin | FST_MOUSE | 38 | 2 | 2 | 8% | 2 | - | - | - | - |
| 8 Follistatin-related protein 1 | FSTL1_MOUSE | 35 | 17 | 22 | 54% | 85 | 22 | 29 | 59% | 116 |
| 264 Follistatin-related protein 3 | FSTL3_MOUSE | 27 | - | - | - | - | 2 | 2 | 14% | 3 |
| 157 Glycan-4 | GPC4_MOUSE | 63 | - | - | - | - | 5 | 5 | 14% | 9 |
| Immunoglobulin superfamily containing leucine-rich | | | | | | | | | | |
| 91 repeat protein | ISLR_MOUSE | 46 | 4 | 4 | 11% | 6 | 6 | 6 | 16% | 14 |
| 546 Integrin beta-like protein 1 | ITGB1L_MOUSE | 54 | 2 | 2 | 6% | 3 | - | - | - | - |
| 429 Leucine-rich repeat LGI family member 2 | LG12_MOUSE | 63 | 4 | 4 | 8% | 9 | - | - | - | - |
| 54 Lumican | LUM_MOUSE | 38 | 6 | 6 | 16% | 24 | 6 | 6 | 16% | 24 |
| 212 Meteorin-like protein | METRL_MOUSE | 35 | 4 | 4 | 15% | 8 | - | - | - | - |
| 403 Microfibril-associated glycoprotein 4 | MFAP4_MOUSE | 29 | - | - | - | - | 2 | 2 | 7% | 3 |
| 126 Microfibrillar-associated protein 5 | MFAP5_MOUSE | 19 | 3 | 4 | 23% | 9 | 3 | 4 | 23% | 10 |
| 77 Lactadherin | MFGM_MOUSE | 51 | 10 | 11 | 23% | 47 | 9 | 9 | 22% | 22 |
| 204 Mimecan | MIME_MOUSE | 34 | 4 | 4 | 11% | 9 | 4 | 4 | 11% | 6 |
| 359 Mesothelin | MSLN_MOUSE | 69 | 4 | 4 | 7% | 8 | - | - | - | - |
| 176 Neutrophil gelatinase-associated lipocalin | NGAL_MOUSE | 23 | 3 | 5 | 17% | 10 | 4 | 5 | 20% | 14 |
| 81 Nitrogen-1 | NID1_MOUSE | 137 | 11 | 11 | 10% | 27 | 8 | 8 | 8% | 27 |
| 108 Nidogen-2 | NID2_MOUSE | 154 | 6 | 6 | 5% | 11 | 10 | 10 | 9% | 33 |
| 147 Protein NOV homolog | NOV_MOUSE | 39 | 5 | 5 | 20% | 12 | 4 | 4 | 17% | 8 |
| 158 Olfactomedin-like protein 3 | OLFL3_MOUSE | 46 | 6 | 6 | 17% | 12 | 5 | 5 | 17% | 15 |
| 406 Olfactomedin-like protein 2B | OLM2B_MOUSE | 84 | - | - | - | - | 2 | 2 | 5% | 3 |
| 338 Inactive serine protease PAMR1 | PAMR1_MOUSE | 80 | 4 | 4 | 7% | 5 | - | - | - | - |
| 86 Procollagen C-endopeptidase enhancer 1 | PCOC1_MOUSE | 50 | 10 | 14 | 31% | 33 | 12 | 14 | 33% | 35 |
| 21 Biglycan | PGS1_MOUSE | 42 | 7 | 9 | 22% | 66 | 9 | 11 | 28% | 51 |
| 26 Decorin | PGS2_MOUSE | 40 | 10 | 11 | 26% | 41 | 9 | 12 | 25% | 51 |
| 92 Periostin | POSTN_MOUSE | 93 | 13 | 14 | 19% | 37 | 7 | 8 | 10% | 24 |
| 30 Prolargin | PRELP_MOUSE | 43 | 9 | 13 | 28% | 55 | 11 | 16 | 30% | 62 |
| 409 Proteoglycan 4 | PRG4_MOUSE | 116 | - | - | - | - | 2 | 2 | 2% | 3 |
| 43 Pentraxin-related protein PTX3 | PTX3_MOUSE | 42 | 9 | 11 | 29% | 29 | 12 | 12 | 39% | 44 |
| 47 Sulfated glycoprotein 1 | SAP_MOUSE | 61 | 9 | 10 | 17% | 29 | 9 | 11 | 19% | 32 |
| 527 Semaphorin-3A | SEM3A_MOUSE | 89 | 2 | 2 | 3% | 4 | - | - | - | - |
| 471 Semaphorin-3C | SEM3C_MOUSE | 85 | 2 | 2 | 4% | 4 | - | - | - | - |
| 231 Semaphorin-3D | SEM3D_MOUSE | 90 | 4 | 4 | 6% | 8 | 3 | 3 | 4% | 5 |
| 170 Semaphorin-3E | SEM3E_MOUSE | 90 | 7 | 9 | 11% | 19 | - | - | - | - |
| 153 Semaphorin-3F | SEM3F_MOUSE | 88 | 7 | 7 | 12% | 14 | - | - | - | - |
| 159 Secreted frizzled-related protein 1 | SFRP1_MOUSE | 35 | - | - | - | - | 5 | 6 | 19% | 12 |
| 141 Secreted frizzled-related protein 3 | SFRP3_MOUSE | 36 | 3 | 3 | 10% | 6 | 3 | 3 | 10% | 11 |
| 309 Slit homolog 2 protein | SLT12_MOUSE | 169 | 7 | 7 | 6% | 10 | 5 | 5 | 3% | 8 |
| 129 Slit homolog 3 protein | SLT13_MOUSE | 168 | 4 | 5 | 3% | 8 | 4 | 4 | 3% | 9 |
| 314 Spondin-2 | SPON2_MOUSE | 36 | 4 | 4 | 11% | 6 | 3 | 3 | 9% | 4 |
| 173 Sushi-repeat-containing protein SRPX2 | SRPX2_MOUSE | 53 | 5 | 5 | 14% | 10 | 3 | 3 | 8% | 12 |
| 38 Tenascin | TENA_MOUSE | 232 | 16 | 18 | 11% | 32 | 25 | 30 | 16% | 61 |
| 295 Tubularinterstitial nephritis antigen-like | TINAL_MOUSE | 53 | 2 | 2 | 6% | 8 | 2 | 2 | 6% | 5 |
| 303 Thrombospondin-1 | TSP1_MOUSE | 130 | 20 | 23 | 23% | 82 | 3 | 3 | 3% | 4 |
| 180 Thrombospondin-2 | TSP2_MOUSE | 130 | 3 | 3 | 3% | 5 | 4 | 4 | 4% | 15 |
| 593 WNT1-inducible-signaling pathway protein 1 | WISP1_MOUSE | 41 | 2 | 2 | 8% | 2 | - | - | - | - |
| 146 WNT1-inducible-signaling pathway protein 2 | WISP2_MOUSE | 27 | 9 | 11 | 31% | 30 | 6 | 6 | 25% | 11 |
| Oxido-reductase | | | | | | | | | | |
| 364 Glutathione peroxidase 3 | GPX3_MOUSE | 25 | 2 | 2 | 13% | 7 | 2 | 2 | 13% | 4 |
| 131 Peroxidasin homolog | PXDN_MOUSE | 165 | 23 | 25 | 20% | 61 | 6 | 6 | 5% | 15 |
| 109 Superoxide dismutase [Cu-Zn] | SDOC_MOUSE | 16 | 6 | 9 | 39% | 20 | 5 | 7 | 36% | 13 |
| 49 Extracellular superoxide dismutase [Cu-Zn] | SODE_MOUSE | 27 | 15 | 17 | 43% | 52 | 10 | 13 | 39% | 37 |
| 175 Lysyl oxidase homolog 1 | LOXL1_MOUSE | 67 | 9 | 11 | 19% | 42 | 6 | 6 | 14% | 10 |
| 228 Lysyl oxidase homolog 2 | LOXL2_MOUSE | 87 | 10 | 14 | 19% | 32 | 4 | 7 | 8% | 13 |
| 200 Lysyl oxidase homolog 3 | LOXL3_MOUSE | 84 | 10 | 12 | 18% | 22 | 7 | 9 | 11% | 16 |
| 40 Sulphydryl oxidase 1 | QSOX1_MOUSE | 83 | 20 | 27 | 30% | 114 | 20 | 26 | 30% | 72 |
| Extracellular matrix | | | | | | | | | | |
| 243 Transforming growth factor-beta-induced protein Ig-h3 | BGH3_MOUSE | 75 | 5 | 5 | 9% | 13 | - | - | - | - |
| 476 Corneodesmosin | CDSN_MOUSE | 54 | 3 | 3 | 7% | 6 | - | - | - | - |
| 479 Collectin-11 | COL11_MOUSE | 29 | 2 | 3 | 10% | 6 | - | - | - | - |
| 265 Versican core protein | CSPG2_MOUSE | 367 | - | - | - | 2 | 2 | 1% | 4 | |
| 134 Fibulin-1 | FBLN1_MOUSE | 78 | 14 | 15 | 25% | 37 | 11 | 12 | 20% | 35 |
| 7 Fibulin-2 | FBLN2_MOUSE | 132 | 24 | 34 | 24% | 262 | 20 | 26 | 20% | 158 |
| 51 Fibulin-5 | FBLN5_MOUSE | 50 | 8 | 10 | 20% | 40 | 6 | 7 | 16% | 30 |
| 66 Galectin-1 | LEG1_MOUSE | 15 | 6 | 8 | 61% | 21 | 4 | 7 | 41% | 21 |
| 437 Galectin-3 | LEG3_MOUSE | 28 | 3 | 3 | 16% | 5 | - | - | - | - |
| 48 Galectin-3-binding protein | LG3BP_MOUSE | 64 | 11 | 16 | 26% | 47 | 10 | 14 | 23% | 41 |
| 72 Protein-lysine 6-oxidase | LYOX_MOUSE | 47 | 5 | 8 | 15% | 25 | 6 | 7 | 19% | 16 |
| 297 Matrin-2 | MATN2_MOUSE | 107 | - | - | - | - | 3 | 3 | 3% | 9 |
| 438 Nephronectin | NPNT_MOUSE | 61 | 3 | 3 | 5% | 4 | - | - | - | - |
| 313 Aggrecan core protein | PGCA_MOUSE | 222 | - | - | - | - | 3 | 3 | 2% | 4 |
| Cell adhesion | | | | | | | | | | |
| 61 Colle-coil domain-containing protein 80 | CCD80_MOUSE | 108 | 4 | 4 | 7% | 7 | 12 | 12 | 15% | 33 |
| 201 Protein CYR61 | CYR61_MOUSE | 42 | 4 | 6 | 12% | 15 | 3 | 3 | 10% | 9 |
| 114 Dermatopontin | DERM_MOUSE | 24 | 7 | 7 | 35% | 19 | 5 | 5 | 30% | 12 |
| Sushi, von Willebrand factor type A, EGF and pentraxin 29 domain-containing protein 1 | SVEP1_MOUSE | 387 | 35 | 45 | 12% | 118 | 33 | 41 | 11% | 121 |
| Growth regulation | | | | | | | | | | |
| 314 Growth arrest-specific protein 6 | GAS6_MOUSE | 75 | 3 | 3 | 4% | 8 | - | - | - | - |
| 239 Growth/differentiation factor 6 | GDF6_MOUSE | 51 | 4 | 4 | 10% | 16 | 4 | 4 | 10% | 6 |
| Serum/Plasma | | | | | | | | | | |
| 216 Serum albumin | ALBU_MOUSE | 69 | 2 | 3 | 4% | 23 | 2 | 3 | 4% | 5 |
| 304 Antithrombin-III | ANT3_MOUSE | 52 | - | - | - | - | 2 | 2 | 5% | 4 |
| 50 Apolipoprotein E | APOE_MOUSE | 36 | 7 | 9 | 28% | 24 | 8 | 11 | 30% | 35 |
| 154 Beta-2-microglobulin | B2MG_MOUSE | 14 | 3 | 3 | 23% | 17 | 2 | 2 | 16% | 14 |
| 419 Complement C1q subcomponent subunit A | C1QA_MOUSE | 26 | 2 | 2 | 11% | 6 | - | - | - | - |
| 371 Complement C1q subcomponent subunit B | C1QB_MOUSE | 27 | 2 | 2 | 10% | 8 | - | - | - | - |
| 268 Complement C1q subcomponent subunit C | C1QC_MOUSE | 26 | 2 | 3 | 13% | 9 | - | - | - | - |
| 179 Complement C1q tumor necrosis factor-related protein 5 | C1QT5_MOUSE | 25 | 4 | 5 | 23% | 9 | - | - | - | - |
| 273 Complement C4-B | C04B_MOUSE | 193 | 10 | 10 | 7% | 18 | 4 | 4 | 2% | 11 |
| 68 Ceruloplasmin | CERU_MOUSE | 121 | 9 | 10 | 11% | 23 | 13 | 14 | 17% | 45 |
| 69 Complement factor H | CFAH_MOUSE | 139 | 32 | 45 | 31% | 160 | 16 | 18 | 18% | 52 |
| 571 Complement factor I | CFAI_MOUSE | 67 | 2 | 2 | 5% | 2 | - | - | - | - |

| | | | | | | | | | | |
|---|--------------|-----|----|----|-----|-----|----|----|-----|----|
| 305 Complement C2 | CO2_MOUSE | 85 | 6 | 6 | 9% | 10 | - | - | - | - |
| 97 Complement C3 | CO3_MOUSE | 186 | 58 | 72 | 38% | 299 | 11 | 12 | 8% | 32 |
| 285 Growth hormone receptor | GHR_MOUSE | 73 | 2 | 2 | 3% | 6 | 2 | 2 | 3% | 5 |
| 57 Granulins | GRN_MOUSE | 63 | 12 | 15 | 29% | 49 | 11 | 13 | 26% | 30 |
| 53 Haptoglobin | HPT_MOUSE | 39 | 8 | 9 | 25% | 25 | 11 | 12 | 27% | 30 |
| 28 Plasma protease C1 inhibitor | IC1_MOUSE | 56 | 11 | 12 | 21% | 36 | 14 | 16 | 27% | 51 |
| 199 Interferon-alpha/beta receptor beta chain | INAR2_MOUSE | 57 | 3 | 3 | 5% | 9 | 2 | 3 | 5% | 9 |
| 521 Inter-alpha-trypsin inhibitor heavy chain H2 | ITIH2_MOUSE | 106 | 2 | 2 | 3% | 4 | - | - | - | - |
| 174 Low-density lipoprotein receptor | LDLR_MOUSE | 95 | 4 | 4 | 5% | 9 | 3 | 3 | 4% | 7 |
| 428 Mast cell protease 8 | MCPT8_MOUSE | 27 | - | - | - | - | 2 | 2 | 10% | 2 |
| 60 Plasma glutamate carboxypeptidase | PGCP_MOUSE | 52 | 8 | 9 | 19% | 30 | 8 | 9 | 20% | 22 |
| 431 Vitamin K-dependent protein S | PROS_MOUSE | 75 | 8 | 8 | 14% | 18 | 2 | 2 | 3% | 2 |
| 286 Ribonuclease 4 | RNASE4_MOUSE | 17 | 3 | 4 | 20% | 8 | 2 | 2 | 19% | 5 |
| 375 Ribonuclease T2 | RNT2_MOUSE | 30 | - | - | - | - | 2 | 2 | 7% | 4 |
| 167 Transcobalamin-2 | TCO2_MOUSE | 48 | 9 | 10 | 24% | 24 | 6 | 8 | 18% | 21 |
| 25 Serotransferrin | TRFE_MOUSE | 77 | 36 | 48 | 46% | 184 | 24 | 27 | 38% | 61 |
| 531 Alpha-2-macroglobulin-P | A2MP_MOUSE | 164 | 2 | 2 | 2% | 3 | - | - | - | - |
| 233 Placenta-specific protein 9 | PLAC9_MOUSE | 11 | 2 | 2 | 28% | 6 | 2 | 2 | 28% | 5 |
| Glycolysis | | | | | | | | | | |
| 140 Fructose-biphosphate aldolase A | ALDOA_MOUSE | 39 | 7 | 8 | 30% | 22 | 6 | 7 | 16% | 17 |
| 193 Glucose-6-phosphate isomerase | G6PI_MOUSE | 63 | 5 | 6 | 13% | 13 | 5 | 5 | 12% | 8 |
| Lysosome | | | | | | | | | | |
| 170 Arylsulfatase A | ARSA_MOUSE | 54 | 2 | 4 | 8% | 9 | 3 | 4 | 10% | 7 |
| 37 Cathepsin B | CATB_MOUSE | 37 | 10 | 15 | 28% | 47 | 9 | 12 | 25% | 33 |
| 138 Gamma-glutamyl hydrolase | GGH_MOUSE | 35 | 3 | 3 | 11% | 10 | 4 | 4 | 15% | 9 |
| 184 Group XV phospholipase A2 | PAG15_MOUSE | 47 | 4 | 4 | 14% | 10 | 4 | 4 | 14% | 14 |
| Membrane | | | | | | | | | | |
| 221 Calyptenin-1 | CSTN1_MOUSE | 109 | 6 | 6 | 9% | 17 | 4 | 5 | 5% | 11 |
| 369 Leukemia inhibitory factor receptor | LIFR_MOUSE | 123 | - | - | - | - | 2 | 2 | 2% | 4 |
| Scavenger receptor cysteine-rich domain-containing | SRCR1_MOUSE | 145 | - | - | - | - | 5 | 5 | 6% | 10 |
| 197 protein LOC284297 homolog | VNN1_MOUSE | 57 | 4 | 4 | 11% | 9 | - | - | - | - |
| Epithelia-mesenchymal transition | | | | | | | | | | |
| 284 Protein FAM3C | FAM3C_MOUSE | 25 | 4 | 4 | 23% | 8 | 3 | 3 | 17% | 6 |
| Glycosylation | | | | | | | | | | |
| 436 Polypeptide N-acetylgalactosaminyltransferase 2 | GALT2_MOUSE | 65 | 3 | 3 | 8% | 5 | - | - | - | - |
| Lipid metabolism/transport | | | | | | | | | | |
| 447 Phospholipase A1 member A | PLA1A_MOUSE | 50 | 3 | 3 | 9% | 8 | - | - | - | - |
| 238 Phospholipid transfer protein | PLTP_MOUSE | 54 | 5 | 6 | 12% | 15 | 5 | 6 | 11% | 16 |
| Apoptosis | | | | | | | | | | |
| 350 Tumor necrosis factor receptor superfamily member 11B | TR11B_MOUSE | 46 | 2 | 2 | 8% | 5 | 2 | 2 | 8% | 5 |
| Others | | | | | | | | | | |
| 317 Cyclic AMP-dependent transcription factor ATF-6 beta | ATF6B_MOUSE | 76 | - | - | - | - | 2 | 2 | 4% | 4 |
| 336 Adenyl cyclase-associated protein 1 | CAP1_MOUSE | 52 | 2 | 3 | 6% | 9 | - | - | - | - |
| 344 Macrophage-capping protein | CAPG_MOUSE | 39 | 2 | 2 | 8% | 5 | - | - | - | - |
| 407 Angiopoietin-related protein 2 | ANGL2_MOUSE | 57 | 2 | 2 | 5% | 4 | - | - | - | - |
| 260 Angiopoietin-2 | ANGP2_MOUSE | 57 | 2 | 2 | 6% | 4 | 5 | 5 | 12% | 9 |
| 195 C-X-C motif chemokine 16 | CXL16_MOUSE | 27 | 3 | 3 | 15% | 10 | 2 | 2 | 8% | 6 |
| 491 von Willebrand factor | VWF_MOUSE | 309 | 3 | 3 | 2% | 5 | - | - | - | - |
| 177 Cofilin-1 | COF1_MOUSE | 19 | 6 | 7 | 31% | 18 | 5 | 6 | 30% | 10 |
| 302 UPF0556 protein C19orf110 homolog | CS010_MOUSE | 18 | 2 | 2 | 16% | 6 | - | - | - | - |
| 181 Gelosin | GELS_MOUSE | 86 | 8 | 11 | 17% | 39 | 9 | 9 | 16% | 19 |
| 220 Beta-galactosidase-1-like protein | GLB1L_MOUSE | 73 | 5 | 5 | 9% | 12 | - | - | - | - |
| 272 Epididymis-specific alpha-mannosidase | MAB22_MOUSE | 116 | 4 | 4 | 6% | 7 | 5 | 5 | 7% | 11 |
| 128 Epididymal secretory protein E1 | NPC2_MOUSE | 16 | 5 | 6 | 34% | 16 | 5 | 5 | 36% | 10 |
| 87 Peptidyl-prolyl cis-trans isomerase A | PPIA_MOUSE | 18 | 7 | 7 | 35% | 25 | 6 | 6 | 35% | 16 |
| 179 Profilin-1 | PROF1_MOUSE | 15 | 8 | 9 | 59% | 15 | 4 | 5 | 32% | 11 |
| 151 Translationally-controlled tumor protein | TCTP_MOUSE | 19 | 2 | 2 | 9% | 4 | 3 | 4 | 16% | 7 |
| 203 Thymosin beta-4 | TYB4_MOUSE | 6 | 3 | 5 | 48% | 11 | 3 | 3 | 48% | 5 |

[a] Sean C. Bendall et al., Mol. Cell. Proteom. 8:421-432,2009;

[b] A. Chui Ping Chin et al. J. of Biotechnology 130 320-328 2007;

[c] N. Buhr et al. Electrophoresis 2007;28, 1615-1623;

[d] L. Xie et al. Mol. Cell. Proteom. 4:1273-1283 2005;

[e] A. B. Prowse et al. Proteomics 2005, 5, 978-989;

[f] J. Wee Eng Lim et al. Proteomics 2002, 2, 1187-1203;

[g] W.A. LaFramboise et al. Am. J. Physiol Cell Physiol 292: C1799-C1808, 2007;

Online-Table II: ECM proteins changes in the secretome of CFs following miR-29b transfection

| # | Identified Proteins | Accession Number | MW (kDa) | Control Anti-miR Sample 1 | Control Anti-miR Sample 2 | Control Anti-miR Sample 3 | Anti-miR-29b Sample 1 | Anti-miR-29b Sample 2 | Anti-miR-29b Sample 3 | t test (paired) | Average Control Anti-miR-29b | Average anti-miR-29b Ratio | Control Pre-miR Sample 1 | Control Pre-miR Sample 2 | Control Pre-miR Sample 3 | Pre-miR-29b Sample 1 | Pre-miR-29b Sample 2 | Pre-miR-29b Sample 3 | t test (paired) | Average Control Pre-miR-29b | Average pre-miR-29b Ratio | Targets can Pictar Diana | |
|-----|--|------------------|----------|---------------------------|---------------------------|---------------------------|-----------------------|-----------------------|-----------------------|-----------------|------------------------------|----------------------------|--------------------------|--------------------------|--------------------------|----------------------|----------------------|----------------------|-----------------|-----------------------------|---------------------------|--------------------------|------------|
| 176 | Cofflin-1 | COF1_MOUSE | 19 | 15.27 | 10.6 | 12.78 | 13.42 | 11.2 | 12.21 | 0.482 | 12.88 | 12.28 | 0.95 | 5.92 | 4.64 | 3.11 | 11.03 | 9.6 | 6.44 | 0.016 | 4.56 | 9.02 | 1.98 |
| 126 | Profilin-1 | PROF1_MOUSE | 15 | 12.89 | 11.48 | 13.76 | 15.2 | 13.76 | 17.39 | 0.025 | 12.71 | 15.45 | 1.22 | 15.75 | 10.09 | 15.75 | 17.3 | 22.49 | 22.78 | 0.155 | 13.86 | 20.86 | 1.50 |
| 1 | Collagen alpha-1(I) chain | COL1A1_MOUSE | 138 | 470.41 | 510.94 | 493.75 | 561.85 | 603.92 | 527.21 | 0.066 | 491.70 | 564.33 | 1.15 | 434.68 | 480 | 455.13 | 204.11 | 214.46 | 244.17 | 0.005 | 456.60 | 220.91 | 0.48 X |
| 4 | Collagen alpha-1(III) chain | COL3A1_MOUSE | 139 | 318.96 | 391.31 | 258.17 | 387.91 | 459.36 | 322.77 | 0.000 | 322.81 | 390.01 | 1.21 | 241.94 | 309.13 | 227.54 | 66.2 | 91.25 | 88.11 | 0.016 | 259.54 | 81.85 | 0.32 X X |
| 29 | Collagen alpha-1(IV) chain | COL4A1_MOUSE | 161 | 35.89 | 69.98 | 40.26 | 76.43 | 78.39 | 55.35 | 0.161 | 48.71 | 70.06 | 1.44 | 37.39 | 71.9 | 41.04 | 9.78 | 19.62 | 26.41 | 0.104 | 50.11 | 18.60 | 0.37 X X X |
| 8 | Collagen alpha-2(IV) chain | COL4A2_MOUSE | 167 | 196.06 | 218.42 | 177.68 | 194.46 | 217.85 | 205.45 | 0.469 | 197.39 | 205.92 | 1.04 | 174.08 | 244.59 | 173.8 | 63.69 | 95.55 | 79.03 | 0.018 | 197.49 | 79.42 | 0.40 X X |
| 85 | Collagen alpha-2(V) chain | COL5A1_MOUSE | 184 | 18.44 | 15.84 | 15.72 | 28.51 | 23.96 | 24.29 | 0.004 | 16.67 | 25.59 | 1.54 | 20.67 | 31.9 | 22.07 | 7.27 | 8.16 | 1 | 0.025 | 24.88 | 5.48 | 0.22 X X |
| 5 | Collagen alpha-2(V) chain | COL5A2_MOUSE | 145 | 295.17 | 303.12 | 268.97 | 276.99 | 369.22 | 288.26 | 0.455 | 289.09 | 311.49 | 1.08 | 219.32 | 269.13 | 254.93 | 39.87 | 85.52 | 68.14 | 0.000 | 247.79 | 64.51 | 0.26 X X X |
| 16 | Collagen alpha-1(VI) chain | COL6A1_MOUSE | 108 | 101.7 | 125.86 | 109.96 | 100.39 | 98.79 | 116.59 | 0.550 | 112.51 | 105.26 | 0.94 | 69.84 | 110.07 | 102.15 | 52.4 | 55.44 | 59.07 | 0.073 | 94.02 | 55.64 | 0.59 |
| 78 | Collagen alpha-2(VI) chain | COL6A2_MOUSE | 110 | 32.72 | 28.94 | 26.52 | 14.31 | 33.31 | 22.57 | 0.463 | 29.39 | 23.40 | 0.80 | 22.64 | 20.09 | 16.8 | 6.02 | 8.16 | 8.26 | 0.034 | 19.84 | 7.48 | 0.38 |
| 113 | Collagen alpha-1(VII) chain | COL8A1_MOUSE | 74 | 21.62 | 21.96 | 16.71 | 21.41 | 21.41 | 22.57 | 0.500 | 20.10 | 21.80 | 1.08 | 5.92 | 9.18 | 6.27 | 1 | 1 | 1 | 0.027 | 7.12 | 1.00 | 0.14 X |
| 267 | Collagen alpha-1(XI) chain | COL8A1_MOUSE | 181 | 4.96 | 7.99 | 5.91 | 8.1 | 12.06 | 9.63 | 0.005 | 6.29 | 9.93 | 1.58 | 4.93 | 10.09 | 5.21 | 2.25 | 3.87 | 6.44 | 0.357 | 6.74 | 4.19 | 0.62 X X X |
| 81 | Collagen alpha-1(XII) chain | COL8A1_MOUSE | 340 | 35.1 | 33.31 | 9.83 | 27.62 | 11.2 | 17.39 | 0.482 | 26.08 | 18.74 | 0.72 | 7.88 | 42.81 | 5.21 | 27.33 | 1 | 1 | 0.669 | 18.63 | 9.78 | 0.52 |
| 623 | Collagen alpha-1(XIV) chain | COL8A1_MOUSE | 193 | 3.38 | 2.75 | 1 | 1 | 1 | 1 | 0.193 | 2.38 | 1.00 | 0.42 | 1 | 1 | 1 | 2.25 | 1 | 1 | 0.423 | 1.00 | 1.42 | |
| 397 | Collagen alpha-1(XV) chain | COL8A1_MOUSE | 140 | 4.96 | 2.75 | 2.96 | 2.77 | 1.85 | 1.86 | 0.073 | 3.56 | 2.16 | 0.61 | 1 | 3.73 | 1 | 1 | 6.73 | 1 | 0.423 | 1.91 | 2.91 | 1.52 X X |
| 121 | Laminin subunit beta-2 | LAMB2_MOUSE | 196 | 10.52 | 22.83 | 19.65 | 15.2 | 21.41 | 12.21 | 0.729 | 17.67 | 16.27 | 0.92 | 15.75 | 22.81 | 11.54 | 4.76 | 5.3 | 1 | 0.029 | 16.70 | 3.69 | 0.22 |
| 523 | TGF-beta receptor type III | TGBR3_MOUSE | 94 | 1 | 1.87 | 2.96 | 4.55 | 1.85 | 1.86 | 0.623 | 1.94 | 2.75 | 1.42 | 1 | 1 | 2.05 | 3.51 | 3.87 | 4.63 | 0.002 | 1.35 | 4.00 | 2.97 |
| 27 | Thrombospondin-1 | TPSP1_MOUSE | 130 | 66.02 | 66.49 | 31.43 | 74.66 | 53.72 | 23.43 | 0.597 | 54.65 | 50.60 | 0.93 | 69.84 | 63.72 | 23.13 | 98.79 | 95.55 | 39.11 | 0.034 | 52.23 | 77.82 | 1.49 |
| 230 | Adenosine deaminase | ADA_MOUSE | 40 | 1.79 | 2.75 | 6.89 | 7.21 | 2.7 | 2.73 | 0.898 | 3.81 | 4.21 | 1.11 | 6.9 | 6.45 | 1 | 21.06 | 18.19 | 10.07 | 0.016 | 4.78 | 16.44 | 3.44 |
| 153 | Calumenin | CALU_MOUSE | 37 | 12.89 | 14.97 | 13.76 | 13.42 | 15.46 | 14.8 | 0.061 | 13.87 | 14.56 | 1.05 | 17.72 | 6.45 | 11.54 | 4.76 | 1 | 1 | 0.049 | 11.90 | 2.25 | 0.19 |
| 124 | Beta-1,4-galactosyltransferase 1 | B4GALT1_MOUSE | 44 | 7.34 | 9.73 | 8.85 | 6.32 | 10.35 | 9.63 | 0.846 | 8.64 | 8.77 | 1.01 | 4.93 | 8.27 | 7.32 | 19.81 | 18.19 | 17.33 | 0.019 | 6.84 | 18.44 | 2.70 |
| 224 | CD109 antigen | CD109_MOUSE | 162 | 8.93 | 12.35 | 6.89 | 3.66 | 3.55 | 5.31 | 0.129 | 9.39 | 4.17 | 0.44 | 14.77 | 9.18 | 7.32 | 3.51 | 1 | 1 | 0.027 | 10.42 | 1.84 | 0.18 |
| 31 | Macrophage colony-stimulating factor 1 | CSF1_MOUSE | 61 | 46.2 | 41.17 | 51.06 | 43.6 | 35.87 | 33.78 | 0.204 | 46.14 | 37.75 | 0.82 | 46.24 | 42.81 | 37.88 | 64.94 | 74.06 | 60.89 | 0.022 | 42.31 | 66.63 | 1.57 |
| 262 | BMP-binding endothelial regulator protein | BMPER_MOUSE | 76 | 9.72 | 8.86 | 7.87 | 8.99 | 11.2 | 4.45 | 0.752 | 8.82 | 8.21 | 0.93 | 5.92 | 4.64 | 5.21 | 1 | 1 | 1 | 0.007 | 5.26 | 1.00 | 0.19 |
| 618 | Cell growth regulator with EF hand domain protein 1 | CGR6L1_MOUSE | 31 | 1.79 | 1 | 1 | 4.55 | 2.7 | 2.73 | 0.027 | 1.26 | 3.33 | 2.63 | 1 | 1 | 1 | 1 | 1 | 1 | NA | 1.00 | 1.00 | |
| 516 | Cartilage oligomeric matrix protein | COMP_MOUSE | 82 | 2.59 | 1 | 3.94 | 1 | 2.7 | 2.73 | 0.758 | 2.51 | 2.14 | 0.85 | 1.98 | 1.91 | 4.16 | 1 | 1 | 2.81 | 0.016 | 2.68 | 1.60 | 0.60 |
| 134 | Mammalian epidymin-related protein 1 | EPDR1_MOUSE | 25 | 9.72 | 12.35 | 8.85 | 13.42 | 12.06 | 12.21 | 0.219 | 10.31 | 12.56 | 1.22 | 12.8 | 11 | 11.54 | 18.55 | 22.49 | 22.78 | 0.037 | 11.78 | 21.27 | 1.81 |
| 11 | EGF-containing fibulin-like extracellular matrix protein 1 | FBLN3_MOUSE | 55 | 112.01 | 104.04 | 129.59 | 111.04 | 118.35 | 115.73 | 0.985 | 115.21 | 115.04 | 1.00 | 110.16 | 100.07 | 131.65 | 174.02 | 194.4 | 233.29 | 0.017 | 113.96 | 200.57 | 1.76 |
| 388 | Fetuin-B | FETUB_MOUSE | 43 | 1.79 | 3.62 | 3.94 | 2.77 | 2.7 | 1.86 | 0.529 | 3.12 | 2.44 | 0.78 | 4.93 | 7.36 | 6.27 | 1 | 1 | 2.81 | 0.036 | 6.19 | 1.60 | 0.26 |
| 19 | Follistatin-related protein 1 | FSTL1_MOUSE | 35 | 64.43 | 75.22 | 56.95 | 73.77 | 81.79 | 74.32 | 0.076 | 65.53 | 76.63 | 1.17 | 61.97 | 76.44 | 80.02 | 38.61 | 41.11 | 48.18 | 0.014 | 72.81 | 42.63 | 0.59 X |
| 506 | Growth-regulated alpha protein | GROA_MOUSE | 10 | 2.59 | 1.87 | 2.96 | 1.89 | 2.7 | 2.73 | 0.948 | 2.47 | 2.44 | 0.99 | 4.93 | 1.91 | 2.05 | 3.51 | 1 | 1 | 0.018 | 2.96 | 1.84 | 0.62 |
| 94 | Haptoglobin | HPT_MOUSE | 39 | 13.69 | 16.72 | 25.54 | 9.87 | 10.35 | 15.66 | 0.063 | 18.65 | 11.96 | 0.64 | 8.87 | 11.91 | 24.18 | 28.58 | 28.22 | 50 | 0.018 | 14.99 | 35.60 | 2.38 |
| 453 | Insulin-like growth factor-binding protein 6 | IGBP6_MOUSE | 25 | 3.38 | 2.75 | 4.93 | 1.89 | 2.7 | 5.31 | 0.565 | 3.69 | 3.30 | 0.90 | 2.97 | 1.91 | 4.16 | 1 | 1 | 2.81 | 0.044 | 3.01 | 1.60 | 0.53 |
| 20 | Insulin-like growth factor-binding protein 7 | IGBP7_MOUSE | 29 | 84.26 | 81.33 | 66.77 | 64.89 | 77.53 | 59.66 | 0.167 | 77.45 | 67.36 | 0.87 | 104.26 | 85.53 | 83.19 | 43.63 | 45.41 | 42.74 | 0.020 | 90.99 | 43.93 | 0.48 |
| 449 | Insulin-like growth factor I | IGF1_MOUSE | 17 | 3.38 | 1.87 | 1.98 | 4.55 | 1 | 2.73 | 0.630 | 2.41 | 2.76 | 1.15 | 3.95 | 2.82 | 3.11 | 1 | 1 | 1 | 0.021 | 3.29 | 1.00 | 0.30 X X |
| 68 | Inhibin beta A chain | INHBA_MOUSE | 47 | 31.13 | 28.07 | 11.8 | 29.4 | 35.02 | 21.7 | 0.286 | 23.67 | 28.71 | 1.21 | 26.57 | 27.36 | 25.23 | 19.81 | 16.76 | 13.7 | 0.022 | 26.39 | 16.76 | 0.64 |
| 432 | Leukemia inhibitory factor | LIF_MOUSE | 22 | 1.79 | 2.75 | 1.98 | 5.44 | 4.4 | 2.73 | 0.143 | 2.17 | 4.19 | 1.93 | 4.93 | 4.64 | 4.16 | 1 | 1 | 1 | 0.004 | 4.58 | 1.00 | 0.22 X X X |
| 77 | Lysyl oxidase homolog 2 | LOXL2_MOUSE | 87 | 23.99 | 21.08 | 19.65 | 24.07 | 22.26 | 24.29 | 0.289 | 21.57 | 23.54 | 1.09 | 15.75 | 30.09 | 25.23 | 6.02 | 8.16 | 10.07 | 0.048 | 23.69 | 8.08 | 0.34 |
| 543 | Latent-transforming growth factor beta-binding protein 1 | LTBP1_MOUSE | 187 | 1 | 1 | 2.96 | 1.89 | 1.85 | 3.59 | 0.010 | 1.65 | 2.44 | 1.48 | 1.98 | 1.91 | 5.21 | 2.25 | 1 | 1 | 0.351 | 3.03 | 1.42 | 0.47 |
| 227 | Meteorin-like protein | METRL_MOUSE | 35 | 7.34 | 6.24 | 5.91 | 5.44 | 5.25 | 3.59 | 0.047 | 6.50 | 4.76 | 0.73 | 6.9 | 8.27 | 8.38 | 7.27 | 18.19 | 19.15 | 0.170 | 7.85 | 14.87 | 1.89 |
| 221 | Neuroserpin | NEUS_MOUSE | 46 | 8.93 | 7.11 | 9.83 | 5.44 | 7.8 | 11.35 | 0.809 | 8.62 | 8.20 | 0.95 | 9.85 | 7.36 | 12.59 | 3.51 | 1 | 1 | 0.044 | 9.93 | 1.84 | 0.18 |
| 209 | Neutrophil gelatinase-associated lipocalin | NGAL_MOUSE | 23 | 7.34 | 3.62 | 8.85 | 6.32 | 1.85 | 7.04 | 0.027 | 6.60 | 5.07 | 0.77 | 9.85 | 9.18 | 11.54 | 8.52 | 5.3 | 8.26 | 0.067 | 10.19 | 7.36 | 0.72 |
| 367 | Pappalysin-1 | PAPP1_MOUSE | 181 | 8.93 | 6.24 | 4.93 | 2.77 | 2.7 | 1.86 | 0.047 | 6.70 | 2.44 | 0.36 | 9.85 | 5.54 | 1 | 1 | 1 | 1 | 0.223 | 5.46 | 1.00 | 0.18 |
| 442 | Phospholipase A1 member A | PLA1A_MOUSE | 50 | 7.34 | 2.75 | 2.96 | 1.85 | 4.45 | 4.53 | 0.435 | 3.02 | 0.70 | 4.93 | 2.82 | 3.11 | 2.25 | 1 | 1 | 0.013 | 3.62 | 1.42 | 0.39 | |
| 108 | Pentraxin-related protein PTX3 | PTX3_MOUSE | 42 | 23.99 | 15.84 | 14.74 | 19.64 | 18.86 | 18.25 | 0.802 | 18.19 | 18.92 | 1.04 | 12.8 | 17.36 | 17.86 | 6.02 | 12.46 | 10.07 | 0.017 | 16.01 | 9.52 | 0.59 X X |
| 18 | Sulfhydryl oxidase 1 | QSOX1_MOUSE | 83 | 73.95 | 76.09 | 86.4 | 61.34 | 60.53 | 76.91 | 0.0 | | | | | | | | | | | | | |

| | | | | | | | | | | | | | | | | | | | | | | | |
|-----|--|--------------|-----|-------|-------|--------|-------|-------|--------|--------------|--------------|--------------|-------------|-------|-------|--------|--------|--------|--------------|--------------|--------------|---------------|-------------|
| 514 | Retinoic acid receptor responder protein 2 | RARR2_MOUSE | 18 | 2.59 | 2.75 | 2.96 | 2.77 | 2.7 | 2.73 | 0.805 | 2.77 | 2.73 | 0.99 | 2.97 | 2.82 | 3.11 | 1 | 2.43 | 4.63 | 0.807 | 2.97 | 2.69 | 0.91 |
| 311 | Ribonuclease 4 | RNASE4_MOUSE | 17 | 2.59 | 4.49 | 4.93 | 3.66 | 3.55 | 4.45 | 0.866 | 4.00 | 3.89 | 0.97 | 8.87 | 7.36 | 5.21 | 7.27 | 6.73 | 4.63 | 0.106 | 7.15 | 6.21 | 0.87 |
| 462 | Semaphorin-3A | SEM3A_MOUSE | 89 | 2.59 | 1.87 | 4.93 | 1 | 3.55 | 4.45 | 0.905 | 3.13 | 3.00 | 0.96 | 1.98 | 1.91 | 4.16 | 1 | 3.87 | 10.07 | 0.369 | 2.68 | 4.98 | 1.86 |
| 565 | Semaphorin-3C | SEM3C_MOUSE | 85 | 1 | 1 | 1 | 1.89 | 1 | 5.31 | 0.318 | 1.00 | 2.73 | 2.73 | 2.97 | 4.64 | 1 | 1 | 1 | 1 | 0.217 | 2.87 | 1.00 | 0.35 |
| 279 | Semaphorin-3D | SEM3D_MOUSE | 90 | 2.59 | 12.35 | 6.89 | 1 | 11.2 | 10.49 | 0.879 | 7.28 | 7.56 | 1.04 | 8.87 | 7.36 | 6.27 | 1 | 6.73 | 2.81 | 0.199 | 7.50 | 3.51 | 0.47 |
| 193 | Semaphorin-3E | SEM3E_MOUSE | 90 | 1 | 7.11 | 12.78 | 5.44 | 4.4 | 13.08 | 0.775 | 6.96 | 7.64 | 1.10 | 19.68 | 9.18 | 6.27 | 6.02 | 5.3 | 15.52 | 0.718 | 11.71 | 8.95 | 0.76 |
| 161 | Semaphorin-3F | SEM3F_MOUSE | 88 | 4.17 | 13.22 | 14.74 | 4.55 | 15.46 | 10.49 | 0.805 | 10.71 | 10.17 | 0.95 | 7.88 | 10.09 | 13.64 | 7.27 | 8.16 | 24.59 | 0.564 | 10.54 | 13.34 | 1.27 |
| 341 | Secreted frizzled-related protein 3 | SFRP3_MOUSE | 36 | 4.96 | 2.75 | 6.89 | 5.44 | 6.95 | 3.59 | 0.851 | 4.87 | 5.33 | 1.09 | 2.97 | 4.64 | 1 | 3.51 | 1 | 1 | 0.514 | 2.87 | 1.84 | 0.64 |
| 444 | Slit homolog 2 protein | SLIT2_MOUSE | 169 | 8.93 | 1 | 1 | 3.66 | 5.25 | 1 | 0.913 | 3.64 | 3.30 | 0.91 | 5.92 | 2.82 | 1 | 1 | 1 | 1 | 0.258 | 3.25 | 1.00 | 0.31 |
| 214 | Slit homolog 3 protein | SLIT3_MOUSE | 168 | 3.38 | 7.11 | 7.87 | 8.1 | 8.65 | 9.63 | 0.121 | 6.12 | 8.79 | 1.44 | 4.93 | 8.27 | 8.38 | 6.02 | 2.43 | 11.89 | 0.896 | 7.19 | 6.78 | 0.94 |
| 90 | Superoxide dismutase [Cu-Zn] | SODC_MOUSE | 16 | 16.86 | 14.1 | 17.69 | 22.3 | 16.31 | 18.25 | 0.196 | 16.22 | 18.95 | 1.17 | 20.67 | 11 | 17.86 | 24.82 | 23.92 | 22.78 | 0.120 | 16.51 | 23.84 | 1.44 |
| 41 | Extracellular superoxide dismutase [Cu-Zn] | SODE_MOUSE | 27 | 35.89 | 46.41 | 47.13 | 33.83 | 33.31 | 45.86 | 0.288 | 43.14 | 37.67 | 0.87 | 28.54 | 25.54 | 43.15 | 16.05 | 39.68 | 44.55 | 0.907 | 32.41 | 33.43 | 1.03 |
| 24 | Serine protease inhibitor A3N | SPA3N_MOUSE | 47 | 77.91 | 56.88 | 54.01 | 43.6 | 45.22 | 59.66 | 0.365 | 62.93 | 49.49 | 0.79 | 54.1 | 77.35 | 68.43 | 120.11 | 119.91 | 93.55 | 0.064 | 66.63 | 111.19 | 1.67 |
| 22 | Sushi, von Willebrand factor type A, EGF and pentraxin domain-containing protein 1 | SVEP1_MOUSE | 387 | 94.56 | 81.33 | 66.77 | 72.88 | 72.43 | 58.8 | 0.101 | 80.89 | 68.04 | 0.84 | 53.12 | 79.17 | 36.82 | 53.66 | 65.47 | 13.7 | 0.221 | 56.37 | 44.28 | 0.79 |
| 79 | Transcobalamin-2 | TCO2_MOUSE | 48 | 20.03 | 15.84 | 17.69 | 20.52 | 18.01 | 19.12 | 0.107 | 17.85 | 19.22 | 1.08 | 15.75 | 19.18 | 16.8 | 14.79 | 26.79 | 26.41 | 0.237 | 17.24 | 22.66 | 1.31 |
| 545 | Translationally-controlled tumor protein | TCTP_MOUSE | 19 | 4.17 | 2.75 | 1 | 1 | 2.7 | 2.73 | 0.762 | 2.64 | 2.14 | 0.81 | 1.98 | 1 | 3.11 | 3.51 | 1 | 1 | 0.872 | 2.03 | 1.84 | 0.90 |
| 132 | Tenascin | TENA_MOUSE | 232 | 2.59 | 21.08 | 3.94 | 13.42 | 18.01 | 13.94 | 0.319 | 9.20 | 15.12 | 1.64 | 14.77 | 30.09 | 1 | 19.81 | 9.6 | 1 | 0.577 | 15.29 | 10.14 | 0.66 |
| 340 | Tissue factor pathway inhibitor | TFPI1_MOUSE | 35 | 2.59 | 7.11 | 2.96 | 5.44 | 6.1 | 4.45 | 0.430 | 4.22 | 5.33 | 1.26 | 4.93 | 5.21 | 4.76 | 1 | 6.44 | 0.613 | 4.93 | 4.07 | 0.83 | |
| 257 | Transforming growth factor beta-2 | TGFB2_MOUSE | 48 | 4.96 | 5.37 | 9.83 | 6.32 | 6.1 | 8.76 | 0.686 | 6.72 | 7.06 | 1.05 | 2.97 | 5.54 | 5.21 | 3.51 | 1 | 1 | 0.237 | 4.57 | 1.84 | 0.40 |
| 556 | Protein-glutamine gamma-glutamyltransferase 2 | TGM2_MOUSE | 77 | 1 | 1 | 1.98 | 4.55 | 4.4 | 1.86 | 0.198 | 1.33 | 3.60 | 2.72 | 1.98 | 1 | 2.05 | 1 | 1 | 2.81 | 0.898 | 1.68 | 1.60 | 0.96 |
| 463 | Thioredoxin OS=Mus musculus GN=Tnx PE=1 SV=3 | THIO_MOUSE | 12 | 1 | 3.62 | 2.96 | 5.44 | 2.7 | 6.18 | 0.300 | 2.53 | 4.77 | 1.89 | 1.98 | 1.91 | 2.05 | 2.25 | 1 | 4.63 | 0.593 | 1.98 | 2.63 | 1.33 |
| 50 | Metalloproteinase inhibitor 1 | TIMP1_MOUSE | 23 | 12.89 | 21.08 | 34.37 | 20.52 | 18.86 | 24.29 | 0.790 | 22.78 | 21.22 | 0.93 | 48.2 | 38.27 | 48.41 | 43.63 | 45.41 | 46.37 | 0.965 | 44.96 | 45.14 | 1.00 |
| 45 | Metalloproteinase inhibitor 2 | TIMP2_MOUSE | 24 | 31.92 | 35.05 | 45.17 | 34.72 | 32.46 | 39.82 | 0.548 | 37.38 | 35.67 | 0.95 | 31.49 | 21.91 | 29.45 | 36.11 | 39.68 | 57.26 | 0.130 | 27.62 | 44.35 | 1.61 |
| 450 | Metalloproteinase inhibitor 3 OS=Mus musculus GN=Timp3 PE=2 SV=1 | TIMP3_MOUSE | 24 | 4.96 | 1.87 | 1 | 1.89 | 6.1 | 1 | 0.872 | 2.61 | 3.00 | 1.15 | 4.93 | 2.82 | 2.05 | 1 | 1 | 1 | 0.119 | 3.27 | 1.00 | 0.31 |
| 416 | Tubulointerstitial nephritis antigen-like | TINAL_MOUSE | 53 | 1 | 2.75 | 5.91 | 1 | 4.4 | 6.18 | 0.337 | 3.22 | 3.86 | 1.20 | 1.98 | 4.64 | 9.43 | 1 | 1 | 1 | 0.184 | 5.35 | 1.00 | 0.19 |
| 466 | Tumor necrosis factor receptor superfamily member 11B | TR11B_MOUSE | 46 | 4.96 | 4.49 | 1 | 3.66 | 6.95 | 4.45 | 0.399 | 3.48 | 5.02 | 1.44 | 1 | 4.64 | 1 | 1 | 1 | 0.423 | 2.21 | 1.00 | 0.45 | |
| 15 | Serotransferrin | TRFE_MOUSE | 77 | 51.75 | 54.26 | 181.61 | 43.6 | 64.78 | 118.32 | 0.456 | 95.87 | 75.57 | 0.79 | 69.84 | 83.71 | 142.19 | 83.75 | 144.26 | 258.69 | 0.165 | 98.58 | 162.23 | 1.65 |
| 301 | Thrombospondin-2 | TSP2_MOUSE | 130 | 4.96 | 5.37 | 1.98 | 4.55 | 6.1 | 1 | 0.704 | 4.10 | 3.88 | 0.95 | 2.97 | 5.54 | 1 | 14.79 | 6.73 | 1 | 0.368 | 3.17 | 7.51 | 2.37 |
| 636 | Thrombospondin-3 | TSP3_MOUSE | 104 | 1 | 1 | 1 | 1 | 1 | 1 | N/A | 1.00 | 1.00 | 1.00 | 1.98 | 1.91 | 1 | 1 | 3.87 | 1 | 0.742 | 1.63 | 1.96 | 1.20 |
| 28 | Vascular cell adhesion protein 1 | VCAM1_MOUSE | 81 | 46.2 | 36.8 | 48.12 | 49.81 | 42.67 | 47.58 | 0.253 | 43.71 | 46.69 | 1.07 | 54.1 | 50.99 | 75.81 | 68.7 | 74.06 | 75.4 | 0.212 | 60.30 | 72.72 | 1.21 |
| 272 | Vascular endothelial growth factor A | VEGFA_MOUSE | 25 | 3.38 | 2.75 | 2.96 | 2.77 | 5.25 | 1.86 | 0.837 | 3.03 | 3.29 | 1.09 | 4.93 | 8.27 | 4.16 | 1 | 8.16 | 2.81 | 0.251 | 5.79 | 3.99 | 0.69 |
| 118 | Vascular endothelial growth factor D | VEGFD_MOUSE | 41 | 10.52 | 23.7 | 17.69 | 12.54 | 13.76 | 19.12 | 0.634 | 17.30 | 15.14 | 0.87 | 6.9 | 10.09 | 14.7 | 14.79 | 22.49 | 19.15 | 0.070 | 10.56 | 18.81 | 1.78 |
| 550 | Pantetheinase OS=Mus musculus GN=Vnn1 PE=1 SV=2 | VNN1_MOUSE | 57 | 1 | 1 | 2.96 | 1 | 1 | 2.73 | 0.423 | 1.65 | 1.58 | 0.95 | 9.85 | 1 | 1 | 6.02 | 1 | 1 | 0.423 | 3.95 | 2.67 | 0.68 |
| 607 | von Willebrand factor | VWF_MOUSE | 309 | 4.96 | 1 | 1 | 3.66 | 1 | 1 | 0.423 | 2.32 | 1.89 | 0.81 | 1 | 1 | 1 | 3.51 | 1 | 1 | 0.423 | 1.00 | 1.84 | 1.84 |
| 611 | WNT1-inducible-signaling pathway protein 1 | WISP1_MOUSE | 41 | 1 | 2.75 | 1 | 1 | 3.55 | 1.86 | 0.184 | 1.58 | 2.14 | 1.35 | 1 | 1.91 | 1 | 1 | 1 | 0.423 | 1.30 | 1.00 | 0.77 | |
| 82 | WNT1-inducible-signaling pathway protein 2 | WISP2_MOUSE | 27 | 9.72 | 17.59 | 9.83 | 10.76 | 17.16 | 16.53 | 0.379 | 12.38 | 14.82 | 1.20 | 30.5 | 16.45 | 17.86 | 19.81 | 19.62 | 11.89 | 0.384 | 21.60 | 17.11 | 0.79 |
| 349 | C-C motif chemokine 2 | CCL2_MOUSE | 16 | 1.79 | 2.75 | 1 | 2.77 | 3.55 | 4.45 | 0.178 | 1.85 | 3.59 | 1.94 | 3.95 | 4.64 | 5.21 | 2.25 | 2.43 | 1 | 0.072 | 4.60 | 1.89 | 0.41 |
| 105 | Complement C4-B | CO4B_MOUSE | 193 | 14.48 | 16.72 | 17.69 | 10.76 | 19.71 | 22.57 | 0.649 | 16.30 | 17.68 | 1.08 | 15.75 | 17.36 | 18.91 | 13.54 | 12.46 | 8.26 | 0.140 | 17.34 | 11.42 | 0.66 |

Online-Table III: ECM proteins changes in the secretome of CFs following miR-30c transfection

| # | Identified Proteins | Accession Number | MW (kDa) | Control Anti-miR Sample 1 | Control Anti-miR Sample 2 | Anti-miR Sample 3 | Control Anti-miR-30c Sample 1 | Anti-miR-30c Sample 2 | Anti-miR-30c Sample 3 | t test (paired) | Average Control Anti-miR-30c | Average anti-miR-30c | Ratio | Control Pre-miR Sample 1 | Control Pre-miR Sample 2 | Control Pre-miR Sample 3 | Pre-miR-30c Sample 1 | Pre-miR-30c Sample 2 | Pre-miR-30c Sample 3 | t test (paired) | Average Control pre-miR | Average pre-miR-30c | Ratio | Targetscan | PicTar | Diana | |
|-----|--|------------------|----------|---------------------------|---------------------------|-------------------|-------------------------------|-----------------------|-----------------------|-----------------|------------------------------|----------------------|-------------|--------------------------|--------------------------|--------------------------|----------------------|----------------------|----------------------|-----------------|-------------------------|---------------------|-------------|-------------|--------|-------|--|
| 228 | Collagen alpha-1(XI) chain | COBA1_MOUSE | 181 | 10.44 | 11.74 | 16.16 | 10.34 | 14.37 | 9.72 | 0.676 | 12.78 | 11.48 | 0.90 | 29.5 | 25.37 | 23.61 | 15.2 | 13.45 | 9.48 | 0.003 | 26.16 | 12.71 | 0.49 | | | | |
| 173 | Calumenin | CALU_MOUSE | 37 | 11.62 | 2.79 | 8.58 | 1 | 4.34 | 1 | 0.268 | 7.66 | 2.11 | 0.28 | 13.83 | 36.74 | 12.9 | 5.73 | 3.77 | 3.12 | 0.169 | 21.16 | 4.21 | 0.20 | X | X | | |
| 66 | Collagen alpha-1(V) chain | C05A1_MOUSE | 184 | 24.6 | 26.07 | 22.22 | 19.68 | 24.4 | 19.69 | 0.089 | 24.30 | 21.26 | 0.87 | 45.18 | 41.61 | 31.94 | 60.18 | 48.02 | 48.68 | 0.058 | 39.58 | 52.29 | 1.32 | | | | |
| 5 | Collagen alpha-2(V) chain | C05A2_MOUSE | 145 | 134.34 | 182.74 | 134.37 | 103.75 | 163.68 | 170.46 | 0.847 | 150.48 | 145.96 | 0.97 | 315.93 | 272.31 | 269.98 | 177.35 | 169.71 | 191.71 | 0.026 | 286.07 | 179.59 | 0.63 | | | | |
| 170 | Collagen alpha-1(XV) chain | C0FA1_MOUSE | 140 | 22.24 | 9.06 | 17.67 | 17.01 | 8.8 | 14.71 | 0.189 | 16.32 | 13.51 | 0.83 | 18.1 | 10.75 | 14.09 | 19.94 | 14.83 | 6.3 | 0.880 | 14.31 | 13.69 | 0.96 | | | | |
| 455 | Leukemia inhibitory factor | LIF_MOUSE | 22 | 1 | 1 | 1 | 1 | 1 | NA | 1.00 | 1.00 | 1.00 | | 10.98 | 10.75 | 2.19 | 4.55 | 5.15 | 2.06 | 0.177 | 7.97 | 3.92 | 0.49 | | | | |
| | Scavenger receptor cysteine-rich domain-containing | | | | | | | | | | | | | | | | | | | | | | | | | | |
| 402 | protein LOC284297 homolog | SRCRL_MOUSE | 145 | 4.54 | 3.69 | 4.03 | 7.67 | 6.57 | 3.49 | 0.263 | 4.09 | 5.91 | 1.45 | 15.25 | 4.25 | 8.14 | 6.92 | 6.53 | 6.3 | 0.484 | 9.21 | 6.58 | 0.71 | | | | |
| 393 | Placenta-specific protein 9 | PLAC9_MOUSE | 11 | 3.36 | 4.58 | 1 | 1 | 3.23 | 1 | 0.212 | 2.98 | 1.74 | 0.59 | 6.7 | 9.12 | 4.57 | 1 | 1 | 1 | 0.048 | 6.80 | 1.00 | 0.15 | | | | |
| 3 | Collagen alpha-1(II) chain | C03A1_MOUSE | 139 | 377.43 | 314.35 | 472.34 | 354.6 | 309.64 | 341.16 | 0.312 | 388.04 | 335.13 | 0.86 | 485.51 | 504.62 | 391.38 | 422.34 | 443.51 | 394.08 | 0.202 | 460.50 | 419.98 | | | | | |
| 148 | Laminin subunit alpha-4 | LAMA4_MOUSE | 202 | 13.98 | 20.7 | 25.25 | 9.01 | 8.8 | 7.23 | 0.091 | 19.98 | 8.35 | 0.42 | 2.43 | 18.87 | 3.38 | 8.1 | 9.3 | 9.48 | 0.900 | 8.23 | 8.96 | 1.09 | | | | |
| 454 | Latent-transforming growth factor beta-binding protein 1 | LTBP1_MOUSE | 187 | 4.54 | 2.79 | 1 | 6.34 | 3.23 | 1 | 0.302 | 2.78 | 3.52 | 1.27 | 6.7 | 5.87 | 3.38 | 2.38 | 2.06 | 0.060 | 5.32 | 2.60 | 0.49 | | | | | |
| 127 | Coiled-coil domain-containing protein 80 | CCD80_MOUSE | 108 | 13.98 | 30.54 | 14.64 | 13.01 | 23.28 | 18.44 | 0.690 | 19.72 | 18.24 | 0.93 | 30.93 | 7.5 | 22.42 | 2.18 | 5.15 | 10.54 | 0.205 | 20.28 | 5.96 | 0.29 | | | | |
| 1 | Collagen alpha-1(I) chain | CO1A1_MOUSE | 138 | 380.97 | 330.46 | 493.56 | 331.92 | 291.81 | 331.19 | 0.170 | 401.66 | 318.31 | 0.79 | 616.61 | 543.61 | 525.87 | 388.01 | 496.06 | 427.98 | 0.147 | 562.03 | 437.35 | 0.78 | | | | |
| 48 | Collagen alpha-1(IV) chain | CO4A1_MOUSE | 161 | 15.16 | 15.32 | 10.09 | 11.67 | 14.37 | 14.71 | 0.982 | 13.52 | 13.58 | 1.00 | 23.8 | 22.12 | 21.23 | 16.39 | 21.74 | 24.31 | 0.662 | 22.38 | 20.81 | 0.93 | | | | |
| 7 | SPARC | SPRC_MOUSE | 34 | 251.17 | 114.7 | 313.2 | 269.21 | 221.62 | 215.31 | 0.893 | 226.36 | 235.38 | 1.04 | 261.78 | 319.42 | 204.52 | 259.01 | 288.63 | 207.61 | 0.434 | 261.91 | 251.75 | 0.96 | | | | |
| 167 | Collagen alpha-1(VIII) chain | C08A1_MOUSE | 74 | 3.36 | 7.27 | 4.03 | 2.33 | 5.46 | 1 | 0.078 | 4.89 | 2.93 | 0.60 | 3.85 | 2.62 | 5.76 | 1 | 1 | 5.24 | 0.132 | 4.08 | 2.41 | 0.59 | | | | |
| 12 | Follistatin-related protein 1 | FSTL1_MOUSE | 35 | 127.26 | 70.83 | 176.8 | 151.78 | 112.42 | 121.86 | 0.912 | 124.96 | 128.69 | 1.03 | 154.9 | 160.21 | 109.31 | 140.66 | 137.9 | 87.88 | 0.017 | 141.47 | 122.15 | 0.86 | | | | |
| 321 | Follistatin-related protein 3 | FSTL3_MOUSE | 27 | 4.54 | 2.79 | 5.55 | 5 | 6.57 | 7.23 | 0.179 | 2.49 | 6.27 | 1.46 | 3.85 | 2.62 | 4.57 | 3.37 | 2.38 | 1 | 0.314 | 3.68 | 2.25 | 0.61 | | | | |
| 340 | Ribonuclease T2 | RNT2_MOUSE | 30 | 5.72 | 4.58 | 5.55 | 5 | 7.69 | 4.74 | 0.723 | 5.28 | 5.81 | 1.10 | 6.7 | 7.5 | 4.57 | 5.15 | 4.18 | 0.120 | 6.26 | 4.63 | 0.74 | | | | | |
| 594 | Proteoglycan 4 | PRG4_MOUSE | 116 | 2.18 | 2.79 | 4.03 | 3.67 | 2.11 | 3.49 | 0.910 | 3.00 | 3.09 | 1.03 | 5.28 | 4.25 | 1 | 3.37 | 3.77 | 1 | 0.299 | 3.51 | 2.71 | 0.77 | | | | |
| | Disintegrin and metalloproteinase domain-containing | | | | | | | | | | | | | | | | | | | | | | | | | | |
| 436 | protein 17 | ADA17_MOUSE | 93 | 3.36 | 1.9 | 4.03 | 3.67 | 3.23 | 3.49 | 0.568 | 3.10 | 3.46 | 1.12 | 1 | 4.25 | 4.57 | 3.37 | 3.77 | 1 | 0.775 | 3.27 | 2.71 | 0.83 | | | | |
| 96 | Protein-lysine 6-oxidase | LYOX_MOUSE | 47 | 17.52 | 12.64 | 22.35 | 15.49 | 17.2 | 0.796 | 17.46 | 18.35 | 1.05 | 19.53 | 23.74 | 20.04 | 9.28 | 10.68 | 10.54 | 0.010 | 21.10 | 10.17 | 0.48 | X | | | | |
| 525 | Anthithrombin-III | ANT3_MOUSE | 52 | 5.72 | 1.9 | 1 | 3.67 | 3.23 | 5.98 | 0.557 | 2.87 | 4.29 | 1.49 | 3.85 | 7.5 | 2.19 | 1 | 3.77 | 5.24 | 0.636 | 4.51 | 3.34 | 0.74 | | | | |
| 366 | Secreted frizzled-related protein 1 | SFRP1_MOUSE | 35 | 8.08 | 11.74 | 2.52 | 3.67 | 8.8 | 7.23 | 0.785 | 7.45 | 6.57 | 0.88 | 6.7 | 9.12 | 5.76 | 3.37 | 5.15 | 1 | 0.010 | 7.19 | 3.17 | 0.44 | | | | |
| 2 | Collagen alpha-2(II) chain | CO1A2_MOUSE | 130 | 296.01 | 274.95 | 352.61 | 322.58 | 269.53 | 323.72 | 0.887 | 307.86 | 305.28 | 0.99 | 499.76 | 399.02 | 369.96 | 345.41 | 431.06 | 360.18 | 0.517 | 422.91 | 378.88 | 0.90 | | | | |
| 162 | Integrin beta-1 | ITB1_MOUSE | 88 | 22.24 | 9.95 | 20.7 | 19.68 | 12.14 | 12.21 | 0.440 | 17.63 | 14.68 | 0.83 | 18.1 | 20.5 | 11.71 | 19.94 | 25.89 | 12.65 | 0.183 | 16.77 | 19.49 | 1.16 | | | | |
| 233 | Gamma-glutamyl hydrolase | GGH_MOUSE | 35 | 5.72 | 9.06 | 13.12 | 11.67 | 9.91 | 8.48 | 0.836 | 9.30 | 10.02 | 1.08 | 10.8 | 9.55 | 14 | 6.95 | 5.73 | 3.77 | 5.24 | 0.177 | 10.17 | 4.91 | 0.48 | | | |
| 193 | Microfibrillar-associated protein 5 | MFAP5_MOUSE | 19 | 12.8 | 6.37 | 8.58 | 9.01 | 6.57 | 5.98 | 0.223 | 9.25 | 7.19 | 0.78 | 13.83 | 14 | 9.33 | 9.28 | 6.53 | 6.3 | 0.061 | 12.39 | 7.37 | 0.59 | | | | |
| 19 | Insulin-like growth factor-binding protein 7 | IPB7_MOUSE | 29 | 93.04 | 83.37 | 61.62 | 95.74 | 87.91 | 100.68 | 0.322 | 79.34 | 94.78 | 1.19 | 90.78 | 85.48 | 98.6 | 89.76 | 95.03 | 108.01 | 0.230 | 91.62 | 97.60 | 1.07 | | | | |
| 414 | Angiopoietin-2 | ANGP2_MOUSE | 57 | 11.62 | 1.9 | 5.55 | 10.34 | 2.11 | 3.49 | 0.258 | 6.36 | 5.31 | 0.84 | 3.85 | 2.62 | 1 | 5.73 | 2.38 | 1 | 0.500 | 2.49 | 3.04 | 1.22 | | | | |
| 10 | Collagen alpha-2(IV) chain | COA42_MOUSE | 167 | 30.5 | 37.71 | 40.4 | 42.37 | 22.17 | 62.05 | 0.644 | 36.20 | 42.20 | 1.17 | 87.93 | 65.98 | 104.55 | 35.32 | 34.19 | 68.81 | 0.024 | 86.15 | 46.11 | 0.54 | | | | |
| 51 | Prolargin | PREL_P MOUSE | 43 | 56.56 | 56.51 | 43.44 | 46.37 | 38.88 | 43.36 | 0.210 | 52.14 | 42.87 | 0.82 | 33.78 | 23.74 | 28.37 | 30.59 | 27.27 | 26.43 | 0.820 | 28.63 | 28.10 | 0.98 | | | | |
| 54 | Collagen alpha-2(VI) chain | CO6A2_MOUSE | 110 | 48.2 | 66.35 | 31.31 | 37.03 | 43.34 | 35.89 | 0.342 | 48.62 | 38.75 | 0.80 | 26.65 | 36.74 | 23.61 | 37.69 | 25.89 | 25.37 | 0.928 | 29.00 | 29.65 | 1.02 | | | | |
| 375 | Receptor-type tyrosine-protein phosphatase gamma | PTPRG_MOUSE | 161 | 4.54 | 1.9 | 2.52 | 1 | 1 | 3.49 | 0.470 | 2.99 | 1.83 | 0.61 | 1 | 2.62 | 3.38 | 3.37 | 2.38 | 6.3 | 0.226 | 2.33 | 4.02 | 1.72 | | | | |
| 142 | Epididymal secretory protein E1 | NPC2_MOUSE | 16 | 12.8 | 6.37 | 7.06 | 15.68 | 9.91 | 7.23 | 0.167 | 8.74 | 10.94 | 1.25 | 15.25 | 12.37 | 9.33 | 6.92 | 9.3 | 7.36 | 0.151 | 12.32 | 7.86 | 0.64 | | | | |
| 101 | Dystroglycan | DAG1_MOUSE | 97 | 15.16 | 11.74 | 16.16 | 10.34 | 15.49 | 12.21 | 0.602 | 14.35 | 12.68 | 0.88 | 22.38 | 23.74 | 23.61 | 18.75 | 10.68 | 9.48 | 0.091 | 23.24 | 12.97 | 0.56 | X | X | | |
| 483 | Aggrecan core protein | PGCA_MOUSE | 222 | 4.54 | 1.9 | 1 | 3.67 | 2.11 | 2.25 | 0.778 | 2.48 | 1.08 | 0.67 | 6.7 | 1 | 3.38 | 5.73 | 3.77 | 1 | 0.911 | 3.69 | 3 | | | | | |

| | | | | | | | | | | | | | | | | | | | | | | | |
|---|--------------|-----|-------|-------|-------|-------|-------|--------------|--------------|--------------|--------------|-------------|------|------|-------|-------|------|--------------|--------------|-------------|-------------|-------------|-----|
| 570 Peroxiredoxin-4 | | | | | | | | | | | | | | | | | | | | | | | |
| 311 Epididymis-specific alpha-mannosidase | PRDX4_MOUSE | 31 | 6.9 | 3.69 | 1 | 1 | 4.34 | 8.48 | 0.865 | 3.86 | 4.61 | 1.19 | 1 | 1 | 1 | 12.84 | 1 | 13.71 | 0.184 | 1.00 | 9.18 | 9.18 | |
| 97 Gelsolin | MA2B2_MOUSE | 116 | 3.36 | 10.85 | 1 | 3.67 | 3.23 | 3.49 | 0.653 | 5.07 | 3.46 | 0.68 | 1 | 1 | 2.19 | 2.18 | 1 | 1 | 0.997 | 1.40 | 1.39 | 1.00 | |
| 117 Lysyl oxidase homolog 3 | GELS_MOUSE | 86 | 9.26 | 18.01 | 2.52 | 3.67 | 5.46 | 7.23 | 0.466 | 9.93 | 5.45 | 0.55 | 1 | 4.25 | 2.19 | 4.55 | 1 | 5.24 | 0.661 | 2.48 | 3.60 | 1.45 | |
| 474 Matrilin-2 | LOXL3_MOUSE | 84 | 8.08 | 15.32 | 4.03 | 5 | 5.46 | 8.48 | 0.564 | 9.14 | 6.31 | 0.69 | 1 | 1 | 3.38 | 2.18 | 1 | 1 | 0.739 | 1.79 | 1.39 | 0.78 | |
| 307 Complement factor B | MATN2_MOUSE | 107 | 2.18 | 9.06 | 1 | 1 | 7.69 | 1 | 0.186 | 4.08 | 3.23 | 0.79 | 1 | 1 | 1 | 1 | 1 | 1 | NA | 1.00 | 1.00 | 1.00 | |
| 379 Angiopoietin-related protein 2 | CFAB_MOUSE | 85 | 1 | 1 | 1 | 3.67 | 4.34 | 1 | 0.189 | 1.00 | 3.00 | 3.00 | 1 | 1 | 1 | 1 | 1 | 1 | NA | 1.00 | 1.00 | 1.00 | |
| 296 Pappalysin-1 | ANGL2_MOUSE | 57 | 2.18 | 2.79 | 4.03 | 2.33 | 2.11 | 9.72 | 0.480 | 3.00 | 4.72 | 1.57 | 1 | 1 | 1 | 1 | 1 | 1 | NA | 1.00 | 1.00 | 1.00 | |
| 99 Transcobalamin-2 | PAPP1_MOUSE | 181 | 6.9 | 3.69 | 1 | 6.34 | 3.23 | 5.98 | 0.546 | 3.86 | 5.18 | 1.34 | 1 | 1 | 1 | 1 | 1 | 1 | NA | 1.00 | 1.00 | 1.00 | |
| 181 Phospholipid transfer protein | TCO2_MOUSE | 48 | 6.9 | 19.8 | 7.06 | 9.01 | 11.03 | 12.21 | 0.916 | 11.25 | 10.75 | 0.96 | 1 | 1 | 3.38 | 3.37 | 6.53 | 6.3 | 0.066 | 1.79 | 5.40 | 3.01 | |
| 22 Complement factor H | PLTP_MOUSE | 54 | 3.36 | 15.32 | 1 | 1 | 3.49 | 0.444 | 6.56 | 1.83 | 0.28 | 1 | 1 | 1 | 1 | 1 | 3.12 | 0.423 | 1.00 | 1.71 | 1.71 | | |
| 89 Nidogen-2 | CFAH_MOUSE | 139 | 21.06 | 47.55 | 7.06 | 15.68 | 12.14 | 14.71 | 0.478 | 25.22 | 14.18 | 0.56 | 2.43 | 1 | 17.66 | 14.02 | 1 | 5.24 | 0.972 | 7.03 | 6.75 | 0.96 | |
| 128 Complement C4-B | NID2_MOUSE | 154 | 12.8 | 30.54 | 7.06 | 11.67 | 14.37 | 7.23 | 0.390 | 16.80 | 11.09 | 0.66 | 9.55 | 2.62 | 3.38 | 1 | 1 | 1 | 0.197 | 5.18 | 1.00 | 0.19 | X X |
| 91 Collagen alpha-1(XII) chain | CO4B_MOUSE | 193 | 2.18 | 10.85 | 1 | 14.34 | 16.6 | 7.23 | 0.060 | 4.68 | 12.72 | 2.72 | 1 | 1 | 2.19 | 2.18 | 1 | 6.3 | 0.286 | 1.40 | 3.16 | 2.26 | |
| 100 Fibulin-1 | COCA1_MOUSE | 340 | 3.36 | 6.37 | 1 | 1 | 5.46 | 3.49 | 0.873 | 3.58 | 3.32 | 0.93 | 1 | 2.62 | 6.95 | 1 | 1 | 1 | 0.291 | 3.52 | 1.00 | 0.28 | X |
| 203 Collagen alpha-1(XIV) chain | FBLN1_MOUSE | 78 | 6.9 | 32.33 | 4.03 | 1 | 7.69 | 7.23 | 0.382 | 14.42 | 5.31 | 0.37 | 1 | 1 | 1 | 1 | 2.06 | 0.423 | 1.00 | 1.35 | 1.35 | | |
| 151 Thrombospondin-2 | COCOA1_MOUSE | 193 | 6.9 | 11.74 | 1 | 1 | 5.46 | 3.49 | 0.376 | 6.55 | 3.32 | 0.51 | 1 | 2.62 | 1 | 1 | 1 | 0.423 | 1.54 | 1.00 | 0.65 | | |
| | TSP2_MOUSE | 130 | 5.72 | 14.43 | 11.61 | 6.34 | 24.4 | 8.48 | 0.589 | 10.59 | 13.07 | 1.23 | 1 | 1 | 1 | 1 | 1 | NA | 1.00 | 1.00 | X X | | |

| | | | | | | | | | | | | | | | | | |
|--|---|---------------------------------|------|------|------|------|------|------|------|------|------|------|-----|------|-----|------|-----|
| Bone morphogenetic protein 1 OS=Mus musculus GN=Bmp1 30 PE=2 SV=1 | BMP1_MOUSE 112 kDa | 95% (0.011) | 26.1 | 32.7 | 23.4 | 27.9 | 26.5 | 34.7 | 54.2 | 41.9 | 42.4 | 27.4 | 4.8 | 29.7 | 4.4 | 46.1 | 7.0 |
| 68 Fibromodulin OS=Mus musculus GN=Fmod PE=2 SV=1 Collagen alpha-2(VI) chain OS=Mus musculus GN=Col6a2 78 PE=2 SV=3 | FMOD_MOUSE 43 kDa CO6A2_MOUSE 110 kDa | 0% (0.93) 95% (0.0078) | 25.3 | 17.4 | 13.3 | 22.7 | 13.9 | 14.2 | 13.5 | 23.2 | 15.8 | 18.6 | 6.1 | 16.9 | 5.0 | 17.5 | 5.1 |
| 132 Complement C4-B OS=Mus musculus GN=C4b PE=1 SV=2 | CO4B_MOUSE 193 kDa | 0% (0.095) | 22.1 | 12.3 | 12.9 | 13.6 | 4.6 | 6.1 | 10.3 | 1.0 | 4.3 | 15.8 | 5.5 | 8.1 | 4.8 | 5.2 | 4.7 |
| 61 Granulins OS=Mus musculus GN=Gm PE=1 SV=2 | GRN_MOUSE 63 kDa | 0% (0.27) | 22.1 | 20.5 | 20.1 | 13.9 | 23.7 | 16.3 | 14.7 | 19.3 | 12.9 | 20.9 | 1.1 | 18.0 | 5.1 | 15.6 | 3.3 |
| 95 Prolargin OS=Mus musculus GN=Prep PE=2 SV=2 Peptidyl-prolyl cis-trans isomerase A OS=Mus musculus 52 GN=Ppi PE=1 SV=2 | PRELP_MOUSE 43 kDa PPIA_MOUSE 18 kDa | 95% (0.00019) 0% (0.25) | 22.1 | 23.7 | 18.6 | 17.7 | 12.8 | 12.4 | 2.4 | 2.7 | 3.7 | 21.4 | 2.6 | 14.3 | 3.0 | 2.9 | 0.7 |
| 59 Stromelysin-1 OS=Mus musculus GN=Mmp3 PE=2 SV=2 Carboxypeptidase E OS=Mus musculus GN=Cpe PE=1 67 SV=2 | MMP3_MOUSE 54 kDa CBPE_MOUSE 53 kDa | 95% (0.0087) 95% (0.0050) | 20.4 | 19.0 | 28.4 | 20.5 | 26.2 | 28.1 | 11.3 | 10.9 | 11.7 | 22.6 | 5.1 | 24.9 | 3.9 | 11.3 | 0.4 |
| 70 Ceruloplasmin OS=Mus musculus GN=Cp PE=1 SV=2 Superoxide dismutase [Cu-Zn] OS=Mus musculus GN=Sod1 109 PE=1 SV=2 | CERU_MOUSE 121 kDa SODC_MOUSE 16 kDa | 0% (0.23) 0% (0.32) | 19.5 | 9.8 | 16.0 | 15.6 | 8.0 | 14.7 | 21.4 | 15.3 | 21.2 | 15.1 | 4.9 | 12.7 | 4.1 | 19.3 | 3.5 |
| 71 Wnt1-inducible-signaling pathway protein 2 OS=Mus musculus GN=Wisp2 PE=2 SV=1 | WISP2_MOUSE 27 kDa | 0% (0.17) | 18.9 | 22.3 | 12.2 | 19.8 | 16.0 | 15.1 | 12.7 | 13.4 | 10.7 | 17.8 | 5.1 | 17.0 | 2.5 | 12.3 | 1.4 |
| 112 PE=2 SV=2 Macrophage colony-stimulating factor 1 OS=Mus musculus 45 GN=Csf1 PE=1 SV=2 | CO5A1_MOUSE 184 kDa CSF1_MOUSE 61 kDa | 95% (0.00043) 95% (0.000052) | 18.5 | 16.7 | 12.2 | 20.5 | 25.3 | 17.5 | 1.0 | 1.0 | 1.0 | 15.8 | 3.3 | 21.1 | 3.9 | 1.0 | 0.0 |
| 103 Dystroglycan OS=Mus musculus GN=Dag1 PE=1 SV=4 Lysyl oxidase homolog 1 OS=Mus musculus GN=Loxl1 PE=2 66 SV=3 Procollagen C-endopeptidase enhancer 1 OS=Mus musculus | DAG1_MOUSE 97 kDa LOXL1_MOUSE 67 kDa | 0% (0.081) 0% (0.10) | 18.5 | 17.9 | 11.1 | 17.2 | 14.5 | 16.8 | 9.4 | 12.9 | 9.2 | 15.8 | 4.1 | 16.2 | 1.4 | 10.5 | 2.1 |
| 56 GN=Pcolce PE=1 SV=2 EGF-containing fibulin-like extracellular matrix protein 2 57 OS=Mus musculus GN=Etemp2 PE=2 SV=1 Plasma glutamate carboxypeptidase OS=Mus musculus | PCOC1_MOUSE 50 kDa FBLN4_MOUSE 49 kDa | 95% (0.031) 95% (0.0040) | 17.9 | 18.7 | 19.7 | 15.3 | 20.3 | 19.3 | 26.2 | 31.8 | 22.2 | 18.8 | 0.9 | 18.3 | 2.7 | 26.8 | 4.8 |
| 85 GN=Pcp PE=2 SV=1 A disintegrin and metalloproteinase with thrombospondin 80 motifs 5 OS=Mus musculus GN=Adams5 PE=2 SV=1 Sulfated glycoprotein 1 OS=Mus musculus GN=Psap PE=1 92 SV=2 | PGCP_MOUSE 52 kDa ATTS5_MOUSE 102 kDa | 0% (0.059) 95% (0.0038) | 15.3 | 14.1 | 12.4 | 16.3 | 16.5 | 13.1 | 11.1 | 12.7 | 10.8 | 13.9 | 1.5 | 15.3 | 1.9 | 11.6 | 1.0 |
| 111 Cathepsin B OS=Mus musculus GN=Ctsb PE=1 SV=2 Coiled-coil domain-containing protein 80 OS=Mus musculus 131 GN=Cdc80 PE=1 SV=2 | CATB_MOUSE 37 kDa CCD80_MOUSE 108 kDa | 95% (0.041) 0% (0.66) | 14.5 | 9.7 | 10.7 | 8.9 | 7.8 | 8.9 | 13.3 | 16.2 | 12.1 | 11.7 | 2.5 | 8.5 | 0.6 | 13.8 | 2.1 |
| 82 Fibulin-5 OS=Mus musculus GN=Fbln5 PE=2 SV=1 Pigment epithelium-derived factor OS=Mus musculus 54 GN=Serpinf1 PE=1 SV=2 Vascular endothelial growth factor D OS=Mus musculus 148 GN=Fgf PE=2 SV=1 | FBLN5_MOUSE 50 kDa PEDF_MOUSE 46 kDa | 0% (0.56) 0% (0.21) | 13.6 | 18.1 | 17.3 | 14.7 | 16.3 | 15.2 | 13.4 | 12.3 | 17.4 | 16.3 | 2.4 | 15.4 | 0.8 | 14.4 | 2.6 |
| 108 Gelsolin OS=Mus musculus GN=Gsn PE=1 SV=3 120 Fibulin-1 OS=Mus musculus GN=Fbln1 PE=1 SV=2 Glucose-6-phosphate isomerase OS=Mus musculus GN=Gpi 125 PE=1 SV=4 | VEGFD_MOUSE 41 kDa GELS_MOUSE 86 kDa | 95% (0.014) 95% (0.029) | 12.0 | 8.5 | 10.4 | 8.3 | 7.0 | 6.6 | 6.4 | 6.7 | 5.3 | 10.3 | 1.7 | 7.3 | 0.9 | 6.1 | 0.7 |
| 118 Lactadherin OS=Mus musculus GN=Mfge8 PE=1 SV=2 145 Dermatopontin OS=Mus musculus GN=Dpt PE=2 SV=1 164 Ribonuclease 4 OS=Mus musculus GN=Rnase4 PE=2 SV=1 | INHBB_MOUSE 51 kDa DERM_MOUSE 24 kDa RNAS4_MOUSE 17 kDa | 0% (0.070) 0% (0.39) | 9.7 | 10.1 | 7.8 | 8.0 | 7.5 | 7.8 | 10.6 | 6.8 | 11.4 | 9.2 | 1.3 | 7.8 | 0.2 | 9.6 | 2.5 |
| 160 Transcobalamin-2 OS=Mus musculus GN=Tcn2 PE=2 SV=1 Inhibin beta B chain OS=Mus musculus GN=Inhhb PE=2 414 SV=4 Thymosin beta-4 OS=Mus musculus GN=Tmsb4x PE=1 | TCO2_MOUSE 48 kDa INHBB_MOUSE 45 kDa | 0% (0.12) 95% (0.048) | 9.7 | 8.0 | 8.1 | 4.1 | 7.8 | 4.5 | 5.8 | 8.6 | 6.6 | 8.6 | 1.0 | 5.4 | 2.0 | 7.0 | 1.5 |
| 168 SV=1 Epididymal secretory protein E1 OS=Mus musculus 154 GN=Npc2 PE=2 SV=1 Probable carboxypeptidase X1 OS=Mus musculus | TYB4_MOUSE 6 kDa NPC2_MOUSE 16 kDa | 0% (0.88) 0% (0.27) | 9.5 | 9.6 | 4.4 | 5.9 | 8.0 | 7.0 | 5.1 | 9.3 | 8.9 | 7.8 | 3.0 | 7.0 | 1.0 | 7.8 | 2.3 |
| 218 GN=Cpxm1 PE=2 SV=1 | CPXM1_MOUSE 81 kDa | 95% (0.0053) | 9.3 | 8.1 | 5.9 | 5.5 | 5.3 | 2.5 | 1.0 | 1.0 | 1.0 | 7.7 | 1.7 | 4.4 | 1.7 | 1.0 | 0.0 |
| 128 Cofilin-1 OS=Mus musculus GN=Cfl1 PE=1 SV=3 166 Protein CYR61 OS=Mus musculus GN=Cyr61 PE=1 SV=1 180 Spondin-2 OS=Mus musculus GN=Spon2 PE=1 SV=2 | COF1_MOUSE 19 kDa CYR61_MOUSE 42 kDa SPON2_MOUSE 36 kDa | 0% (0.082) 0% (0.73) | 9.2 | 10.3 | 7.9 | 10.2 | 8.5 | 11.1 | 10.4 | 13.0 | 14.6 | 9.1 | 1.2 | 9.9 | 1.3 | 12.6 | 2.1 |
| 73 Biglycan OS=Mus musculus GN=Bgn PE=2 SV=1 Phospholipid transfer protein OS=Mus musculus GN=Pltp 165 PE=1 SV=1 | PGS1_MOUSE 42 kDa PLTP_MOUSE 54 kDa | 95% (0.048) 0% (0.23) | 9.0 | 11.4 | 11.6 | 11.7 | 20.1 | 14.0 | 24.1 | 15.5 | 27.7 | 10.7 | 1.4 | 15.3 | 4.4 | 22.4 | 6.3 |

| Beta-2-microglobulin OS=Mus musculus GN=B2m PE=1 | | | | | | | | | | | | | | | | | | | | | |
|---|---|---|---|--------------|--------------|--------------|------|------|------|------|------|------|------|------|------|------|------|------|------|------|-----|
| 175 | SV=1 | B2MG_MOUSE | 14 kDa | 0% (0.79) | 8.8 | 1.0 | 1.0 | 1.0 | 6.9 | 1.0 | 1.0 | 11.7 | 3.8 | 3.6 | 4.5 | 3.0 | 3.4 | 5.5 | 5.5 | | |
| Peroxidasin homolog OS=Mus musculus GN=Pxdn PE=2 | | PXDN_MOUSE | 165 kDa | 0% (0.24) | 8.8 | 17.6 | 16.7 | 17.8 | 24.1 | 20.1 | 7.3 | 9.5 | 21.0 | 14.4 | 4.9 | 20.7 | 3.2 | 12.6 | 7.4 | | |
| 81 | SV=1 | PGS2_MOUSE | 40 kDa | 0% (0.18) | 8.5 | 6.7 | 10.3 | 7.1 | 8.0 | 6.0 | 11.5 | 8.2 | 9.7 | 8.5 | 1.8 | 7.1 | 1.0 | 9.8 | 1.7 | | |
| 136 | Decorin OS=Mus musculus GN=Dcn PE=2 SV=1 | TSP1_MOUSE | 130 kDa | 95% (0.0091) | 8.2 | 8.2 | 5.2 | 7.8 | 6.3 | 10.0 | 2.9 | 1.0 | 2.8 | 7.2 | 1.7 | 8.0 | 1.9 | 2.2 | 1.1 | | |
| Thrombospondin-1 OS=Mus musculus GN=Thbs1 PE=1 | | NID1_MOUSE | 137 kDa | 0% (0.060) | 8.1 | 3.6 | 6.1 | 4.6 | 1.0 | 4.1 | 1.0 | 1.0 | 1.0 | 5.9 | 2.3 | 3.2 | 1.9 | 1.0 | 0.0 | | |
| 194 | SV=1 | MMP2_MOUSE | 74 kDa | 95% (0.0084) | 7.8 | 15.4 | 12.3 | 19.4 | 18.7 | 15.6 | 4.6 | 9.4 | 4.8 | 11.9 | 3.8 | 17.9 | 2.0 | 6.3 | 2.7 | | |
| 272 | Nidogen-1 OS=Mus musculus GN=Nid1 PE=1 SV=1 | ISLR_MOUSE | 46 kDa | 95% (0.026) | 7.6 | 1.0 | 2.7 | 1.0 | 1.0 | 1.0 | 7.0 | 7.5 | 6.5 | 3.8 | 3.4 | 1.0 | 0.0 | 7.0 | 0.5 | | |
| 72 | kDa type IV collagenase OS=Mus musculus GN=Mmp2 | CRLF1_MOUSE | 47 kDa | 0% (0.58) | 7.3 | 5.5 | 6.6 | 7.9 | 3.7 | 4.1 | 6.3 | 5.6 | 3.6 | 6.5 | 0.9 | 5.2 | 2.4 | 5.2 | 1.4 | | |
| 110 | PE=2 SV=1 | NGAL_MOUSE | 23 kDa | 95% (0.020) | 6.7 | 8.9 | 6.8 | 12.1 | 9.6 | 9.8 | 3.5 | 4.5 | 7.6 | 7.5 | 1.3 | 10.5 | 1.4 | 5.2 | 2.1 | | |
| Immunoglobulin superfamily containing leucine-rich repeat | | Lysyl oxidase homolog 2 OS=Mus musculus GN=Loxl2 PE=2 | LOXL2_MOUSE | 87 kDa | 95% (0.029) | 6.6 | 10.9 | 11.1 | 8.5 | 14.3 | 14.8 | 4.8 | 5.9 | 4.2 | 9.5 | 2.5 | 12.5 | 3.5 | 4.9 | 0.9 | |
| A disintegrin and metalloproteinase with thrombospondin | | ATS2_MOUSE | 135 kDa | 0% (0.62) | 6.4 | 7.5 | 7.2 | 1.0 | 7.7 | 7.8 | 4.3 | 7.1 | 4.4 | 7.0 | 0.5 | 5.5 | 3.9 | 5.3 | 1.6 | | |
| 183 | motifs 2 OS=Mus musculus GN=Adams2 PE=1 SV=2 | C-X-C motif chemokine 5 OS=Mus musculus GN=Cxcl5 | CXCL5_MOUSE | 14 kDa | 0% (0.10) | 6.3 | 8.2 | 4.4 | 7.1 | 9.1 | 5.9 | 1.0 | 5.3 | 3.8 | 6.3 | 1.9 | 7.4 | 1.6 | 3.4 | 2.2 | |
| 205 | PE=1 SV=1 | Semaphorin-3D OS=Mus musculus GN=Sema3d PE=1 | SEM3D_MOUSE | 90 kDa | 95% (0.0027) | 6.3 | 6.5 | 7.8 | 6.9 | 4.5 | 4.9 | 2.4 | 1.0 | 1.8 | 6.9 | 0.8 | 5.4 | 1.3 | 1.7 | 0.7 | |
| 210 | SV=1 | Kalliukrein-8 OS=Mus musculus GN=Klk8 PE=1 SV=1 | KLK8_MOUSE | 29 kDa | 0% (0.13) | 6.2 | 1.0 | 3.2 | 1.0 | 3.1 | 4.5 | 1.0 | 1.0 | 1.0 | 3.5 | 2.6 | 2.9 | 1.8 | 1.0 | 0.0 | |
| A disintegrin and metalloproteinase with thrombospondin | | 287 | motifs 1 OS=Mus musculus GN=Adams1 PE=1 SV=3 | ATS1_MOUSE | 106 kDa | 95% (0.027) | 6.1 | 3.0 | 3.9 | 1.0 | 5.7 | 3.9 | 1.0 | 1.0 | 1.0 | 4.3 | 1.6 | 3.5 | 2.3 | 1.0 | 0.0 |
| Slit homolog 3 protein OS=Mus musculus GN=Slc3 PE=2 | | 243 | SV=1 | SLC3_MOUSE | 168 kDa | 0% (0.14) | 5.8 | 6.0 | 1.0 | 3.1 | 4.3 | 1.8 | 1.0 | 2.9 | 2.8 | 4.3 | 2.8 | 3.1 | 1.3 | 2.2 | 1.1 |
| Penetratin-related protein PTX3 OS=Mus musculus GN=Ptix3 | | 221 | PE=1 SV=2 | PTX3_MOUSE | 42 kDa | 95% (0.012) | 5.8 | 12.0 | 11.9 | 1.0 | 6.2 | 3.9 | 1.0 | 1.0 | 1.0 | 9.9 | 3.6 | 3.7 | 2.6 | 1.0 | 0.0 |
| Disintegrin and metalloproteinase domain-containing protein | | 187 | 9 OS=Mus musculus GN=Adam9 PE=1 SV=1 | ADAM9_MOUSE | 92 kDa | 95% (0.048) | 5.8 | 5.4 | 3.4 | 5.2 | 4.8 | 3.6 | 7.8 | 8.9 | 5.9 | 4.8 | 1.3 | 4.5 | 0.8 | 7.5 | 1.5 |
| 44 | | Periostin OS=Mus musculus GN=Postn PE=1 SV=2 | POSTN_MOUSE | 93 kDa | 0% (0.16) | 5.8 | 11.1 | 12.9 | 13.1 | 40.9 | 36.2 | 27.8 | 13.8 | 42.7 | 9.9 | 3.7 | 30.1 | 14.9 | 28.1 | 14.5 | |
| 268 | | Mimecan OS=Mus musculus GN=Ogn PE=2 SV=1 | MIME_MOUSE | 34 kDa | 0% (0.49) | 5.2 | 1.0 | 1.0 | 3.3 | 5.2 | 4.8 | 3.8 | 4.3 | 1.0 | 2.4 | 2.4 | 4.4 | 1.0 | 3.0 | 1.8 | |
| Mammalian ependymin-related protein 1 OS=Mus musculus | | 276 | GN=Epdrl PE=2 SV=1 | EPDR1_MOUSE | 25 kDa | 0% (0.95) | 5.1 | 2.7 | 1.0 | 1.0 | 1.0 | 4.2 | 4.5 | 1.0 | 1.0 | 2.9 | 2.1 | 2.1 | 1.8 | 2.2 | 2.0 |
| Protein CTLA-2-alpha OS=Mus musculus GN=Ctla2a PE=2 | | 242 | SV=2 | CTL2A_MOUSE | 16 kDa | 0% (0.097) | 4.9 | 4.0 | 6.1 | 4.0 | 7.0 | 5.1 | 1.0 | 3.0 | 3.9 | 5.0 | 1.0 | 5.3 | 1.5 | 2.6 | 1.5 |
| Glia-derived nexin OS=Mus musculus GN=Serpine2 PE=2 | | 239 | SV=2 | GDN_MOUSE | 44 kDa | 0% (0.21) | 4.8 | 5.0 | 3.6 | 1.0 | 3.5 | 2.7 | 1.0 | 5.8 | 2.8 | 4.5 | 0.8 | 2.4 | 1.3 | 3.2 | 2.4 |
| Complement C1q tumor necrosis factor-related protein 5 | | 138 | OS=Mus musculus GN=C1qrnf5 PE=2 SV=1 | C1Q1T5_MOUSE | 25 kDa | 95% (0.0010) | 4.8 | 5.4 | 4.3 | 5.2 | 4.8 | 6.6 | 9.5 | 12.1 | 13.1 | 4.8 | 0.6 | 5.5 | 0.9 | 11.5 | 1.8 |
| 215 | | Protein FAM3C OS=Mus musculus GN=Fam3c PE=1 SV=1 | FAM3C_MOUSE | 25 kDa | 0% (0.43) | 4.8 | 3.6 | 7.0 | 5.3 | 4.3 | 6.4 | 4.3 | 4.5 | 3.4 | 5.1 | 1.8 | 5.3 | 1.1 | 4.0 | 0.6 | |
| Growth-regulated alpha protein OS=Mus musculus | | 389 | GN=Cxcl1 PE=1 SV=1 | GROA_MOUSE | 10 kDa | 95% (0.0069) | 4.8 | 1.0 | 3.3 | 2.4 | 3.4 | 1.0 | 1.0 | 1.0 | 1.0 | 3.0 | 1.9 | 2.3 | 1.2 | 1.0 | 0.0 |
| Interleukin-1 receptor accessory protein OS=Mus musculus | | 277 | GN=Il1trap PE=1 SV=1 | IL1AP_MOUSE | 66 kDa | 95% (0.024) | 4.5 | 2.8 | 2.5 | 3.1 | 1.0 | 4.1 | 1.0 | 1.0 | 1.0 | 3.3 | 1.1 | 2.7 | 1.6 | 1.0 | 0.0 |
| Semaphorin-3E OS=Mus musculus GN=Sema3e PE=2 | | 285 | SV=2 | SEM3E_MOUSE | 90 kDa | 0% (0.27) | 4.5 | 3.8 | 4.1 | 1.0 | 1.0 | 1.0 | 1.0 | 1.0 | 4.1 | 0.4 | 1.0 | 0.0 | 1.0 | 0.0 | |
| 252 | | Biotinidase OS=Mus musculus GN=Btd PE=1 SV=2 | BTD_MOUSE | 58 kDa | 95% (0.024) | 4.5 | 1.0 | 1.0 | 3.1 | 1.0 | 1.7 | 7.4 | 9.4 | 4.8 | 2.2 | 2.0 | 1.9 | 1.0 | 7.2 | 2.3 | |
| Protein NOV homolog OS=Mus musculus GN=Nov PE=2 | | 413 | SV=1 | NOV_MOUSE | 39 kDa | 0% (0.27) | 3.9 | 1.0 | 2.7 | 1.0 | 1.0 | 1.0 | 1.0 | 1.0 | 2.5 | 1.4 | 1.0 | 0.0 | 1.0 | 0.0 | |
| 162 | | Calsyntenin-1 OS=Mus musculus GN=Cln1 PE=1 SV=1 | CSTN1_MOUSE | 109 kDa | 0% (0.14) | 3.7 | 8.1 | 4.2 | 10.1 | 7.1 | 8.2 | 4.8 | 6.7 | 6.1 | 5.3 | 2.4 | 8.4 | 1.5 | 5.8 | 1.0 | |
| 98 | | EMILIN-1 OS=Mus musculus GN=Emilin1 PE=1 SV=1 | EMIL1_MOUSE | 108 kDa | 95% (0.0089) | 3.7 | 8.1 | 4.2 | 13.7 | 18.6 | 13.1 | 11.1 | 15.3 | 16.7 | 5.3 | 2.4 | 15.1 | 3.0 | 14.4 | 2.9 | |
| Inter-alpha-trypsin inhibitor heavy chain 2 OS=Mus | | 353 | musculus GN=Iith2 PE=1 SV=1 | ITIH2_MOUSE | 106 kDa | 0% (0.72) | 3.7 | 1.8 | 1.0 | 7.2 | 1.0 | 1.0 | 1.0 | 1.0 | 2.2 | 1.4 | 3.1 | 3.6 | 1.0 | 0.0 | |
| Beta-nerve growth factor OS=Mus musculus GN=Ngf PE=1 | | 371 | SV=2 | NGF_MOUSE | 27 kDa | 0% (0.42) | 3.7 | 3.0 | 1.0 | 1.0 | 1.0 | 5.7 | 1.0 | 1.0 | 1.0 | 2.6 | 1.4 | 2.6 | 2.7 | 1.0 | 0.0 |
| Serine protease 23 OS=Mus musculus GN=Prss23 PE=2 | | 274 | SV=2 | PRSS23_MOUSE | 43 kDa | 0% (0.79) | 3.7 | 1.0 | 2.9 | 3.0 | 1.0 | 4.1 | 3.9 | 3.0 | 2.9 | 2.5 | 1.4 | 2.7 | 1.6 | 3.3 | 0.5 |
| Polypeptide N-acetylgalactosaminyltransferase 2 OS=Mus | | 420 | musculus GN=Galnt2 PE=2 SV=1 | GALT2_MOUSE | 65 kDa | 95% (0.0056) | 3.6 | 1.0 | 3.3 | 1.0 | 1.0 | 1.0 | 1.0 | 1.0 | 2.6 | 1.4 | 1.0 | 0.0 | 1.0 | 0.0 | |
| Microfibrillar-associated protein 5 OS=Mus musculus | | 193 | GN=Mfap5 PE=2 SV=1 | MFAP5_MOUSE | 19 kDa | 0% (0.24) | 3.1 | 1.0 | 5.5 | 5.6 | 6.2 | 4.6 | 1.0 | 4.8 | 5.6 | 3.2 | 2.2 | 5.5 | 0.8 | 3.8 | 2.4 |
| Fructose-bisphosphate aldolase A OS=Mus musculus | | 99 | GN=Aldoa PE=1 SV=2 | ALDOA_MOUSE | 39 kDa | 95% (0.0023) | 2.9 | 7.3 | 12.5 | 7.5 | 12.0 | 10.7 | 25.2 | 21.3 | 22.9 | 7.6 | 4.8 | 10.0 | 2.3 | 23.1 | 2.0 |
| Beta-2-microglobulin OS=Mus musculus GN=B2m PE=1 | | 222 | Calumenin OS=Mus musculus GN=Calu PE=1 SV=1 | CALU_MOUSE | 37 kDa | 95% (0.0020) | 2.9 | 2.0 | 3.6 | 8.3 | 8.9 | 6.3 | 2.9 | 1.0 | 2.8 | 0.8 | 7.8 | 1.4 | 1.6 | 1.1 | |
| Haptoglobin OS=Mus musculus GN=Hp PE=1 SV=1 | | 122 | Disintegrin and metalloproteinase domain-containing protein | HPT_MOUSE | 39 kDa | 95% (0.0064) | 2.9 | 10.5 | 6.2 | 8.1 | 7.7 | 8.8 | 16.6 | 21.7 | 15.4 | 6.5 | 3.8 | 8.2 | 0.6 | 17.9 | 3.3 |
| 294 | | 15 OS=Mus musculus GN=Adam15 PE=1 SV=2 | ADA15_MOUSE | 93 kDa | 0% (0.44) | 2.9 | 4.7 | 1.0 | 1.0 | 1.0 | 1.0 | 1.7 | 5.8 | 1.0 | 2.9 | 1.9 | 1.0 | 0.0 | 2.8 | 2.6 | |
| Translationaly-controlled tumor protein OS=Mus musculus | | 231 | GN=Tctp PE=1 SV=1 | TCTP_MOUSE | 19 kDa | 0% (0.63) | 2.9 | 5.4 | 4.3 | 5.2 | 4.8 | 3.6 | 1.0 | 1.0 | 5.6 | 4.2 | 1.2 | 4.5 | 0.8 | 2.5 | 2.6 |
| Olfactomedin-like protein 3 OS=Mus musculus GN=Olfml3 | | 198 | PE=2 SV=2 | OLFL3_MOUSE | 46 kDa | 95% (0.0059) | 2.7 | 1.9 | 3.4 | 4.1 | 2.8 | 2.5 | 5.7 | 9.1 | 10.0 | 2.7 | 0.8 | 3.1 | 0.9 | 8.3 | 2.3 |

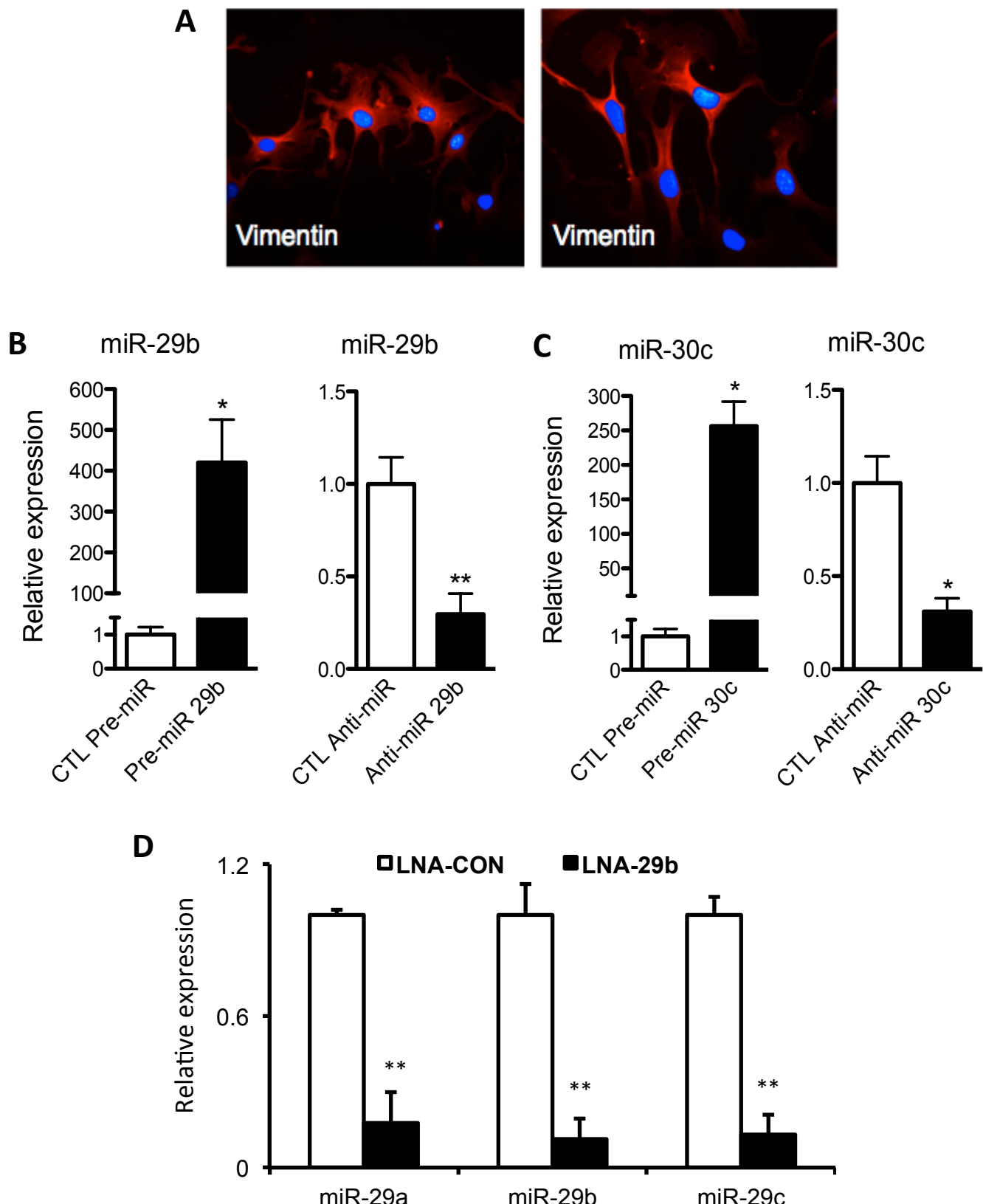
| Follistatin-related protein 3 OS=Mus musculus GN=Fstl3 | FSTL3_MOUSE 27 kDa | 0% (0.17) | 2.6 | 4.8 | 4.3 | 7.7 | 7.3 | 3.6 | 5.6 | 9.7 | 6.4 | 3.9 | 1.2 | 6.2 | 2.3 | 7.3 | 2.1 | |
|--|--|---------------------|---------------|-----|-----|-----|------|------|------|------|------|------|-----|-----|------|-----|------|-----|
| 178 PE=1 SV=1 | | | | | | | | | | | | | | | | | | |
| UPF0556 protein C19orf10 homolog OS=Mus musculus | CS010_MOUSE 18 kDa | 0% (0.093) | 2.4 | 1.0 | 2.9 | 1.0 | 1.0 | 1.0 | 2.9 | 2.0 | 1.0 | 2.1 | 1.0 | 1.0 | 0.0 | 2.0 | 1.0 | |
| 384 GN=D17Vsu104E PE=2 SV=1 | Disintegrin and metalloproteinase domain-containing protein | ADA19_MOUSE 101 kDa | 95% (0.0074) | 1.9 | 1.0 | 2.6 | 2.6 | 1.0 | 2.7 | 1.0 | 1.0 | 1.8 | 0.8 | 2.1 | 0.9 | 1.0 | 0.0 | |
| 400 19 OS=Mus musculus GN=Adam19 PE=2 SV=2 | Acid sphingomyelinase-like phosphodiesterase 3a OS=Mus | ASM3A_MOUSE 50 kDa | 95% (0.0047) | 1.8 | 1.0 | 1.0 | 1.0 | 1.0 | 1.0 | 1.0 | 1.0 | 1.3 | 0.5 | 1.0 | 0.0 | 1.0 | 0.0 | |
| 495 musculus GN=Smpd3a PE=2 SV=1 | Disintegrin and metalloproteinase domain-containing protein | ADA10_MOUSE 84 kDa | 95% (0.035) | 1.0 | 1.0 | 1.0 | 1.0 | 1.0 | 1.0 | 3.2 | 7.3 | 1.8 | 1.0 | 0.0 | 1.0 | 0.0 | 4.1 | 2.8 |
| 365 Agrin OS=Mus musculus GN=Agrn PE=2 SV=1 | Apolipoprotein A-I-binding protein OS=Mus musculus | AGRIN_MOUSE 208 kDa | 95% (0.050) | 1.0 | 1.0 | 3.4 | 1.0 | 1.0 | 3.6 | 1.0 | 1.0 | 1.8 | 1.4 | 1.9 | 1.5 | 1.0 | 0.0 | |
| 391 GN=Apoa1bp1 PE=1 SV=1 | Aminocarboxyl tRNA synthetase complex-interacting multifunctional protein 1 OS=Mus musculus GN=Aimp1 | AIBP_MOUSE 31 kDa | 95% (0.027) | 1.0 | 1.8 | 1.0 | 1.0 | 1.0 | 1.0 | 3.5 | 1.8 | 3.4 | 1.3 | 0.5 | 1.0 | 0.0 | 2.9 | 0.9 |
| 453 PE=1 SV=2 | | | | | | | | | | | | | | | | | | |
| 151 Serum albumin OS=Mus musculus GN=Alb PE=1 SV=3 | Albumin OS=Mus musculus | ALBU_MOUSE 69 kDa | 0% (0.22) | 1.0 | 9.0 | 5.9 | 1.0 | 1.0 | 1.0 | 12.5 | 1.0 | 8.1 | 5.3 | 4.0 | 1.0 | 0.0 | 7.2 | 5.8 |
| Angiopoietin-related protein 2 OS=Mus musculus | ANGL2_MOUSE 57 kDa | 0% (0.31) | 1.0 | 1.0 | 1.0 | 1.0 | 3.1 | 1.0 | 1.0 | 1.0 | 1.8 | 1.0 | 0.0 | 1.7 | 1.2 | 1.3 | 0.5 | |
| 449 GN=Angpt2 PE=2 SV=1 | 279 Arylsulfatase A OS=Mus musculus GN=Arsa PE=2 SV=1 | ARSA_MOUSE 54 kDa | 0% (0.20) | 1.0 | 1.0 | 1.0 | 1.0 | 1.0 | 1.0 | 2.4 | 1.0 | 2.7 | 1.0 | 0.0 | 1.0 | 0.0 | 2.0 | 0.9 |
| Beta-1,4-galactosyltransferase 1 OS=Mus musculus | 340 GN=B4galt1 PE=2 SV=1 | B4GT1_MOUSE 44 kDa | 0% (0.18) | 1.0 | 1.0 | 1.0 | 1.0 | 2.6 | 1.0 | 2.7 | 1.9 | 5.6 | 1.0 | 0.0 | 1.5 | 0.9 | 3.4 | 2.0 |
| Brain-derived neurotrophic factor OS=Mus musculus | 442 GN=Bdnf PE=1 SV=1 | BDNF_MOUSE 28 kDa | 0% (0.60) | 1.0 | 1.0 | 1.0 | 1.0 | 1.0 | 1.0 | 1.0 | 1.0 | 1.0 | 1.0 | 0.0 | 1.3 | 0.5 | 1.0 | 0.0 |
| Adenyl cyclase-associated protein 1 OS=Mus musculus | 439 GN=Cap1 PE=1 SV=3 | CAP1_MOUSE 52 kDa | 0% (0.20) | 1.0 | 1.0 | 1.0 | 1.0 | 1.0 | 1.0 | 1.0 | 1.0 | 4.5 | 1.0 | 0.0 | 1.0 | 0.0 | 2.2 | 2.0 |
| Macrophage-capping protein OS=Mus musculus GN=Capg | 293 PE=1 SV=2 | CAPG_MOUSE 39 kDa | 95% (0.048) | 1.0 | 1.0 | 1.0 | 1.0 | 4.3 | 3.6 | 4.8 | 4.8 | 2.8 | 1.0 | 0.0 | 3.0 | 1.7 | 4.1 | 1.1 |
| 485 CD109 antigen OS=Mus musculus GN=Cd109 PE=2 SV=1 | CD109_MOUSE 162 kDa | 0% (0.61) | 1.0 | 1.0 | 1.0 | 1.0 | 1.0 | 1.0 | 3.1 | 1.0 | 1.0 | 1.0 | 0.0 | 1.0 | 0.0 | 1.7 | 1.2 | |
| Complement factor B OS=Mus musculus GN=Cfb PE=1 | 421 SV=2 | CFAB_MOUSE 85 kDa | 0% (0.46) | 1.0 | 1.0 | 1.0 | 1.0 | 1.0 | 1.0 | 3.2 | 1.0 | 1.0 | 1.0 | 0.0 | 1.0 | 0.0 | 1.7 | 1.3 |
| 208 Clustering OS=Mus musculus GN=Clu PE=1 SV=1 | Collagen alpha-1(VIII) chain OS=Mus musculus GN=Col8a1 | CLUS_MOUSE 52 kDa | 0% (0.54) | 1.0 | 9.7 | 7.5 | 1.0 | 5.2 | 7.2 | 3.8 | 10.8 | 9.2 | 6.1 | 4.5 | 4.5 | 3.2 | 7.9 | 3.7 |
| 220 PE=1 SV=3 | Collagen alpha-1(XI) chain OS=Mus musculus GN=Col11a1 | C08A1_MOUSE 74 kDa | 95% (0.032) | 1.0 | 8.7 | 8.7 | 1.0 | 7.3 | 1.0 | 1.0 | 1.0 | 1.0 | 6.2 | 4.5 | 3.1 | 3.6 | 1.0 | 0.0 |
| 246 PE=1 SV=1 | Collagen triple helix repeat-containing protein 1 OS=Mus | COBA1_MOUSE 181 kDa | 95% (0.00089) | 1.0 | 1.0 | 1.0 | 7.9 | 13.3 | 11.3 | 1.0 | 1.8 | 1.0 | 1.0 | 0.0 | 10.8 | 2.8 | 1.3 | 0.5 |
| 214 musculus GN=Cthrc1 PE=2 SV=1 | CTHR1_MOUSE 26 kDa | 95% (0.021) | 1.0 | 3.6 | 3.4 | 1.0 | 4.2 | 3.7 | 5.3 | 7.6 | 7.1 | 2.7 | 1.4 | 2.9 | 1.7 | 6.7 | 1.2 | |
| C-X-C motif chemokine 16 OS=Mus musculus GN=Cxcl16 | 248 PE=1 SV=2 | CXL16_MOUSE 27 kDa | 95% (0.013) | 1.0 | 1.0 | 1.0 | 1.0 | 1.0 | 1.0 | 6.4 | 7.9 | 7.0 | 1.0 | 0.0 | 1.0 | 0.0 | 7.1 | 0.7 |
| Dickkopf-related protein 3 OS=Mus musculus GN=Dkk3 | 176 PE=1 SV=1 | DKK3_MOUSE 38 kDa | 95% (0.00038) | 1.0 | 2.8 | 2.5 | 1.0 | 1.0 | 4.9 | 9.6 | 11.0 | 12.7 | 2.1 | 1.0 | 2.3 | 2.3 | 11.1 | 1.6 |
| 451 Elastin OS=Mus musculus GN=Eln PE=2 SV=1 | Growth/differentiation factor 15 OS=Mus musculus | ELN_MOUSE 72 kDa | 95% (0.00024) | 1.0 | 1.0 | 1.0 | 1.0 | 1.0 | 1.0 | 1.9 | 3.1 | 2.9 | 1.0 | 0.0 | 1.0 | 0.0 | 2.6 | 0.7 |
| 377 GN=Gdf15 PE=2 SV=1 | Gamma-glutamyl hydrolase OS=Mus musculus GN=Ggh | GDF15_MOUSE 33 kDa | 95% (0.0026) | 1.0 | 4.1 | 4.4 | 1.0 | 4.6 | 1.0 | 1.0 | 1.0 | 1.0 | 3.2 | 1.9 | 2.2 | 2.1 | 1.0 | 0.0 |
| 447 PE=1 SV=1 | Serine protease HTRA1 OS=Mus musculus GN=Htra1 PE=2 | GGH_MOUSE 35 kDa | 95% (0.021) | 1.0 | 2.0 | 1.0 | 1.0 | 1.0 | 1.0 | 1.0 | 1.0 | 1.0 | 1.3 | 0.6 | 1.0 | 0.0 | 1.0 | 0.0 |
| 362 SV=1 | Insulin-like growth factor-binding protein 6 OS=Mus | HTRA1_MOUSE 51 kDa | 0% (0.72) | 1.0 | 1.0 | 2.9 | 1.0 | 1.0 | 1.8 | 1.0 | 1.0 | 1.0 | 1.6 | 1.1 | 1.3 | 0.5 | 1.0 | 0.0 |
| 440 musculus GN=Igfbp6 PE=2 SV=1 | Insulin-like growth factor I OS=Mus musculus GN=Igf1 PE=2 | IBP6_MOUSE 25 kDa | 0% (0.48) | 1.0 | 1.0 | 1.0 | 1.7 | 1.0 | 1.0 | 1.0 | 1.0 | 1.0 | 1.0 | 0.0 | 1.2 | 0.4 | 1.0 | 0.0 |
| 227 SV=2 | Interleukin-6 OS=Mus musculus GN=Il6 PE=1 SV=1 | IGF1_MOUSE 17 kDa | 95% (0.0076) | 1.0 | 1.0 | 1.0 | 4.8 | 6.9 | 5.9 | 3.8 | 1.0 | 3.8 | 1.0 | 0.0 | 5.8 | 1.1 | 2.9 | 1.6 |
| 344 Interleukin-6 OS=Mus musculus GN=Il6 PE=1 SV=1 | Interferon-alpha/beta receptor beta chain OS=Mus musculus | IL6_MOUSE 24 kDa | 0% (0.84) | 1.0 | 1.8 | 2.6 | 1.0 | 3.2 | 1.0 | 1.0 | 1.0 | 4.3 | 1.8 | 0.8 | 1.7 | 1.3 | 2.1 | 1.9 |
| 327 GN=Infrar2 PE=1 SV=1 | Inar2_MOUSE 57 kDa | 0% (0.53) | 1.0 | 1.0 | 1.0 | 1.0 | 1.0 | 1.0 | 1.0 | 6.4 | 1.0 | 1.0 | 1.0 | 0.0 | 1.0 | 0.0 | 2.8 | 3.1 |
| Laminin subunit alpha-1 OS=Mus musculus GN=Lama1 | 490 PE=1 SV=1 | LAMA1_MOUSE 338 kDa | 0% (0.42) | 1.0 | 1.0 | 1.0 | 1.0 | 2.1 | 1.0 | 1.0 | 1.0 | 1.0 | 1.0 | 0.0 | 1.4 | 0.6 | 1.0 | 0.0 |
| Laminin subunit alpha-2 OS=Mus musculus GN=Lama2 | 259 PE=1 SV=1 | LAMA2_MOUSE 343 kDa | 0% (0.11) | 1.0 | 4.6 | 1.0 | 8.1 | 4.2 | 1.0 | 1.0 | 1.0 | 1.0 | 2.2 | 2.0 | 4.4 | 3.5 | 1.0 | 0.0 |
| Laminin subunit alpha-5 OS=Mus musculus GN=Lama5 | 348 PE=1 SV=3 | LAMA5_MOUSE 404 kDa | 0% (0.36) | 1.0 | 8.0 | 1.0 | 1.0 | 6.3 | 1.0 | 1.0 | 1.0 | 1.0 | 3.3 | 4.0 | 2.8 | 3.1 | 1.0 | 0.0 |
| Laminin subunit beta-2 OS=Mus musculus GN=Lamb2 PE=2 | 497 SV=1 | LAMB2_MOUSE 196 kDa | 0% (0.62) | 1.0 | 1.0 | 1.0 | 1.0 | 2.2 | 1.0 | 1.0 | 1.0 | 2.7 | 1.0 | 0.0 | 1.4 | 0.7 | 1.6 | 1.0 |
| Laminin subunit gamma-1 OS=Mus musculus GN=Lamc1 | 403 PE=1 SV=2 | LAMC1_MOUSE 177 kDa | 0% (0.27) | 1.0 | 1.0 | 1.0 | 2.1 | 1.0 | 1.0 | 6.3 | 1.0 | 1.8 | 1.0 | 0.0 | 1.4 | 0.6 | 3.0 | 2.8 |
| Leukemia inhibitory factor OS=Mus musculus GN=Lif PE=1 | 305 SV=1 | LIF_MOUSE 22 kDa | 95% (0.0093) | 1.0 | 1.0 | 1.0 | 3.1 | 4.3 | 5.4 | 1.0 | 1.0 | 1.0 | 1.0 | 0.0 | 4.3 | 1.2 | 1.0 | 0.0 |
| Lysyl oxidase homolog 3 OS=Mus musculus GN=Lox3 PE=2 | 83 SV=1 | LOXL3_MOUSE 84 kDa | 95% (0.00074) | 1.0 | 2.7 | 3.4 | 3.7 | 8.0 | 9.0 | 30.5 | 40.0 | 24.1 | 2.4 | 1.2 | 6.9 | 2.8 | 31.5 | 8.0 |
| Latent-transforming growth factor beta-binding protein 1 | 321 OS=Mus musculus GN=Ltpb1 PE=2 SV=2 | LTBP1_MOUSE 187 kDa | 95% (0.0051) | 1.0 | 1.0 | 1.0 | 4.8 | 4.6 | 4.7 | 1.0 | 4.0 | 3.8 | 1.0 | 0.0 | 4.7 | 0.1 | 2.9 | 1.7 |
| Latent-transforming growth factor beta-binding protein 2 | 60 OS=Mus musculus GN=Ltpb2 PE=1 SV=2 | LTBP2_MOUSE 196 kDa | 95% (0.00021) | 1.0 | 1.0 | 1.0 | 11.8 | 23.1 | 19.5 | 30.5 | 33.9 | 39.9 | 1.0 | 0.0 | 18.1 | 5.8 | 34.8 | 4.7 |
| Latent-transforming growth factor beta-binding protein 4 | 206 OS=Mus musculus GN=Ltpb4 PE=2 SV=1 | LTBP4_MOUSE 179 kDa | 95% (0.0064) | 1.0 | 1.0 | 1.0 | 3.1 | 4.2 | 1.0 | 6.3 | 14.2 | 13.7 | 1.0 | 0.0 | 2.8 | 1.6 | 11.4 | 4.4 |
| 217 Lumican OS=Mus musculus GN=Lum PE=1 SV=2 | LUM_MOUSE 38 kDa | 0% (0.084) | 1.0 | 2.9 | 1.0 | 1.0 | 4.5 | 4.2 | 5.0 | 10.7 | 4.6 | 1.6 | 1.1 | 3.2 | 1.9 | 6.8 | 3.4 | |

| | | | | | | | | | | | | | | | | | | | |
|---|-------------|---------|---------------|--|-----|-----|-----|-----|-----|-----|-----|-----|-----|-----|-----|-----|-----|-----|-----|
| Mesencephalic astrocyte-derived neurotrophic factor | | | | | | | | | | | | | | | | | | | |
| 320 OS=Mus musculus GN=Manf PE=1 SV=1 | MANF_MOUSE | 20 kDa | 95% (0.038) | | 1.0 | 1.0 | 1.0 | 4.2 | 1.0 | 1.0 | 2.9 | 1.0 | 1.0 | 1.0 | 0.0 | 2.1 | 1.8 | 1.6 | 1.1 |
| Multiple epidermal growth factor-like domains protein 6 | MEGF6_MOUSE | 165 kDa | 95% (0.0012) | | 1.0 | 1.0 | 1.0 | 1.0 | 1.0 | 1.0 | 4.8 | 3.8 | 2.3 | 1.0 | 0.0 | 1.0 | 0.0 | 3.6 | 1.3 |
| 406 OS=Mus musculus GN=Megf6 PE=2 SV=3 | METRL_MOUSE | 35 kDa | 95% (0.040) | | 1.0 | 1.0 | 2.2 | 1.0 | 4.2 | 1.0 | 3.8 | 4.3 | 4.6 | 1.4 | 0.7 | 2.1 | 1.8 | 4.2 | 0.4 |
| 302 SV=1 | MFAP4_MOUSE | 29 kDa | 95% (0.010) | | 1.0 | 1.0 | 1.0 | 1.0 | 3.1 | 1.0 | 4.7 | 8.6 | 4.6 | 1.0 | 0.0 | 1.7 | 1.2 | 6.0 | 2.3 |
| 300 GN=Mfap4 PE=1 SV=1 | MIF_MOUSE | 13 kDa | 0% (0.16) | | 1.0 | 1.0 | 4.4 | 3.6 | 1.0 | 4.7 | 6.4 | 6.7 | 3.8 | 2.1 | 2.0 | 3.1 | 1.9 | 5.6 | 1.6 |
| Macrophage migration inhibitory factor OS=Mus musculus | MMP19_MOUSE | 59 kDa | 0% (0.47) | | 1.0 | 1.0 | 1.8 | 1.0 | 1.8 | 2.6 | 1.9 | 3.1 | 1.9 | 1.3 | 0.4 | 1.8 | 0.8 | 2.3 | 0.7 |
| 251 GN=Mif PE=1 SV=2 | NEUS_MOUSE | 46 kDa | 95% (0.00026) | | 1.0 | 1.0 | 2.0 | 2.8 | 2.5 | 1.0 | 1.0 | 1.0 | 1.0 | 1.0 | 0.0 | 2.4 | 0.4 | 1.0 | 0.0 |
| Matrix metalloproteinase-19 OS=Mus musculus GN=Mmp19 | NID2_MOUSE | 154 kDa | 0% (0.11) | | 1.0 | 1.0 | 1.0 | 1.0 | 1.0 | 1.0 | 1.0 | 3.9 | 9.1 | 1.0 | 0.0 | 1.0 | 0.0 | 4.7 | 4.1 |
| 428 Neuroserpin OS=Mus musculus GN=Serpini1 PE=1 SV=1 | PAPP1_MOUSE | 181 kDa | 95% (0.0069) | | 1.0 | 1.0 | 2.1 | 1.0 | 1.0 | 2.2 | 6.3 | 3.8 | 7.3 | 1.4 | 0.6 | 1.4 | 0.7 | 5.8 | 1.8 |
| Proprotein convertase subtilisin/kexin type 5 OS=Mus | PCSK5_MOUSE | 209 kDa | 0% (0.25) | | 1.0 | 1.0 | 1.0 | 1.0 | 5.3 | 1.0 | 4.0 | 3.8 | 3.0 | 1.0 | 0.0 | 2.4 | 2.5 | 3.6 | 0.5 |
| 317 musculus GN=Pcsk5 PE=2 SV=2 | PDGF6_MOUSE | 43 kDa | 95% (0.010) | | 1.0 | 3.0 | 3.6 | 3.1 | 2.6 | 2.7 | 1.0 | 1.0 | 1.0 | 2.5 | 1.4 | 2.8 | 0.3 | 1.0 | 0.0 |
| Platelet-derived growth factor D OS=Mus musculus | PLA1A_MOUSE | 50 kDa | 95% (0.041) | | 1.0 | 2.8 | 1.0 | 1.0 | 3.7 | 3.3 | 1.0 | 1.0 | 1.0 | 1.6 | 1.0 | 2.6 | 1.4 | 1.0 | 0.0 |
| 323 GN=Pdgfd PE=2 SV=1 | PLAC9_MOUSE | 11 kDa | 95% (0.00025) | | 1.0 | 1.0 | 3.2 | 5.6 | 6.5 | 5.5 | 1.0 | 1.0 | 1.0 | 1.7 | 1.2 | 5.8 | 0.5 | 1.0 | 0.0 |
| Phospholipase A1 member A OS=Mus musculus GN=Pla1a | PROS_MOUSE | 75 kDa | 0% (0.099) | | 1.0 | 2.9 | 3.5 | 4.1 | 1.0 | 1.0 | 3.7 | 6.3 | 5.7 | 2.5 | 1.3 | 2.0 | 1.8 | 5.2 | 1.3 |
| 379 PE=2 SV=2 | SFRP3_MOUSE | 36 kDa | 0% (0.11) | | 1.0 | 2.4 | 1.0 | 1.0 | 5.2 | 2.4 | 1.0 | 1.0 | 1.8 | 1.5 | 0.8 | 2.9 | 2.1 | 1.3 | 0.5 |
| Placenta-specific protein 9 OS=Mus musculus GN=Plac9 | SLIT2_MOUSE | 169 kDa | 0% (0.19) | | 1.0 | 1.0 | 1.0 | 1.0 | 1.0 | 2.7 | 1.0 | 1.0 | 1.0 | 1.0 | 0.0 | 1.6 | 1.0 | 1.0 | 0.0 |
| 310 PE=2 SV=1 | TENAA_MOUSE | 232 kDa | 0% (0.065) | | 1.0 | 1.0 | 1.0 | 1.0 | 1.0 | 1.0 | 4.2 | 1.0 | 1.0 | 1.0 | 0.0 | 1.0 | 0.0 | 2.1 | 1.8 |
| Vitamin K-dependent protein S OS=Mus musculus | TGFB2_MOUSE | 48 kDa | 95% (0.029) | | 1.0 | 4.1 | 4.4 | 1.0 | 4.6 | 4.4 | 1.0 | 1.0 | 1.0 | 3.2 | 1.9 | 3.3 | 2.0 | 1.0 | 0.0 |
| 271 GN=Pros1 PE=2 SV=1 | TR11B_MOUSE | 46 kDa | 95% (0.028) | | 1.0 | 1.0 | 1.0 | 1.0 | 4.9 | 1.0 | 1.0 | 1.0 | 1.0 | 1.0 | 0.0 | 2.3 | 2.2 | 1.0 | 0.0 |
| Secreted frizzled-related protein 3 OS=Mus musculus | UCRP_MOUSE | 18 kDa | 0% (0.53) | | 1.0 | 1.0 | 1.0 | 1.0 | 2.8 | 1.0 | 1.0 | 1.0 | 1.0 | 1.0 | 0.0 | 1.6 | 1.1 | 1.0 | 0.0 |
| 241 GN=Frzb PE=1 SV=1 | VNN1_MOUSE | 57 kDa | 0% (0.42) | | 1.0 | 1.0 | 1.0 | 1.0 | 1.6 | 1.0 | 1.0 | 1.0 | 1.0 | 1.0 | 0.0 | 1.2 | 0.4 | 1.0 | 0.0 |
| Slit homolog 2 protein OS=Mus musculus GN=Slit2 PE=2 | | | | | | | | | | | | | | | | | | | |
| 436 SV=1 | | | | | | | | | | | | | | | | | | | |
| Sushi repeat-containing protein SRPX2 OS=Mus musculus | | | | | | | | | | | | | | | | | | | |
| 318 GN=Srpox2 PE=2 SV=1 | | | | | | | | | | | | | | | | | | | |
| 455 Tenascin OS=Mus musculus GN=Tnc PE=1 SV=1 | | | | | | | | | | | | | | | | | | | |
| Transforming growth factor beta-2 OS=Mus musculus | | | | | | | | | | | | | | | | | | | |
| 335 GN=Tgb2 PE=2 SV=1 | | | | | | | | | | | | | | | | | | | |
| Tumor necrosis factor receptor superfamily member 11B | | | | | | | | | | | | | | | | | | | |
| 370 OS=Mus musculus GN=Trnfrsf11b PE=2 SV=1 | | | | | | | | | | | | | | | | | | | |
| Ubiquitin cross-reactive protein OS=Mus musculus | | | | | | | | | | | | | | | | | | | |
| 481 GN=Igsg15 PE=1 SV=4 | | | | | | | | | | | | | | | | | | | |
| 501 Pantetheinase OS=Mus musculus GN=Vnn1 PE=1 SV=2 | | | | | | | | | | | | | | | | | | | |

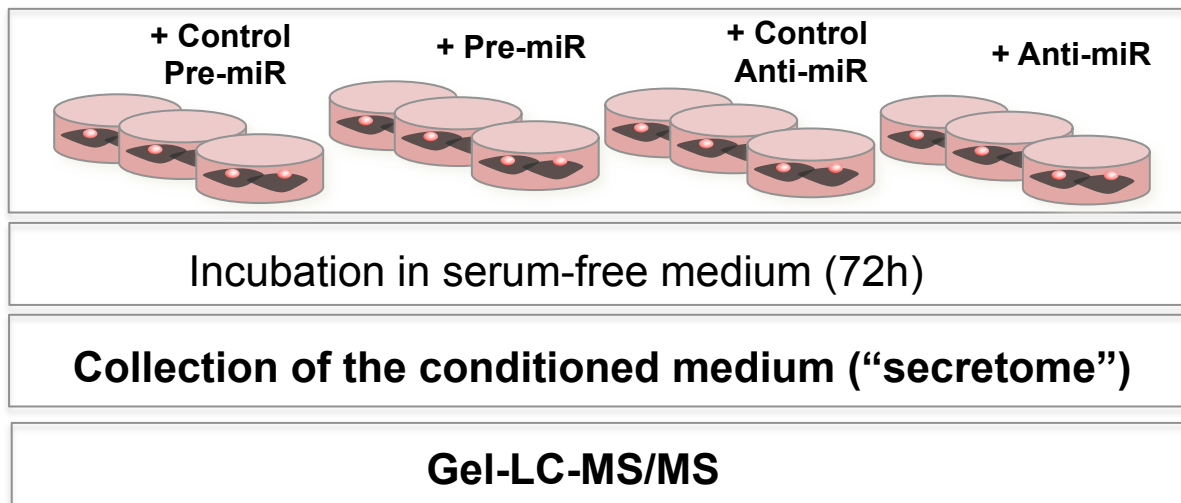
Online-Table V: Echocardiography data of antagomiR-29b treated hearts after TAC (n=9 per group)

| | Control | | | antagomir | | | T-test |
|--|-------------|------------|------------|-------------|------------|------------|-------------|
| | Mean (9) | SD | SE | Mean (9) | SD | SE | |
| Body weight (baseline) | 20.2 | 2.6 | 0.9 | 20.1 | 2.4 | 0.8 | 0.81 |
| Body weight (2 week) | 22.6 | 2.9 | 1.0 | 22.9 | 3.2 | 1.1 | 0.99 |
| HW/T | 9.0 | 1.8 | 0.6 | 9.9 | 1.5 | 0.5 | 0.28 |
| M-mode (combined PSLAX and SAX) | | | | | | | |
| Heart Rate | 517.8 | 54.8 | 18.3 | 513.2 | 51.6 | 17.2 | 0.82 |
| Diameter;s | 3.3 | 0.3 | 0.1 | 3.3 | 0.5 | 0.2 | 0.84 |
| Diameter;d | 4.1 | 0.2 | 0.1 | 4.1 | 0.4 | 0.1 | 0.96 |
| Volume;s | 43.4 | 11.0 | 3.7 | 46.1 | 15.7 | 5.2 | 0.77 |
| Volume;d | 73.6 | 9.8 | 3.3 | 74.9 | 17.2 | 5.7 | 0.95 |
| Stroke Volume | 30.2 | 4.6 | 1.5 | 28.8 | 3.1 | 1.0 | 0.41 |
| Ejection Fraction | 41.7 | 7.8 | 2.6 | 39.7 | 7.1 | 2.4 | 0.64 |
| Fractional Shortening | 20.3 | 4.3 | 1.4 | 19.2 | 3.8 | 1.3 | 0.62 |
| Cardiac Output | 15.6 | 2.5 | 0.8 | 14.8 | 2.0 | 0.7 | 0.41 |
| B-mode (SAX) | | | | | | | |
| IVS;d | 0.9 | 0.1 | 0.0 | 0.9 | 0.1 | 0.0 | 0.46 |
| IVS;s | 1.2 | 0.2 | 0.1 | 1.2 | 0.1 | 0.0 | 0.97 |
| LVID;d | 4.2 | 0.5 | 0.2 | 4.3 | 0.5 | 0.2 | 0.81 |
| LVID;s | 3.2 | 0.5 | 0.2 | 3.4 | 0.5 | 0.2 | 0.45 |
| LVPW;d | 0.9 | 0.1 | 0.0 | 1.1 | 0.2 | 0.1 | 0.13 |
| LVPW;s | 1.2 | 0.1 | 0.0 | 1.2 | 0.1 | 0.0 | 0.91 |

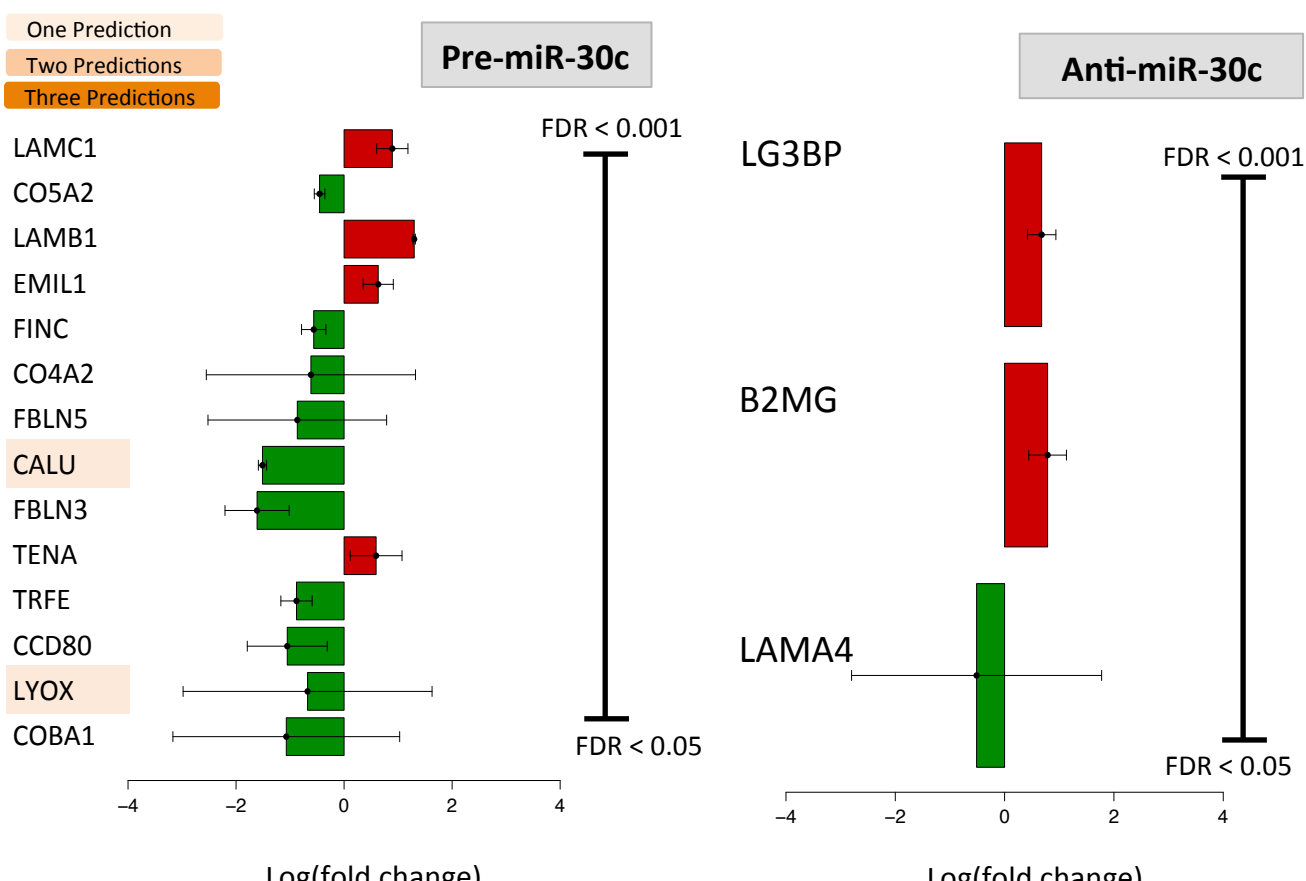
Online Figure I: A) Vimentin immunostaining after collagenase-based digestion of mouse hearts. Following collagenase-based digestion of mouse hearts, primary mouse CFs were cultured on gelatin 0.1% and grown in DMEM medium supplemented with L-Glutamine, 10% heat-inactivated FBS and antibiotics (100 U/ml penicillin and 100 µg/ml streptomycin) at 37°C in a humidified atmosphere of 95% air / 5% CO₂. Cells were detached with 0.05% trypsin for passaging. At passage 2, the cells were plated on 8-well chamber slides for immunostaining (Vimentin: red, DAPI:blue). **B, C)** Confirmation of over-expression and inhibition of miR-29b and miR-30c by qPCR. **D)** LNA-anti-miRs to miR-29b also reduced the expression of the other miR-29 family members. *P<0.05, **P<0.01.



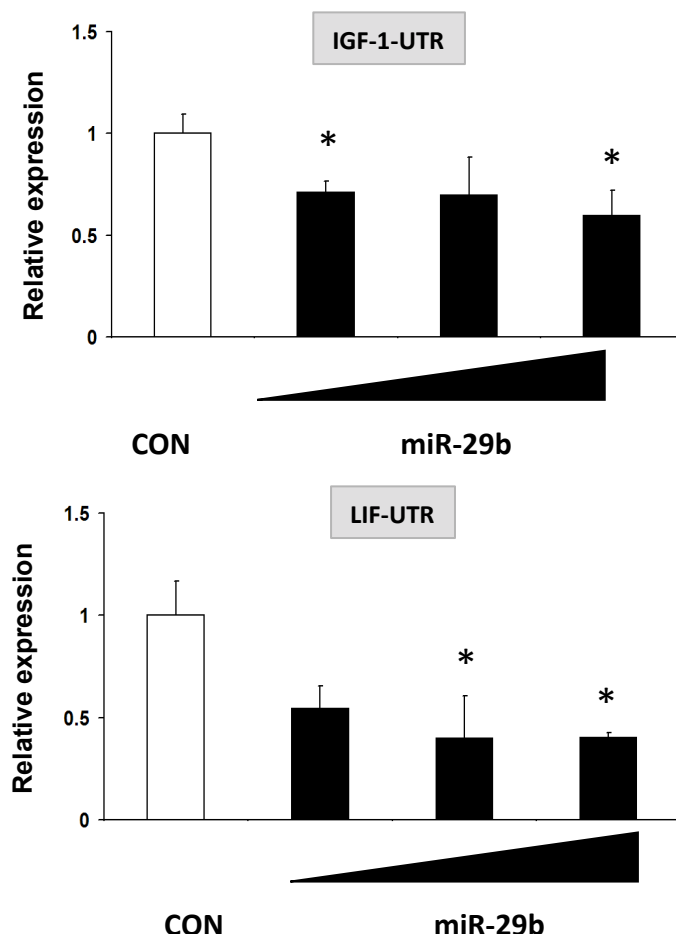
Online Figure II: Schematic description of the proteomics workflow. CFs were isolated from mouse heart by collagenase-based digestion. At passage 2-3, CFs (3 biological replicates per experimental condition) were transfected with a miRNA construct and then, incubated in serum-free medium. After 72h, the conditioned medium was collected, cleared from cell debris by centrifugation, desalting, and resuspended in loading buffer. An equal volume of sample (30 µl) was separated on a SDS-PAGE gel, digested with trypsin and analysed by LC-MS/MS using a high mass accuracy LTQ-Orbitrap XL.



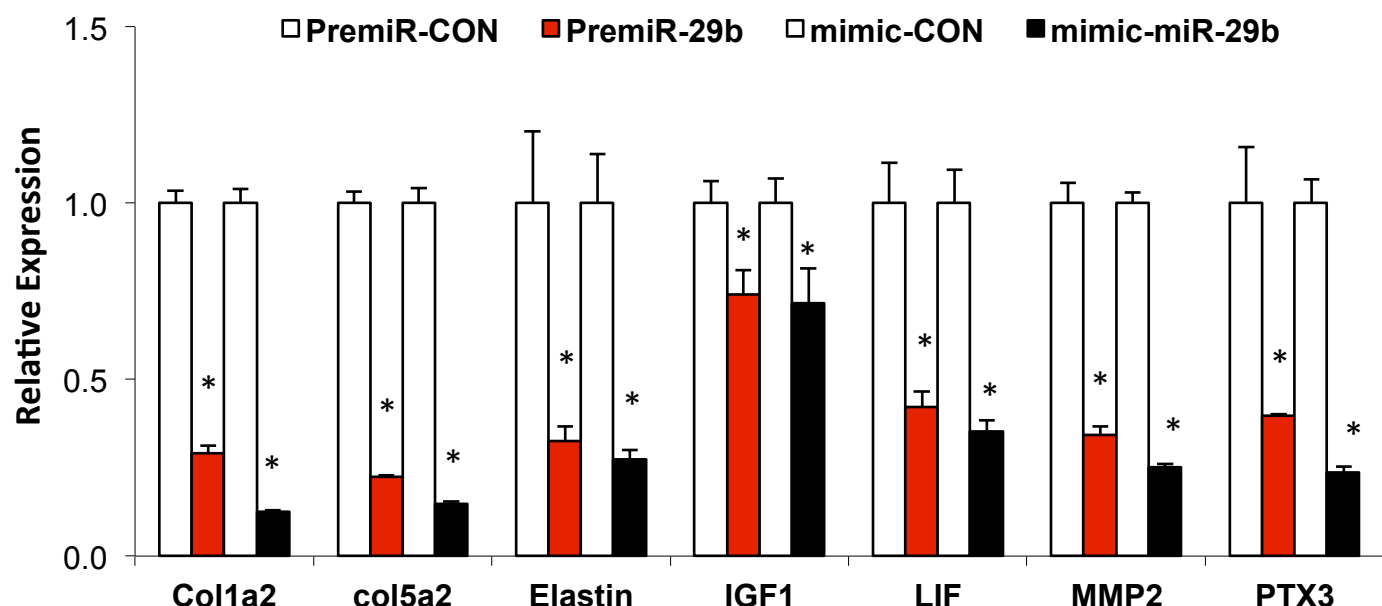
Online Figure III: The log(fold change) for each of the differentially released proteins in the miR-30c experiment is illustrated. The proteins are ordered from the smallest to largest False Discovery Rate (FDR) with significant differential expression set at a FDR 5% (<0.05). The differential release and corresponding FDR was calculated using the Qspec method which utilises a model based on a hierarchical Bayes estimation of generalized linear mixed effects model (GLMM). The FDR, as per the Qspec method, was calculated using the Bayes Factors and a mixture model-based method of controlling the local FDR. All protein identifications are listed in **Online Table III**.



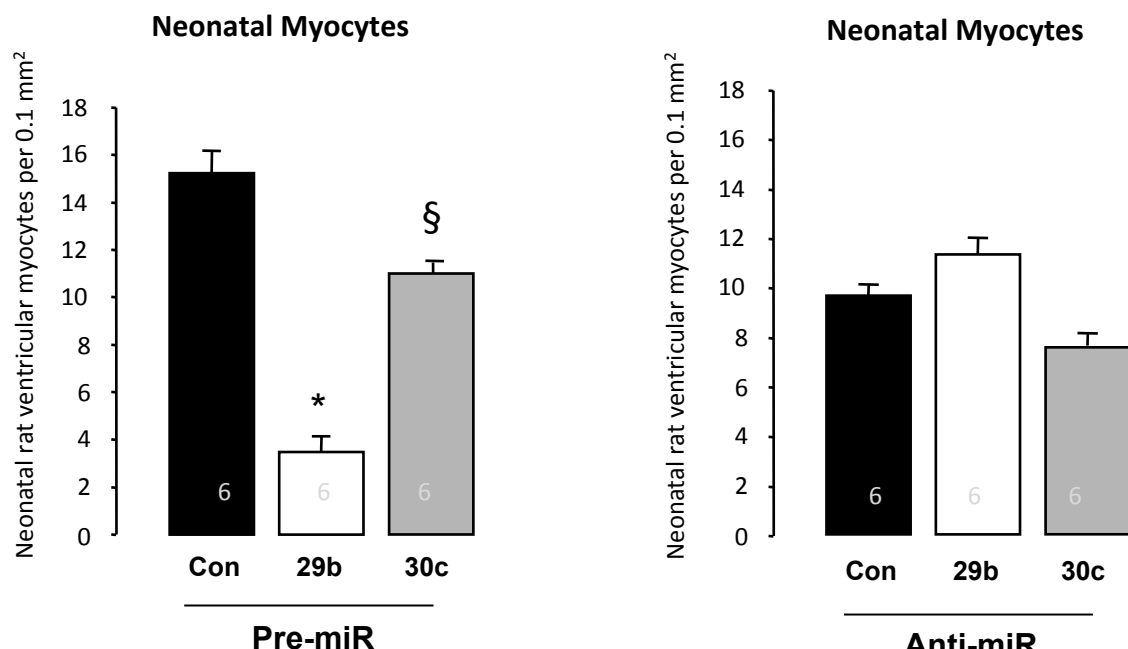
Online Figure IV: Luciferase reporter assay. The 3' untranslated regions of mouse IGF-1, LIF and PTX3 harboring putative binding sites of the miR-29 family were cloned into the dual-luciferase reporter vector psiCheck2 (Promega). The reporter vectors (100 ng of psiCheck2 construct) were transfected together with 30-100 nM of miR-29b mimic or the mimic negative control (CON) in triplicate into mouse aortic smooth muscle cells using Lipofectamine 2000 (Lifetech). Renilla 3'UTR-coupled luciferase activity was normalized to constitutive firefly luciferase activity for each well. Unlike IGF-1 and LIF, no significant inhibition was obtained for PTX3 (data not shown). *, denotes P<0.05 compared to respective CON.



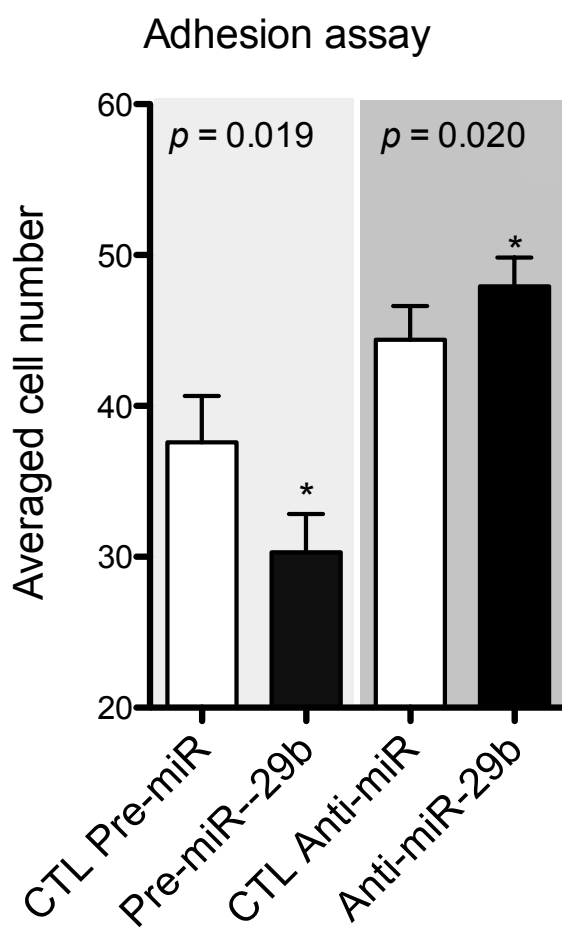
Online Figure V: Effect of miR-29b mimics on expression of miR-29b targets in CFs as assessed by qPCR (minimum of n=3 per group). * denotes P<0.05.



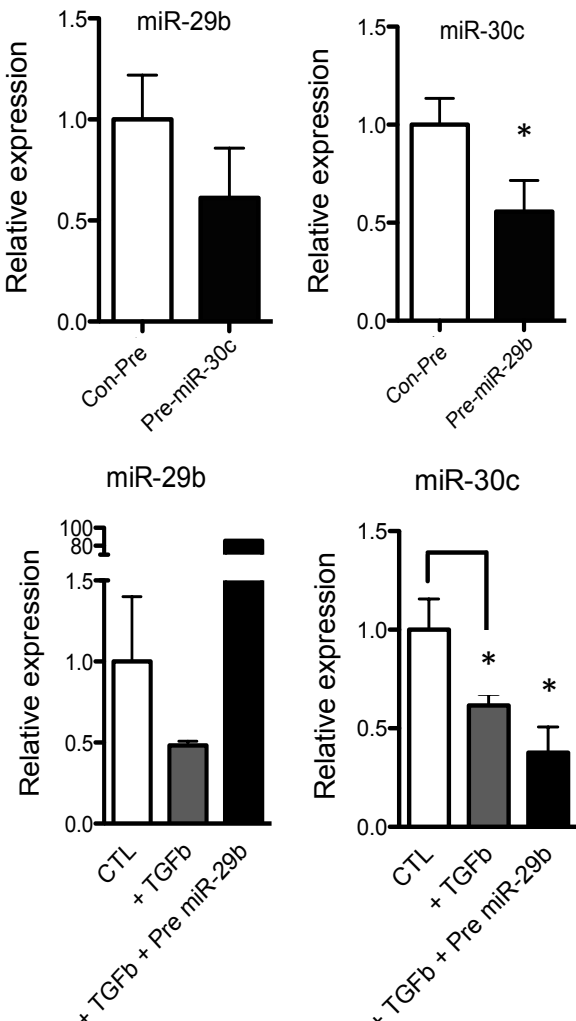
Online Figure VI: Number of adherent NRVM is displayed by the bar chart per 0.1 mm^2 . The bar chart demonstrates the myocyte count of 3 areas per coverslip in 6 independent experiments. § $P<0.05$ vs corresponding control group (CON).



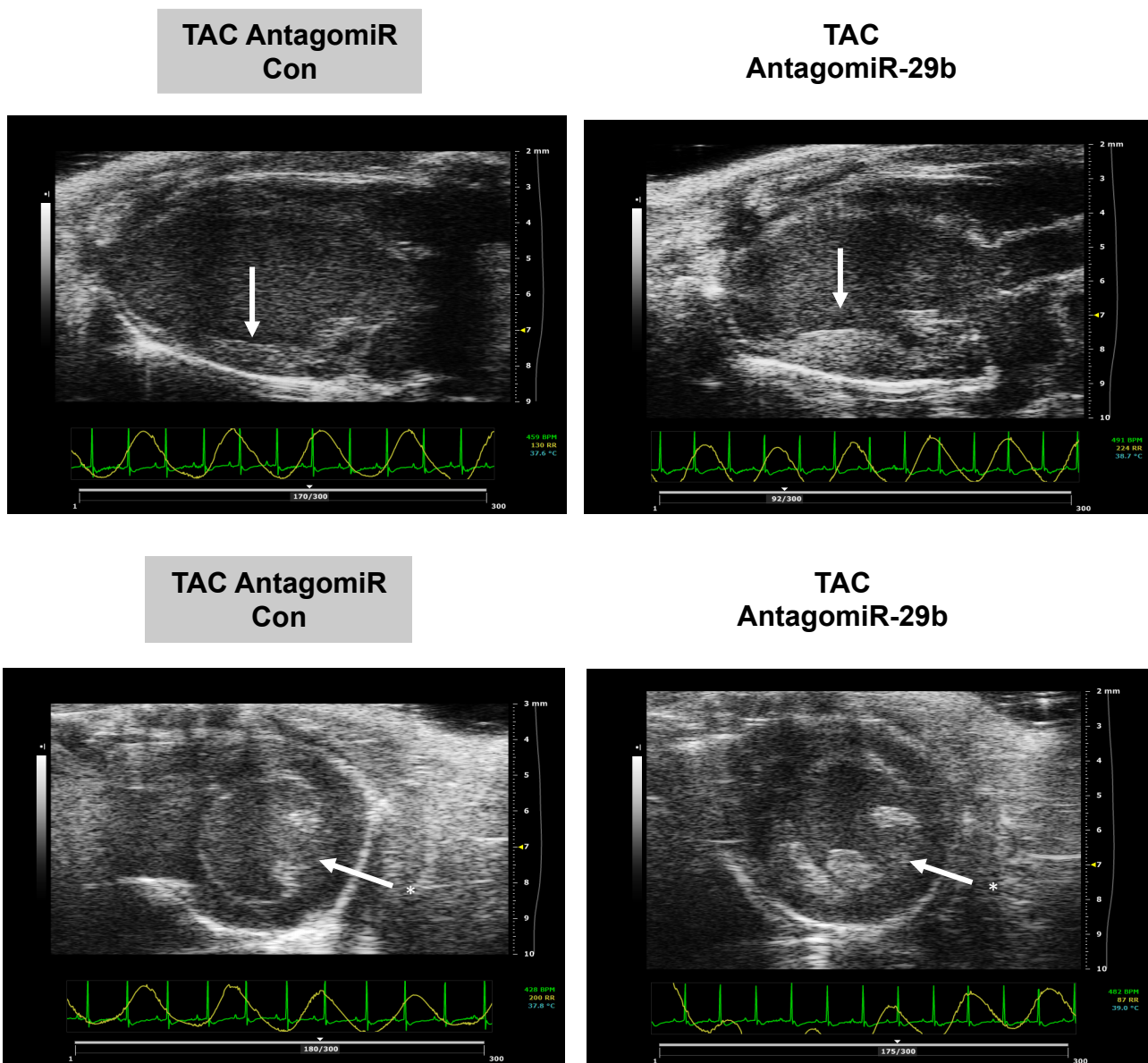
Online Figure VII: Number of adherent CFs is displayed as averaged cell number per 0.1 mm^2 . * $P<0.05$ vs control (CON) for the averaged CF count of 3 areas per coverslip.



Online Figure VIII: Cross-talk between miR-29b and miR-30c in CFs as assessed by qPCR. * $P<0.05$ vs control (CON) in three independent experiments.



Online Figure IX: Representative parasternal long axis B mode image from antagomiR-treated mice that showed the most pronounced inhibition of miR-29b after TAC. A cross section of the papillary muscle (white arrows) is in view rather than the true inferolateral (posterior) wall. The latter (*) has the same thickness as revealed in the short axis B-mode but the papillary muscle was abnormally thickened and hyperechogenic.



Online Figure X: Q-PCR. Bean plots visualizing 27 transcript levels in LVH normalized to U6.

